



Scientific Excellence • Resource Protection & Conservation • Benefits for Canadians
Excellence scientifique • Protection et conservation des ressources • Bénéfices aux Canadiens

Interannual Variability of Oceanographic Conditions in the Southeastern Beaufort Sea

by
D.B. Fissel
Arctic Sciences Limited
and
H. Melling
Institute of Ocean Sciences

Department of Fisheries and Oceans
Institute of Ocean Sciences
Sidney, B.C.

1990

**Canadian Contractor Report of
Hydrography and Ocean Sciences
No. 35**



Fisheries
and Oceans

Pêches
et Océans

Canada

Canadian Contractor Report of Hydrography and Ocean Sciences

Contractor reports are unedited final reports from scientific and technical projects contracted by the Ocean Science and Surveys (OSS) sector of the Department of Fisheries and Oceans.

The contents of the reports are the responsibility of the contractor and do not necessarily reflect the official policies of the Department of Fisheries and Oceans.

If warranted, contractor reports may be rewritten for other publications of the Department, or for publication outside the government.

Contractor reports are abstracted in *Aquatic Sciences and Fisheries Abstracts* and indexed in the Department's annual index to scientific and technical publications.

Contractor reports are produced regionally but are numbered nationally. Requests for individual reports will be filled by the issuing establishment listed on the front cover and title page. Out of stock reports will be supplied for a fee by commercial agents.

Regional and headquarters establishments of Ocean Science and Surveys ceased publication of their various report series as of December 1981. A complete listing of these publications is published in the *Canadian Journal of Fisheries and Aquatic Sciences*, Volume 39: Index to Publications 1982. The current series, which begins with report number 1, was initiated in January 1982.

Rapport canadien des entrepreneurs sur l'hydrographie et les sciences océaniques

Cette série se compose des rapports finals non révisés préparés dans le cadre des projets scientifiques et techniques réalisés par des entrepreneurs travaillant pour le service des Sciences et levés océaniques (SLO) du ministère des Pêches et des Océans.

Le contenu des rapports traduit les opinions de l'entrepreneur et ne reflète pas nécessairement la politique officielle du ministère des Pêches et des Océans.

Le cas échéant, certains rapports peuvent être rédigés à nouveau de façon à être publiés dans une autre série du Ministère, ou à l'extérieur du gouvernement.

Les rapports des entrepreneurs sont résumés dans la publication *Résumés des sciences halieutiques et aquatiques* et ils sont classés dans l'index annuel des publications scientifiques et techniques du Ministère.

Les rapports des entrepreneurs sont produits à l'échelon régional, mais numérotés à l'échelon national. Les demandes de rapports seront satisfaites par l'établissement auteur dont le nom figure sur la couverture et la page du titre. Les rapports épuisés seront fournis contre rétribution par des agents commerciaux.

Les établissements des Sciences et levés océaniques dans les régions et à l'administration centrale ont cessé de publier leurs diverses séries de rapports en décembre 1981. Une liste complète de ces publications figure dans le volume 39, Index des publications 1982 du *Journal canadien des sciences halieutiques et aquatiques*. La série actuelle a commencé avec la publication du rapport numéro 1 en janvier 1982.

1990

**INTERANNUAL VARIABILITY
OF OCEANOGRAPHIC CONDITIONS IN THE
SOUTHEASTERN BEAUFORT SEA**

by

D.B. Fissel
Arctic Sciences Limited

and

H. Melling
Institute of Ocean Sciences

Department of Fisheries and Oceans
Institute of Ocean Sciences
Sidney, B.C.

The contents of this report are the sole responsibility of Arctic Sciences Limited, and do not reflect policy or opinions of the Government of Canada.

Copyright Minister of Supply and Services, Canada - 1990
Cat. NO. Fs 97 - 17/35 ISSN 0711-6748

Correct citation for this publication:

D.B. Fissel and H. Melling. 1990. Interannual Variability of Oceanographic Conditions in the Southeastern Beaufort Sea. Can. Contr. Rep. Hydrogr. Ocean Sci. No. 35, 102 pages (plus 6 microfiche).

ACKNOWLEDGEMENTS

This project represents the cumulative efforts of many people and organizations. A key contribution was made by Mr. Rick Birch of Arctic Sciences Limited, who was instrumental in the compiling of, and the preliminary quality control of, most of the data sets used in this report. We also thank other Arctic Sciences Limited personnel for their dedicated efforts: Owen Byrne, Gordon Lacey and Rene Chave in computer programming; Ferne Welsman and Dave Stover in report production.

Funding for this project was provided by Supply and Services Canada's Unsolicited Proposal Fund, the Panel on Energy Research and Development (PERD), the Institute of Ocean Sciences (IOS), the Freshwater Institute (FWI), Indian and Northern Affairs Canada (INAC) and the Atlantic Geoscience Centre (AGC) of Energy Mines and Resources Canada. Special thanks for support in this regard are directed to: Bob Wilson and Brian Smiley (IOS), Mike Lawrence (FWI), Phil Hill (AGC), Jon Moen (INAC), Langley Muir (COGLA) and Brian Wright (Gulf Canada).

Many people assisted in providing data and information for this study. We especially wish to thank: the late Fred Geddes and Phil Côté of Ice Centre (AES), Val Swail (Canadian Climate Centre, AES), Glen Hopky (FWI), Luc Cuypers (IOS) and Rob MacDonald (IOS).

ABSTRACT

D.B. Fissel and H. Melling. 1990. *Interannual Variability of Oceanographic Conditions in the Southeastern Beaufort Sea*. Can. Contr. Rep. Hydrogr. Ocean Sci. No. 35, 102 pages (plus 6 microfiche).

Interannual variations in summertime oceanic conditions in the southeastern Beaufort Sea have been studied through analysis of temperature and salinity data collected between 1950 and 1987. Causes for observed oceanic variations have been sought in variations in wind, ice cover and river discharge over the same period. The largest interannual variation has occurred in salinity, with an amplitude of 5 over decadal periods. Related variations were noted in temperature. The area of sea ice in summer has varied over slightly shorter periods, with an amplitude equal to 80% of the mean ice-covered area. Correlations between oceanic parameters and wind, or ice-covered area, or river discharge, have been generally low. However, over the continental shelf, with the exception of the coastal zone, increased temperature and salinity have been correlated with reduced sea ice cover. In the coastal zone, temperature and salinity have been correlated with discharge from the Mackenzie River.

Budgets of freshwater and heat were computed during spring and summer over a ten-year period for the shelf region. In this area, approximately 70% of the fresh water in summer originates as river discharge, and most of the remainder from melting sea ice. The fresh water budget undergoes large variations from year to year, due to varying losses of fresh water from the shelf by advection. Such transport is controlled primarily by the extent of sea-ice clearing and, in years of moderate sea ice clearing, by the response to seasonal wind patterns. The heat budget is dominated by radiation and exchange with the atmosphere. Inflow of warm river water, and ice melting are relatively insignificant. The amounts of both fresh water and heat vary from year to year, but only the heat content drops dramatically towards the end of each summer.

Key words: temperature, salinity, ice, Beaufort, variability, budget

RÉSUMÉ

D.B. Fissel and H. Melling. 1990. Interannual Variability of Oceanographic Conditions in the Southeastern Beaufort Sea. Can. Contr. Rep. Hydrogr. Ocean Sci. No. 35, 102 pages (plus 6 microfiche).

Les variations interannuelles des conditions océaniques en été dans le sud-est del la mer de Beaufort ont été étudiées grâce à l'analyse des données sur la température et sur la salinité recueillies entre 1950 et 1957. On a cherché les causes des variations océaniques observées en étudiant les variations au niveau du vent, de la couverture de glace et du débit fluvial au cours de cette même période. La variation interannuelle la plus importante a été celle de la salinité avec une amplitude de 5 d'une décennie à l'autre. Des variations connexes ont été observées au niveau des températures. La superficie couverte par la glace de mer en été variait sur des périodes légèrement plus courtes, avec une amplitude égale à 80% de la superficie moyenne couverte par les glaces. Les corrélations entre les paramètres océaniques et le vent, ou la superficie couverte par les glaces ou encore le débit fluvial on été généralement faibles. Sur le plateau continental cependant, à l'exception de la zone côtière, la hausse des températures et de la salinité correspondait à la réduction de la superficie couverte par la glace de mer. Dans la zone côtière, on a établi la corrélation entre la température et la salinité d'une part, et le débit du Mackenzie d'autre part.

Le bilan des eaux douces et le bilan thermique on été calculés au printemps et en été au cours d'une période de 10 ans dans la région bordière. Dans cette région, environ 70% des eaux douces en été proviennent du fleuve, et la majeure partie des 30% qui restent provient de la fonte del la glace de mer. Le bilan de l'eau douce connaît d'importantes variations d'une année à l'autre dues à la variation des pertes d'eau douce par advection sur le plateau continental. Ce transport est dirigé dans une large mesure par la dimension de polynies et, au cours des années de polynies modérées, la réaction aux vents locaux. Le budget thermique est dominé par le rayonnement et les échanges de chaleur avec l'atmosphère. L'apport des eaux fluviales chaudes et la fonte des glaces sont relativement peu importants. Les quantités d'eau douce et la chaleur varient d'une année à l'autre, mais seule la teneur en chaleur diminue considérablement vers la fin de chaque été.

Mots clés: température, salinité, glace, Beaufort, variabilité, bilan

TABLE OF CONTENTS

	<u>Page</u>
ACKNOWLEDGEMENTS	iii
ABSTRACT	iv
RÉSUMÉ	v
TABLE OF CONTENTS	vi
LIST OF TABLES	viii
LIST OF FIGURES	ix
 1 INTRODUCTION	 1
1.1 Background	1
1.2 Study Objectives	3
1.3 Project Scope: Spatial and Temporal Coverage	3
 2 OCEANOGRAPHIC DATA	 6
2.1 Data Base	6
2.2 Data Collection	6
2.3 Data Processing	6
2.4 Quality Control	8
2.5 Data Display Products	9
2.6 Derived Integral Quantities	10
 3 WIND, SEA-ICE AND RIVER DISCHARGE DATA	 12
3.1 Wind Data	12
3.2 Sea-Ice Data	12
3.3 River Discharge Data	16
 4 RESULTS	 18
4.1 Interannual Variations of Oceanographic Conditions	18
<u>Long Term Means - Seasonal Variations</u>	24
<u>Surface Temperature and Salinity</u>	24
<u>Heat and Freshwater Content (Upper 50 m)</u>	26
<u>Extreme and Unusual Conditions</u>	29
<u>Interannual-Variability</u>	30
<u>Long-Term Trends in Oceanographic Properties</u>	32
<u>Temperature at Salinity = 31</u>	32
4.2 Wind, Ice and River Discharges	36
<u>Interannual Variations</u>	36
<u>Sea-Ice</u>	36
<u>Wind</u>	36
<u>Mackenzie River Discharge</u>	39
<u>Wind vs. Sea-Ice Area</u>	39
<u>Comparison of Oceanographic Parameters with Wind, Ice</u> <u>and River Discharges</u>	 39
<u>Non-Ice Area</u>	39
<u>Winds</u>	45
<u>River Discharge</u>	50

TABLE OF CONTENTS, cont...

	<u>Page</u>
4.3 Heat and Freshwater Budget Considerations	50
<u>Freshwater Budget</u>	53
<u>Seasonal Variations - May to August</u>	55
<u>Advection of Freshwater</u>	55
<u>Heat Budget</u>	61
<u>Uncertainties in Estimated Heat Budget Terms</u>	66
<u>Atmospheric Heat Fluxes</u>	69
<u>Ice Melt and River Heat Fluxes</u>	73
<u>Oceanic Heat Storage</u>	73
<u>Advection of Ocean Heat</u>	78
<u>Early Summer Quantities with Predictive Value for Net Heat</u> <u>Transfers</u>	81
4.4 Upwelling Conditions	81
5 SUMMARY AND DISCUSSION	86
5.1 Study Objectives	86
5.2 Data Sources and Methods	86
5.3 Interannual Variability of Oceanographic Conditions	86
5.4 Interannual Variability of Sea-Ice, Wind and River Discharges and Correlation with Oceanographic Conditions	87
5.5 Freshwater Budget	88
5.6 Heat Budget	89
5.7 Upwelling Conditions	90
5.8 Recommendations	90
6 REFERENCES	92
APPENDIX A: Information on Data Sets	97
(Appendices B to H are contained as microfiche in an envelope on the back cover of the report.)	
APPENDIX B: Maps of Temperature and Salinity Contours	
APPENDIX C: Maps of Freshwater and Heat Content	
APPENDIX D: Temperature-Salinity Diagrams	
APPENDIX E: Temperature and Salinity Contours on Vertical Cross Sections	
APPENDIX F: Marine Geostrophic Winds: Progressive Vector Diagrams and Wind Event Analysis	
APPENDIX G: Maps of Sea-Ice Concentrations	
APPENDIX H: Plots of Mackenzie River Discharges at Arctic Red River and at East Channel - Inuvik	

LIST OF TABLES

	<u>Page</u>
Table 1: Information for each of the five subregions used in computing monthly mean values of oceanographic parameter.	18
Table 2: A summary of data sources, computational techniques and estimated uncertainties for quantities used in the heat budget computations.	63

LIST OF FIGURES

	<u>Page</u>
Figure 1: Comparison of the mean temperature of the upper mixed layer in August between 1974 (upper), a year of severe ice conditions, and 1975, a year of more typical ice conditions (from Tummers, 1980).	2
Figure 2: A map of the study area showing subareas used in data categories in the temperature-salinity diagrams. The regions used to categorize displays of the vertical cross-sections of temperatures and salinities are indicated by the dashed lines.	4
Figure 3: The quantity of temperature-salinity profiles used in this study by (a) year and month; and by (b) subregions within the southeastern Beaufort Sea.	7
Figure 4: The distribution of the speeds and durations of wind events by direction (1950-1987).	13
Figure 5: An example of the display of sea-ice concentrations for mid-July of (a) 1974, having the maximum sea-ice concentration; and (b) 1977, having the minimum sea-ice concentration. Also shown are the two separate areas ('continental shelf' and 'full area') in which the areas of open water and ice concentrations <u>s</u> even-tenths were computed.	15
Figure 6: A map of the Mackenzie River drainage area. Note the river gauging sites at Arctic Red River, Inuvik and Norman Wells from which data were used in this study. The number along the Mackenzie River designate the distance from the head waters (in Great Slave Lake) in kilometers (and in miles).	17
Figure 7: The monthly mean values of temperature at 1 m depth during July, August and September of each year in which data were available.	19
Figure 8: The monthly mean values of salinity at 1 m depth during July, August and September of each year in which data were available.	20
Figure 9: The monthly mean values of heat integral over the uppermost 50 m during July, August and September of each year in which data were available.	21
Figure 10: The monthly mean values of freshwater integral over the uppermost 50 m during July, August and September of each year in which data were available.	22

LIST OF FIGURES, cont...

	<u>Page</u>
Figure 11: The monthly mean values of: temperature at 1 m; salinity at 1 m; heat integral; freshwater integral; for the March-April period of each year in which data were available. The results are displayed individually for the continental shelf and slope subregions.	23
Figure 12: The mean monthly temperature and salinity values (at 1 m depth) averaged from those years where the available data are of the highest or intermediate reliability category (see text).	25
Figure 13: The mean monthly heat and freshwater integrals (over the uppermost 50 m) averaged from those years where the available data are of the highest or intermediate reliability category (see text).	27
Figure 14: Two examples of vertical cross-sections of temperature and salinity (1975 and 1986) which reveal that at depths exceeding 25-30 m, contributions to the heat integral are positive, while contributions to the freshwater integral are small or negative.	28
Figure 15: Monthly mean values of temperature at a salinity of 31. The results are displayed separately for five subregions of the study area.	33
Figure 16: Monthly mean values of temperature at a salinity of 31. The results are presented for the portions of the continental shelf and slope subregions (shown in inset map of Figure 15).	34
Figure 17: Maps of temperature and salinity over the eastern Alaskan continental shelf showing the presence of warm subsurface water of Bering Sea origin (from Fissel et al., 1987a).	35
Figure 18: (a) The surface area, in thousands of km ² , with ice cover of less than seven-tenths concentration for: (a) the S.E. Beaufort Sea; and (b) the portion of the S.E. Beaufort Sea spanning the continental shelf (regions are shown in Figure 5). The areas are plotted for mid-July, mid-August and the average of the two. (b) A scatter plot between the area of reduced (C<0.7) ice concentration during August in the S.E. Beaufort Sea (this study) and the areal-ice extent of the much larger region (see inset) of Mysak and Manak (1989).	37

LIST OF FIGURES, cont...

Page

Figure 19:	(a) The net wind displacement of the easterly wind component (in km) for April 15 to June 15, mid-June to mid-July and mid-July to mid-August, as computed from the marine geostrophic wind data.	38
	(b) The cumulative volume discharge of the Mackenzie River (at Arctic Red River) for May-June, July and August.	
Figure 20:	A scatter plot of the change in "non-ice area" (ice concentrations <0.7) against the net easterly wind run from mid-July to mid-August.	40
Figure 21:	Scatter plot and linear regression results for salinity at 1 m versus area where ice concentration <0.7 for (a) continental shelf (shf) and slope (slp) subregions and, (b) nearshore Mackenzie shelf (nsh) and Mackenzie Bay/Yukon (mck) subregions.	41
Figure 22:	Scatter plot and linear regression results for freshwater content to 50 m versus area where ice concentration <0.7 for (a) continental shelf (shf) and slope (slp) subregions, and (b) nearshore Mackenzie shelf (nsh) and Mackenzie Bay/Yukon (mck) subregions.	42
Figure 23:	Scatter plot and linear regression results for temperature at 1 m versus area where ice concentration <0.7 for (a) continental shelf (shf) and slope (slp) subregions, and (b) nearshore Mackenzie shelf (nsh) and Mackenzie Bay/Yukon (mck) subregions.	43
Figure 24:	Scatter plot and linear regression results for heat content to 50 m versus area where ice concentration <0.7 for (a) continental shelf (shf) and slope (slp) subregions, and (b) nearshore Mackenzie shelf (nsh) and Mackenzie Bay/Yukon (mck) subregions.	44
Figure 25:	Scatter plot and linear regression results for salinity at 1 m versus easterly wind run for (a) continental shelf (shf) and slope (slp) subregions, and (b) nearshore Mackenzie shelf (nsh) and Mackenzie Bay/Yukon (mck) subregions.	46
Figure 26:	Scatter plot and linear regression results for freshwater content to 50 m versus easterly wind run for (a) continental shelf (shf) and slope (slp) subregions, and (b) nearshore Mackenzie shelf (nsh) and Mackenzie Bay/Yukon (mck) subregions.	47

LIST OF FIGURES, cont...

Page

- Figure 27: Scatter plot and linear regression results for 48
 temperature at 1 m versus easterly wind run for (a)
 continental shelf (shf) and slope (slp) subregions,
 and (b) nearshore Mackenzie shelf (nsh) and Mackenzie
 Bay/Yukon (mck) subregions.
- Figure 28: Scatter plot and linear regression results for heat 49
 content to 50 m, versus easterly wind run for (a)
 continental shelf (shf) and slope (slp) subregions,
 and (b) nearshore Mackenzie shelf (nsh) and Mackenzie
 Bay/Yukon (mck) subregions.
- Figure 29: Scatter plot and linear regression results for (a) 51
 salinity at 1 m, and (b) freshwater content to 50 m
 versus Mackenzie River discharge for inshore areas:
 nearshore Mackenzie shelf (nsh) and Mackenzie
 Bay/Yukon (mck).
- Figure 30: Scatter plot and linear regression results for (a) 52
 temperature at 1 m and (b) heat content to 50 m versus
 Mackenzie River discharge for inshore areas:
 nearshore Mackenzie shelf (nsh) and Mackenzie
 Bay/Yukon (mck).
- Figure 31: The area of the continental shelf (61,950 km²) for 54
 which the freshwater and heat budgets were computed.
- Figure 32: (a) The monthly mean values of freshwater input to 56
 the continental shelf including River
 discharges, melt of sea-ice in place, and the
 excess of precipitation over evaporation. The
 mean values are given for May, June, July and
 August, as well as the cumulative value for
 the five month period of December to April.
 (b) Total freshwater inputs to the continental shelf
 by individual years for the averaging periods
 shown in (a).
- Figure 33: Freshwater input to the continental shelf resulting 57
 from (a) River discharge, and (b) ice melt by
 individual years for the months May, June, July,
 August as well as the five month averaging period:
 December-April.

LIST OF FIGURES, cont...

Page

- Figure 34: (a) Estimated freshwater stored in the continental shelf by year for the periods: (1) mid-July to mid-August, and (2) mid-August to mid-September. See the text for the method used to estimate the uncertainties shown as error bars. 58
- (b) The accumulated value of the freshwater budget terms over the period December to August, by individual years. The numbers displayed below the bars represent the estimated percentage uncertainty (of total freshwater input) in the ocean storage values for each year.
- Figure 35: The computed values of (a) freshwater lost from the continental shelf and (b) freshwater retained on the continental shelf, as a percentage of total freshwater input. The values displayed represent the cumulative losses from the period beginning in December to either: mid-July to mid-August; or mid-August to mid-September. 60
- Figure 36: Water temperature measurement data for the Mackenzie River near Arctic Red River (Davies, 1975; B.C. Hydro, unpubl. data) and at points in the Mackenzie Delta. The included average temperature versus time curve is used in the heat budget computations (From Marko et al., 1983). 67
- Figure 37: The long-term mean (computed over ten years) values of the heat budget terms, accumulated over the period May-August, along with the estimated uncertainty. 68
- Figure 38: The long-term monthly means for all terms related to exchange of heat from the atmosphere computed with incident solar radiation determined (a) case 1 - from Sachs Harbour direct measurements and (b) case 2 - including an additional factor to simulate losses due to increased cloudiness over the ocean. 70
- Figure 39: A comparison of heat fluxes from this study with those of previous heat budget studies in the Canadian Arctic. 71
- Figure 40: The monthly mean values of net surface heat transferred to the ocean (Q_A) by individual years for May, June, July, August and the average of these four months (a) without, and (b) with the additional simulation for effects of marine cloudiness. 72

LIST OF FIGURES, cont...

Page

- Figure 41: The surface heat transfer, river input, ice melt and the net input to the ocean (for case 1 net radiation) displayed as: (a) long-term mean values, by individual months; and (b) values from May to August by individual years. 74
- Figure 42: The surface heat transfer, river input, ice melt and the net input to the ocean (for case 2 net radiation) displayed as: (a) long-term mean values, by individual months; and (b) values from May to August by individual years. 75
- Figure 43: Estimates of heat storage in the continental shelf for those years with sufficient observations: (a) mid-July to mid-August; and (b) mid-August to mid-September. 76
- Figure 44: Yearly estimated values of heat storage (August) plotted versus net surface heat input from May to August. 77
- Figure 45: Estimates of freshwater content plotted versus heat content in the continental shelf for the period mid-August to mid-September. 79
- Figure 46: The computed values of heat lost from the continental shelf as a percentage of total heat input. The displayed values represent the cumulative losses from the period beginning in May to either: mid-July to mid-August, or mid-August to mid-September. 80
- Figure 47: A scatter plot of net solar radiation to the end of June with (a) cumulative net surface heat transfer (May to August) and (b) cumulative net heat transfer to the ocean (May to August). 82
- Figure 48: A scatter plot of amount of open water at the end of June with (a) cumulative net surface heat transfer (May to August) and (b) cumulative net heat transfer to the ocean (May to August). 83
- Figure 49: The number of up- or down-welling events plotted versus wind direction and magnitude categories for two different ranges of time lags between the winds and oceanographic conditions. One to two days for (a) the Mackenzie Shelf and (b) the Mackenzie Trough, and three to five days for (c) the Mackenzie Shelf and (d) the Mackenzie Trough. 85

1 INTRODUCTION

1.1 BACKGROUND

An extended set of oceanographic data is available for the southeastern Beaufort Sea, where systematic data collection began in 1950, nearly 40 years ago. While the dominant oceanographic features of the region have been reasonably well described (eg. Cameron, 1953; Herlinveaux and de Lange Boom, 1975; Melling and Lewis, 1982; MacDonald et al., 1987), comparatively little effort has been directed at examining the longer period variability of the Beaufort Sea, particularly on year-to-year time scales (interannual) or longer.

Large changes in summer oceanographic conditions can occur between years, as is evident in the data collected in 1974 and 1975, during the Beaufort Sea Project. In 1974, sea-ice remained abnormally close to shore through most of the summer, while in 1975, extensive areas of open water were present in July and August. The large difference in open water areas between 1974 and 1975 had a substantial effect on other parameters, including solar radiation absorbed (Tummers, 1980), and surface water advection over the continental shelf. As a result, oceanographic distributions were much different between the two years, as shown in Figure 1. Considerable differences between 1974 and 1975 were also evident in the distribution of nutrients and in the inferred levels of primary productivity (MacDonald et al., 1987).

While the differences in sea-ice concentrations were important in explaining the difference in oceanographic conditions between 1974 and 1975, sea-ice conditions are not the only factor influencing oceanographic variability. Other important (and interrelated) factors include prevailing wind patterns, Mackenzie River discharge and the vagaries of oceanic exchanges with adjacent regions to the west, east, and offshore.

The importance of interannual variability of the oceanography of the southeastern Beaufort Sea leads to a need for information to document and quantify the nature of these variations. Fortunately, a great deal of oceanographic and sea-ice data have been accumulated over the past 30-40 years, on an opportunistic basis. However, this information is contained in a multitude of research reports, papers and operational data reports. A first step towards better utilization of these many sources of data was the compilation and appraisal of Beaufort Sea physical oceanographic data, recently updated to include data to 1986 (Birch et al., 1987).

A few previous oceanographic studies have examined oceanographic variability over periods longer than meteorological time scales (one day to one month): Melling and Lewis (1982) and Melling (1983) examined shelf drainage flows driven by autumnal freezing; the roles of physical oceanographic processes were studied in determining sediment transport (Fissel and Birch, 1984); and data from the 1974-1975 Beaufort Sea Project have been analyzed, as described above. Among the data collected in the 24-year period 1950-1973, only the Cancolim II data of 1951-1952 have been subjected to a systematic analysis (Cameron, 1953), and that analysis was quite limited. Moreover, several large-scale synoptic data sets have been collected since 1974-1975, which have not been examined in terms of long-period variability.

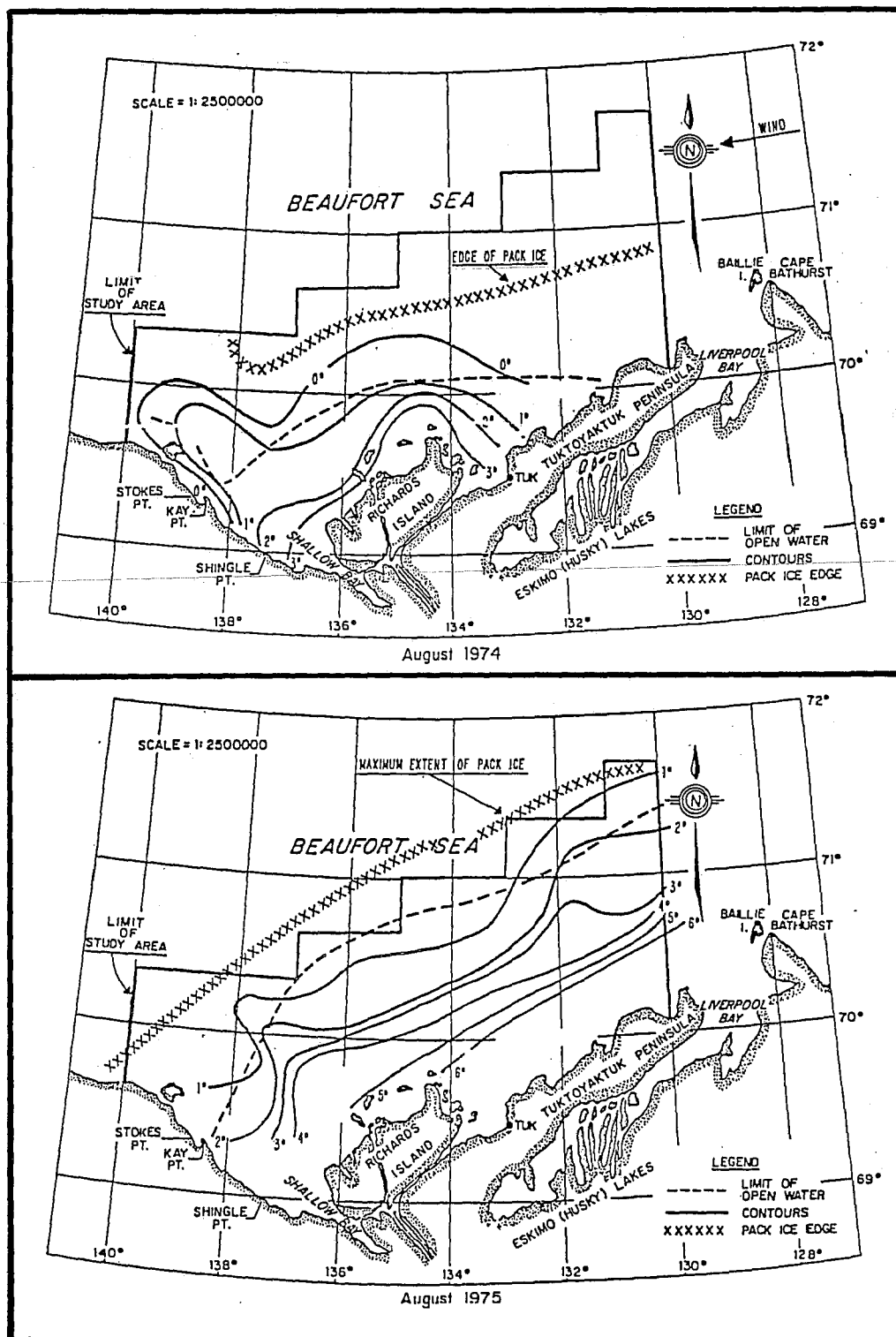


Figure 1: Comparison of the mean temperature of the upper mixed layer in August between 1974 (upper), a year of severe ice conditions, and 1975, a year of more typical ice conditions (from Tummers, 1980).

1.2 STUDY OBJECTIVES

Our general objective was to examine variations in Beaufort Sea oceanographic conditions over periods of one year or longer, and to compare these variations with measurable changes in external factors which may be important, including surface winds, sea-ice concentrations and Mackenzie River discharge volumes.

To achieve the general objective, the following specific tasks were carried out:

- (1) Acquire and process all sets of available oceanographic data, which provided sufficient areal coverage to be useful in representing oceanographic conditions. The data processing consisted of conversion into a uniform data format and removal of erroneous or suspect data values.
- (2) Display the available data sets in a uniform and consistent manner. The data displays consisted of: contoured maps of temperature and salinity at several depths (0, 20, 50 and 100 m) and temperature on an isohaline (salinity = 31) surface; temperature-salinity diagrams; and contoured temperature and salinity fields on selected vertical transects oriented perpendicular to the coastline.
- (3) Computation of integral quantities consisting of: heat content (surface to 50 m) and freshwater (or reduction in salt) content (surface to 50 m). These quantities were displayed as contours on maps. The heat and freshwater content values were also averaged over selected sub-areas of the study region to simplify the study of changes occurring over many years.
- (4) Available information on surface winds, sea-ice concentrations and river discharges was acquired and processed. Fluctuations in these quantities were compared with fluctuations in the observed and derived oceanographic properties (tasks 2 and 3 above), in order to identify similarities in patterns of variability.
- (5) Computation of all relevant terms in the heat and freshwater budgets for selected years having reasonably complete observations of oceanographic, meteorological and river discharge parameters.

This study is the first systematic examination of longer period variations in the oceanography of the southeastern Beaufort Sea. While the available historical data are incomplete in some important respects (eg. a six-year gap in summer data collection between 1963 and 1968), the study was designed to quantify the information available in existing data. The results of the study are intended to provide the basis for planning improved future oceanographic programs to study the long-term variability of the Beaufort Sea.

1.3 PROJECT SCOPE: SPATIAL AND TEMPORAL COVERAGE

The full study area, shown in Figure 2, extends westward to the Canada-US offshore boundary, northward to a latitude of 72.5°N and eastward to include the mouth of Amundsen Gulf (longitude of 124°W) and the west coast of Banks Island. The North American continental coastline forms the southern boundary of the study

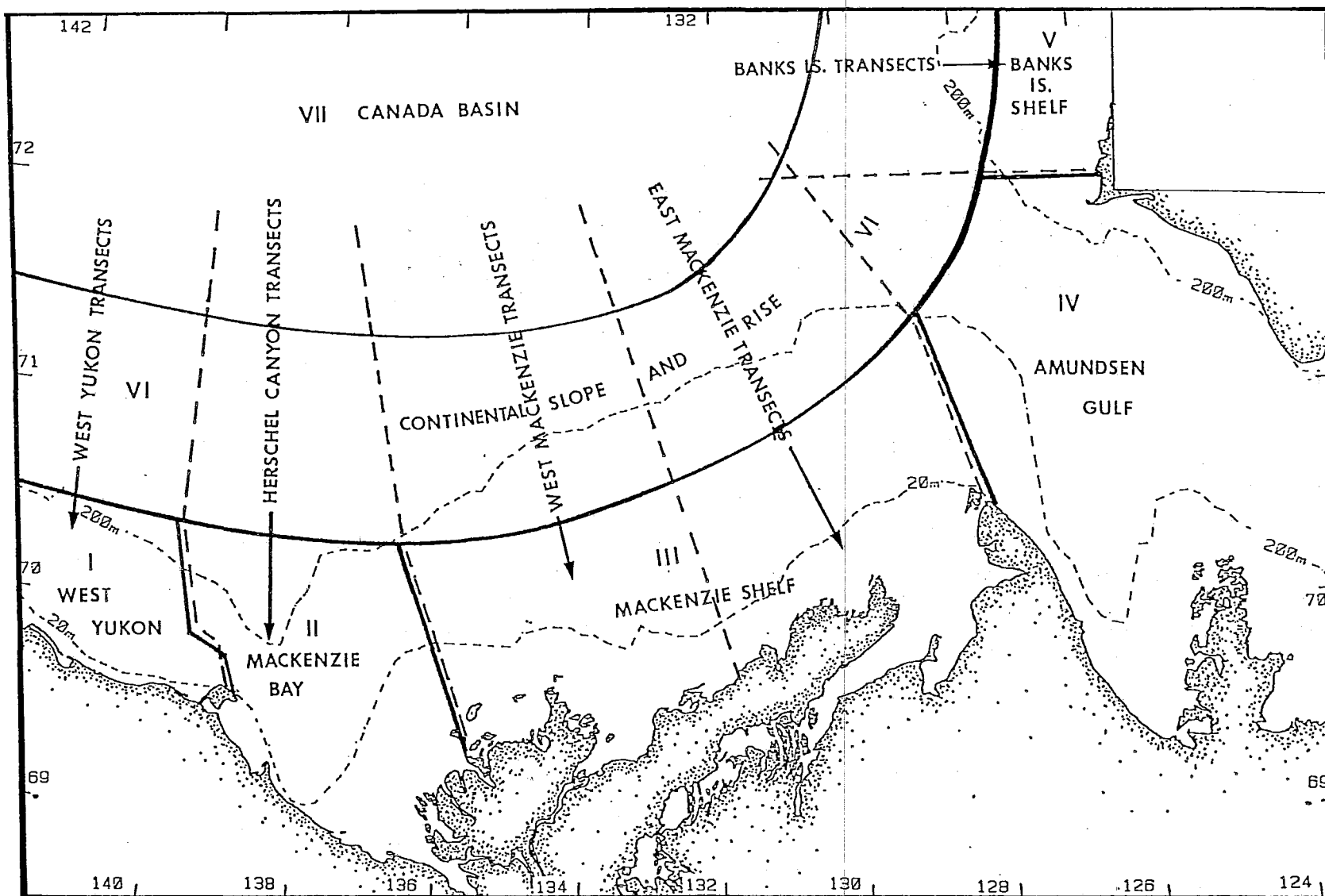


Figure 2: A map of the study area showing subareas used in data categories in the temperature-salinity diagrams. The regions used to categorize displays of the vertical cross-sections of temperatures and salinities are indicated by the dashed lines.

area. While the focus of this project is the continental shelf and areas immediately adjoining, where offshore activities are concentrated (and where the bulk of oceanographic observations have been obtained), the study area has been extended northward and eastward. This extension ensures that significant oceanographic features occurring over the continental margin of the Canada Basin, the continental shelf off Banks Island and in the mouth of Amundsen Gulf, are also displayed on the maps of oceanographic distributions prepared for this study.

The full study area was divided into subregions (Figure 2) which reflect distinctive bathymetry. A broad, shallow continental shelf, extending from Richards Island to Cape Dalhousie, is designated as subregion III - Mackenzie Shelf. Two small portions of the continental shelf are also represented as subregions I and V, situated off the western Yukon coastline and off Banks Island respectively. Subregion II contains Mackenzie Bay and the Herschel Canyon or Trough. This latter feature impinges on the continental shelf, bringing comparatively deep water of 100 m or more to within 35 km of the coastline. Subregion IV, the approaches to western portions of Amundsen Gulf, also cuts across the continental shelf, having water depths to over 400 m. Region VI includes the continental slope and rise, and consists of water depths ranging from 50 m to approximately 2000 m. Areas of greater depths are in subregion VII - Canada Basin.

The subregions were used as distinct categories for presenting data on the temperature-salinity diagrams (Appendix D). Subareas were also devised for the presentation of temperature and salinity distributions on vertical transects directed offshore from the coastline (Appendix E). The categories for the vertical transects are also shown on Figure 2 as the areas delineated by dashed lines.

To the extent that the sampling in the historical data permitted, oceanographic display products were prepared at bimonthly intervals. The display products were limited to the spring and summer seasons, the seasons encompassing virtually all oceanographic data collection in the Beaufort Sea. In the summer, oceanographic data are concentrated over the period mid-July to late September, while smaller quantities of oceanographic data are available in the spring from mid-March to late May. Very few data are available over the continental shelf in June and early July, during the break-up and dispersal of the sea-ice.

2 OCEANOGRAPHIC DATA

2.1 DATA BASE

Selection of data sets was based on their coverage (both spatially and temporally), quality and availability. The objective was to acquire sufficient data to map oceanographic distributions over the Beaufort Sea shelf area, for the spring through fall period, for as many years as possible between 1950 and 1987.

Depending heavily on the recently updated physical oceanographic data inventory for the Beaufort Sea (Birch et al, 1987), a total of approximately 1500 vertical profiles of temperature and salinity were selected for use in this study, from 72 different data sets (see Appendix A). The availability of oceanographic data varies enormously among individual years, as illustrated in Figure 3. The level of oceanographic research activity was comparatively high in the 1950's, and from the mid-1970's to mid-1980's, due to defense-related surveillance and offshore oil activities (and related environmental studies), respectively. However, during the 1960's the quantity of oceanographic data collected was very small, and generally limited to nearshore areas. As a result, no useable data sets were available for the eight year period, 1961 to 1968. The selected data sets provided spatial coverage of summer water property distributions in 28 years. The number of useable springtime data sets was limited to eight.

2.2 DATA COLLECTION

Data were obtained from seven main sources:

- (1) Marine Environmental Data Service, Ottawa (MEDS)
- (2) National Oceanographic data Centre, Washington (NODC)
- (3) Institute of Ocean Sciences, Sidney, British Columbia (IOS)
- (4) Department of Fisheries and Oceans, Winnipeg, Manitoba (DFO)
- (5) Canadian Marine Drilling (CANMAR), Dome Petroleum, Calgary, Alberta
- (6) Arctic Sciences Ltd., Sidney B.C. and Dartmouth, N.S.
- (7) published reports

Some data (85-0007, 86-0004 and 86-0008), having been collected by Arctic Sciences Ltd., were already available on its in-house computing facilities. MEDS supplied 27 data sets and NODC supplied two. Several data sets were coded manually using data tabulated in reports. DFO Winnipeg and IOS each provided several data sets on computer-compatible tape.

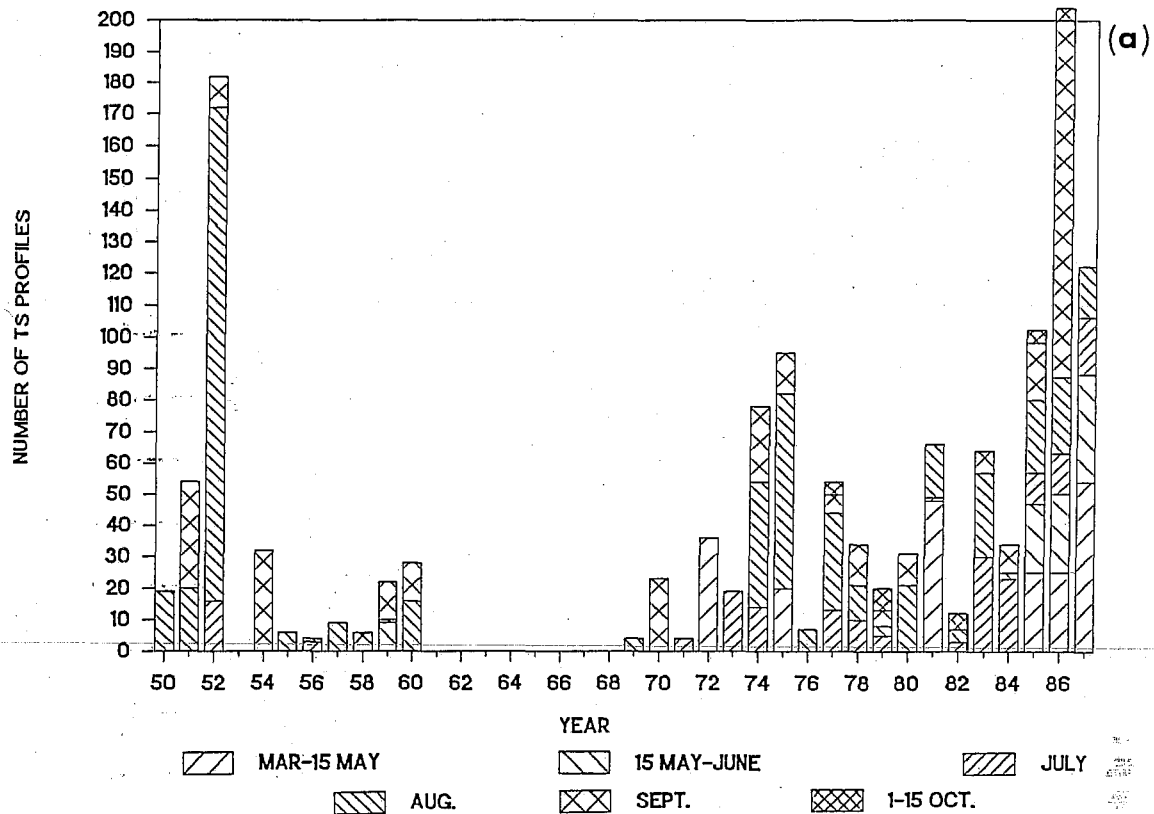
The CANMAR data were collected from drillships during summer operations. Only selected casts were used, ones which provided synoptic coverage at generally three or more sites.

2.3 DATA PROCESSING

All data were converted to binary format for processing on Arctic Sciences' computers.

The MEDS and NODC data were primarily collected using bottle casts. The data were provided at measured as well as interpolated depths.

DATA QUANTITY BY YEAR



DISTRIBUTION OF DATA

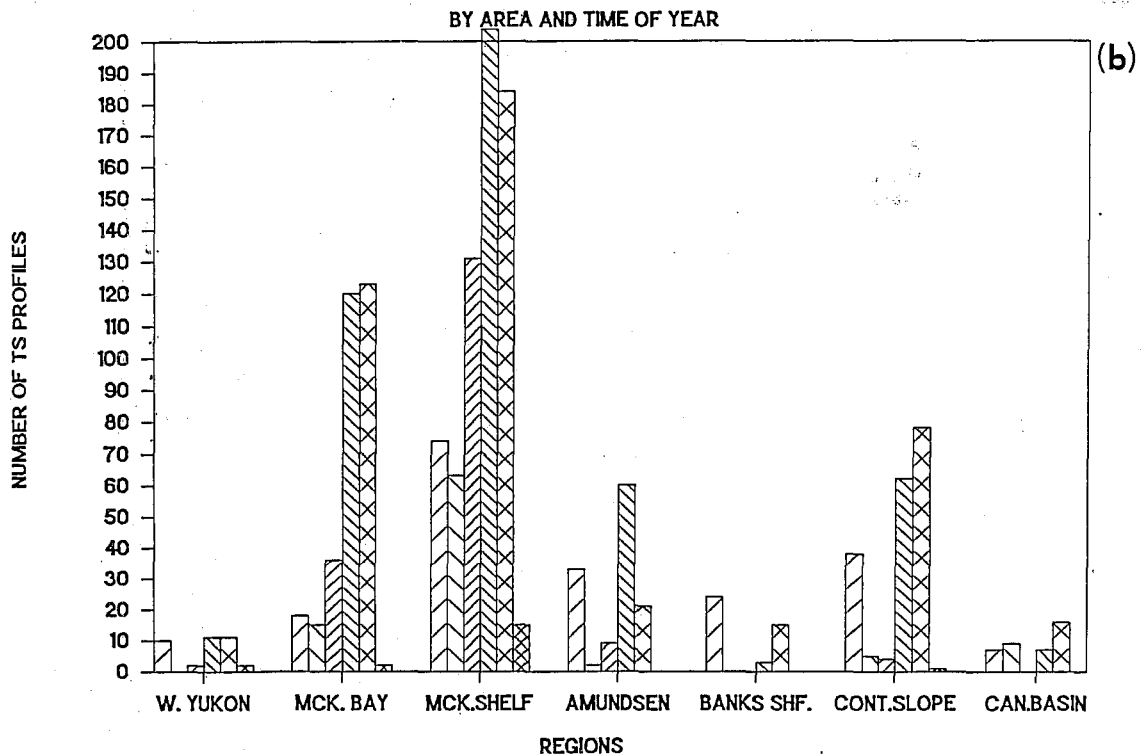


Figure 3: The quantity of temperature-salinity profiles used in this study by (a) year and month; and by (b) subregions within the southeastern Beaufort Sea.

Standard depths (to 1000 m) for interpolation are:

0, 10, 20, 30, 50, 75, 100, 125, 150, 175 (MEDS only), 200, 225 (MEDS only), 250, 300, 400, 500, 600, 700, 800, 900 (NOD only), and 1000 m.

In some cases there are insufficient data to do interpolations, whereas in others the interpolated values, particularly near the surface, may be unrealistic.

Beginning in the 1970's, data collection with continuous profiling instruments (CTD's - Conductivity, Temperature and Depth) has largely replaced bottle cast data collection. For this project, CTD data were typically subsampled over 1-5 m depth intervals.

In most cases pressure as well as depth were provided. In the remaining cases pressures were computed using the formula $P(\text{db}) = 1.00962 (m)$ which is based on an average water density of 1.029 gm/cc for waters above 400 m (Sweers, 1970).

For the error checking routines, density (σ_t) and the freezing point for water of that salinity were also computed.

2.4 QUALITY CONTROL

The data were examined for erroneous or suspect data in three stages. Initially, data were processed using computer programs to check for unrealistic values, spikes (large deviations from the profile over short distances), density inversions, temperatures less than the freezing point and decreasing pressure. The following criteria were used to detect suspect data on the pressure, temperature and salinity values. (No checks were performed on the oxygen and nutrient data.)

- density inversion of 0.02 σ_t (bottle), 0.04 (CTD)
- temperature more than 0.03 (bottle) or 0.05°C (CTD) below freezing
- pressures not increasing
- absolute and first difference values falling outside the bounds:

DEPTH RANGE	ABSOLUTE VALUES	FIRST DIFFERENCE
$0 \leq P < 50$	$-2 < T < 20$ $1 < S < 35$	$T \leq 8$ (bottle), 7 (CTD) $S \leq 15$ (bottle, 10 (CTD)
$50 \leq P < 300$	$-2 < T < 1$ $30 < S < 35.2$	$T \leq 1.0$ (bottle), 0.1 (CTD) $S \leq 1.0$ (bottle), 0.1 (CTD)
$300 \leq P$	$-0.5 < T < 1$ $34 < S < 35.2$	$T \leq 0.5$ (bottle), 0.1 (CTD) $S \leq 0.3$ (bottle), 0.1 (CTD)

Suspect values were not edited automatically, but were flagged for further inspection of each cast. Minor errors, particularly if not at standard depths, were often not corrected. Generally, temperatures below freezing were replaced

with the freezing temperature value. Density inversions were usually eliminated by editing the salinity value deemed to be suspect. If no reasonable value could be determined, the data were replaced with either 9.999 (temp) or 99.999 (sal) and the values flagged.

The second stage of error removal involved preparation of temperature-salinity (TS) diagrams to search for data points that were inconsistent with historical data. This error detection technique was most useful at salinities of 32 or more, where the levels of natural variability are comparatively small. For some data sets, having comparatively low accuracies (i.e. temperature and salinity accuracies of 0.1 or more), such as much of the drillship data from 1976 to 1985, the technique was not applied since the scatter in TS values resulting from low instrument accuracy exceeded the expected natural variations. Because of these limitations, the use of the less accurate data sets was restricted to the upper layers where natural variability is much larger.

A third level of error detection involved invalid data points which had escaped detection using the procedures described above. Such invalid data would occasionally become evident in a contour map as an anomalously high or low value. When this situation occurred, the data value in question was manually removed. Erroneous data values detected in this manner amounted to a very small number, less than 100, out of several thousand data values used in this study. The most common occurrence of these errors was in the oceanographic data collected from drillships, where subsurface measurements were often judged to be too inconsistent, particularly the conductivity (salinity) data.

A summary of the quality control results for individual data sets is provided in Appendix A. Note that a data set having a large number of errors is not necessarily of poorer quality than a data set with fewer detected errors. For example, CTD data are of greater vertical resolution (higher number of values per meter depth) than bottle data, and therefore tend to result in more density inversions. However, the overall data quality of the CTD data may be superior to that of the bottle cast.

2.5 DATA DISPLAY PRODUCTS

The temperature and salinity data are displayed in three standard formats:

- (1) Temperature-Salinity (TS) Diagrams (Appendix D): Scatter plots of temperature and salinity were prepared for individual time periods, typically extending over a few days to three to four weeks. Data values were identified by seven different symbols, according to measurement location in the seven subregions (Figure 2) of the study area. Up to three different TS diagrams were generated for each period:
 - Temperature: -2 to 20°C, Salinity 0-30, which emphasized the large variability occurring in the upper layer;
 - Temperature: -2 to 8°C, Salinity 20-35, which illustrated variations in areas having a strong influence from colder, more saline Arctic Water;
 - Temperature: -2 to 0.5°C, Salinity 33-35, which portrayed variations at depth where the influence of warmer, more saline Atlantic Water is

evident. Note only comparatively accurate data sets were displayed on this high resolution TS diagram.

- (2) Contoured Maps of Temperature and Salinity (Appendix B): The spatial distribution of water properties within the study area was displayed through computer-generated contour maps, using the computer program CONMAP. CONMAP was originally developed by the Marine Environmental Data Service (Taylor, 1976); the version applied in this project was revised at the Institute of Ocean Sciences for easier portability among computers (Jorgenson, pers. com., 1987). The computer program selects all data available for the specified quantity and time of interest. It then averages these data onto a square grid, which measured approximately 17 km on each side in this study. Contours are generated with a finite difference smoothing algorithm, setting the parameter CAY = 10. For each group of quasi-synoptic data profiles, sequence of maps routinely generated. These maps are:

QUANTITY	CONTOUR INTERVAL
Temperature at 1 m depth	1.0°C
Temperature at 20 m depth	0.5°C
Temperature at 100 m depth	0.1°C
Salinity at 1 m depth	1 or 2
Salinity at 20 m depth	0.5
Salinity at 100 m depth	0.1
Temperature at Salinity = 31.00	0.5°C

The full suite of display maps was not generated for all data sets. For example, in some time periods, measurements were limited to comparatively shallow depths of less than 50 m. Other data sets were not sufficiently accurate to provide useable results for examination of distributions at larger depths (100 m), where the variation in oceanographic parameters is small in comparison to that of the surface layer.

- (3) Temperature and Salinity Distributions along Vertical Transects (Appendix E): Sets of three or more vertical profiles, oriented in a line directed offshore from the coast, were selected. The contouring program CONMAP was used to display the distribution of temperature and salinity from the surface to depths of 150 m. Based on empirical testing, the contouring grid was chosen to have a depth resolution of 9 m, with a spatial resolution of either 8 or 16 km. A moderate value for the smoothing parameter (CAY=10) was applied. The contouring parameters provided reasonably good results over the bulk of the water column, but features in and just beneath the surface layer, associated with strong vertical gradients, typically 3-7 m in depth, are often distorted due to the spatial filtering implicit in the contouring program.

2.6 DERIVED INTEGRAL QUANTITIES

For analysis purposes, two integral quantities were routinely computed from the temperature and salinity profile data:

- (1) Heat content was computed as:

$$H = \rho C_p \int (T - T_R) dz$$

where H is the heat content, expressed in units of J/m^2 ,

ρ = density of seawater, 1025 kg/m^3

C_p = specific heat of water, taken as $4,211 \text{ J/kg/C}$ (for temperature of 2°C)

T_R is a reference temperature, taken as -1.5°C

z is the depth in metres.

For this study, we chose 50 m as the depth limit, since this value approximates the limit of diabatic heating in summer, and the limit of convective heat losses in winter. The lower limit was taken as 1 m, to avoid contributions from large (and questionable) vertical gradients observed in the upper metre of the water column. Computation of heat content was limited to those sites where measurements extended to 3 m or more.

- (2) Freshwater content was computed as:

$$F = \frac{1}{S_R} \int (S_R - S) dz$$

where F is the volume per square meter of fresh water added to reference salinity (S_R), to produce the same average salinity as was observed. The reference salinity was chosen as 31, approximately midway in the seasonal range. The limits of integration are depths of 1 and 50 m. Computation is limited to profile data having measurements extending to depths of 3 m or greater.

Maps of heat and freshwater content are presented in Appendix E.

3 WIND, SEA-ICE AND RIVER DISCHARGE DATA

3.1 WIND DATA

As in most marine areas, surface winds are the most important driving force in influencing oceanographic conditions of the Beaufort Sea. Previous oceanographic studies of the area (eg. Cameron, 1953; MacNeill and Garrett, 1975; Tummers, 1980; Fissel, 1981; Fissel and Birch, 1984; Thomson et al., 1986; Fissel et al., 1987a; Fissel et al., 1987b) demonstrate that major wind events result in a pronounced redistribution of surface layer waters over large areas of the southeastern Beaufort Sea.

For this study, wind results were computed using geostrophic winds derived for Canadian marine areas, 1946-1987 (Swail, 1985). While geostrophic winds have some distinct limitations (Appendix F), their availability over four decades was the major reason in choosing this wind data set. The analytical methods applied to the wind data and detailed results are presented in Appendix F.

Over the 30 years (1950-1960, 1969-1987) of wind records analysed between July 1 and October 15, a total of 342 individual wind events were identified, amounting to an average of 11 wind events each year (Appendix F). The directional distribution of these wind events (Figure 4) reveals a bimodal wind regime with the dominant directions being east-southeast winds (49%) and west-northwest winds (28%). The duration of wind events within the two dominant directional categories differs considerably: east-southeasterly winds tend to occur over longer periods (53% exceeding seven days) than west-northwesterly winds (25% exceeding seven days). Note that wind 'events' as defined in this study (Appendix F) can contain two, or even three, distinct periods of enhanced wind activity. Combined wind events are counted as one, as long as the winds continue to blow from the same general direction. Successive periods of easterly winds tend to occur more frequently than those originating from the west.

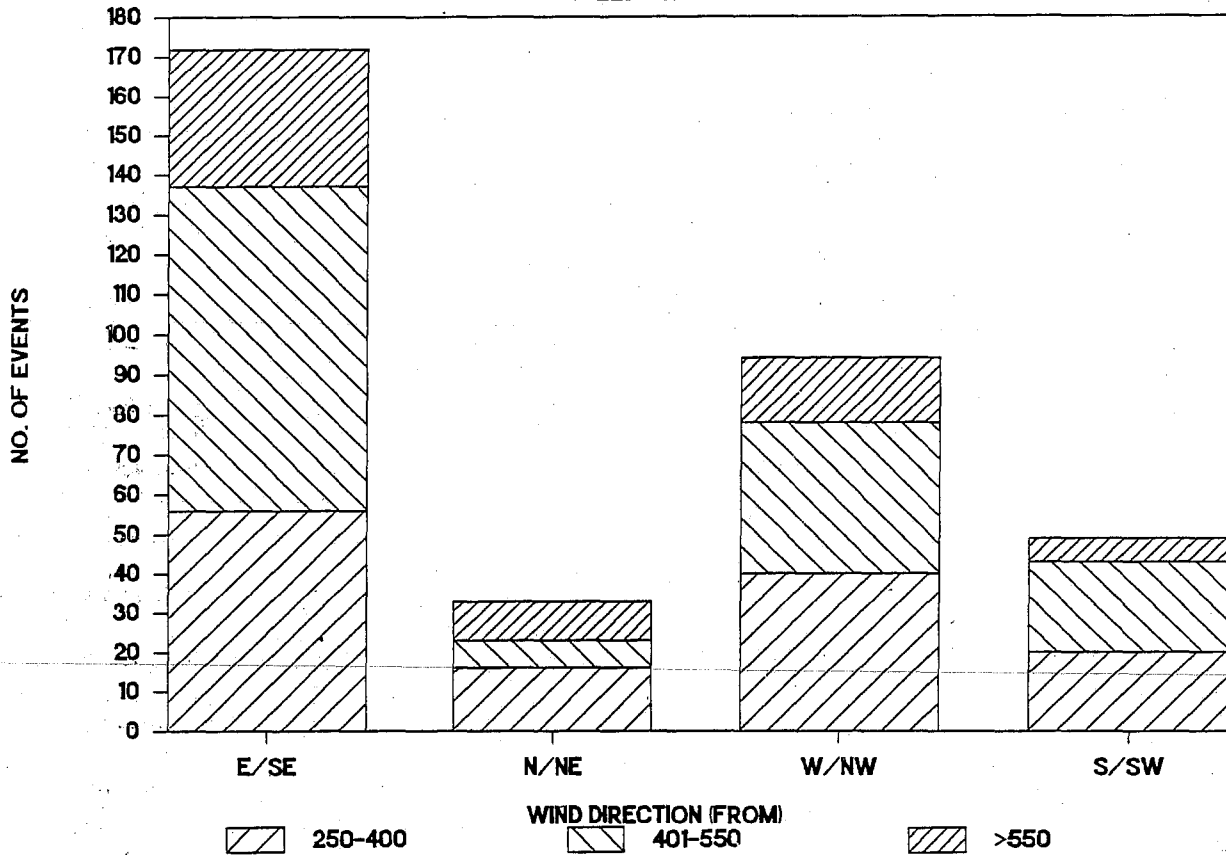
The mean velocity of west-northwest wind events also tended to be smaller in magnitude: for example, only 33% of easterly winds had mean geostrophic wind velocities less than 400 km/d, while 43% of westerly wind events were in the lower wind magnitude category. Conversely, of the 36 wind events having the largest mean velocity magnitude (>650 km/d or 7.5 m/s), one-half (18) blew from the east-southeast quadrant, while only 12 were from the west-northwest quadrant, with the remaining five being from the north-northeast sector, and one from the south sector. However, the frequency of strong west-northwesterly winds may be somewhat greater than the statistics derived from geostrophic winds would indicate. As noted in Appendix F, westerly winds associated with rapidly moving cyclonic disturbances occasionally occur over short periods (two days or less). The magnitude of short duration wind events will be significantly attenuated with the analytical methods of this study.

3.2 SEA-ICE DATA

Maps of sea-ice concentrations were prepared for selected dates in the months from July to October. The selected dates varied from year to year, according to the availability of sea-ice data, and the amount of oceanographic data coverage. To the extent that the sea-ice information permitted, at least one map of sea-ice was prepared for each summer month in which oceanographic data were

MEAN SPEED OF WIND EVENTS

SPEEDS IN KM/D



DURATION OF WIND EVENTS

DURATIONS IN DAYS (D)

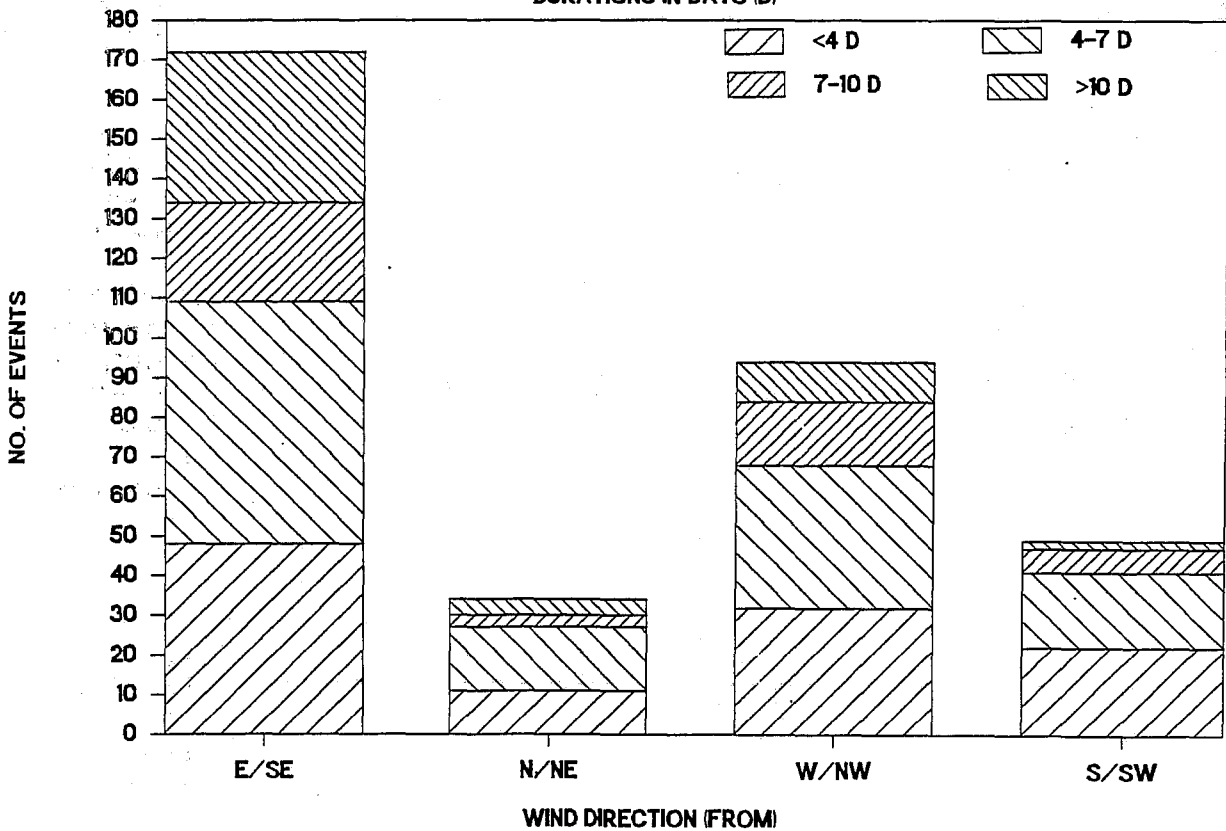


Figure 4: The distribution of the speeds and durations of wind events by direction (1950-1987).

assembled for this study. Particular emphasis was placed on providing sea-ice maps in the early summer (July 1-20). These ice charts were needed to examine the effects of sea-ice extent immediately following break-up of landfast ice on oceanographic conditions through the remainder of the summer.

Information on sea-ice was very sparse in the early 1950's. From 1950 to 1953, the only source of information was the Ice Atlas of Swithenback (1960). Unfortunately, observations available for the southeastern Beaufort Sea were virtually non-existent until the latter part of the summer (from mid-August). In 1951 and 1952, the sparse information from the Ice Atlas was supplemented by descriptions of sea-ice conditions obtained from the M.V. Cancolim as part of the oceanographic surveys of Cameron (1953).

For the years 1954 to 1960, information on sea-ice concentrations was available from charts prepared by the United States Air Force and Navy (to 1958) and from ice maps of the Canadian Ice Branch (1959 to 1963). These ice charts were a marked improvement over the information of the early 1950's, but spatial coverage was still somewhat limited, particularly further from shore beyond the coastal shipping routes. In particular, the ice charts of 1959 and 1960 lacked observations over extensive portions of the continental shelf and slope.

From 1964 to 1973, sea-ice information was available from reports titled "Ice Summary and Analysis for the Canadian Arctic", an annual publication of the Ice Branch of Environment Canada. These reports were excellent in terms of areal coverage on bi-weekly ice charts, reflecting the increased level of the aircraft, and later - satellite ice reconnaissance data collection. The reports also included weather maps and other meteorological data.

Since 1971, weekly ice charts have been issued once each week for the Canadian Western Arctic by Ice Branch of Environment Canada. Selected ice charts from this series of maps were used for this study during the period 1974 to 1987.

The sea-ice maps prepared for this study (Appendix G) made use of a simplified scale for ice concentrations, in order to reduce the space required to display the maps. Ice concentrations are represented by a four level scale, which varies somewhat according to data sources:

CATEGORY		YEARS	
		1950-1962	1963-1987
O	open water		
A	ice concentration of	1-4 tenths	1-3 tenths
B	ice concentrations of	5-7 tenths	4-6 tenths
C	ice concentrations of	8-10 tenths	7-10 tenths

An example of the format used to display sea-ice data is provided in Figure 5, showing the minimum (1977) and maximum (1974) sea-ice conditions experienced in mid-summer. The complete set of ice charts for the 28 years considered in this study (1950-1960; 1969-1987) are presented in Appendix G.

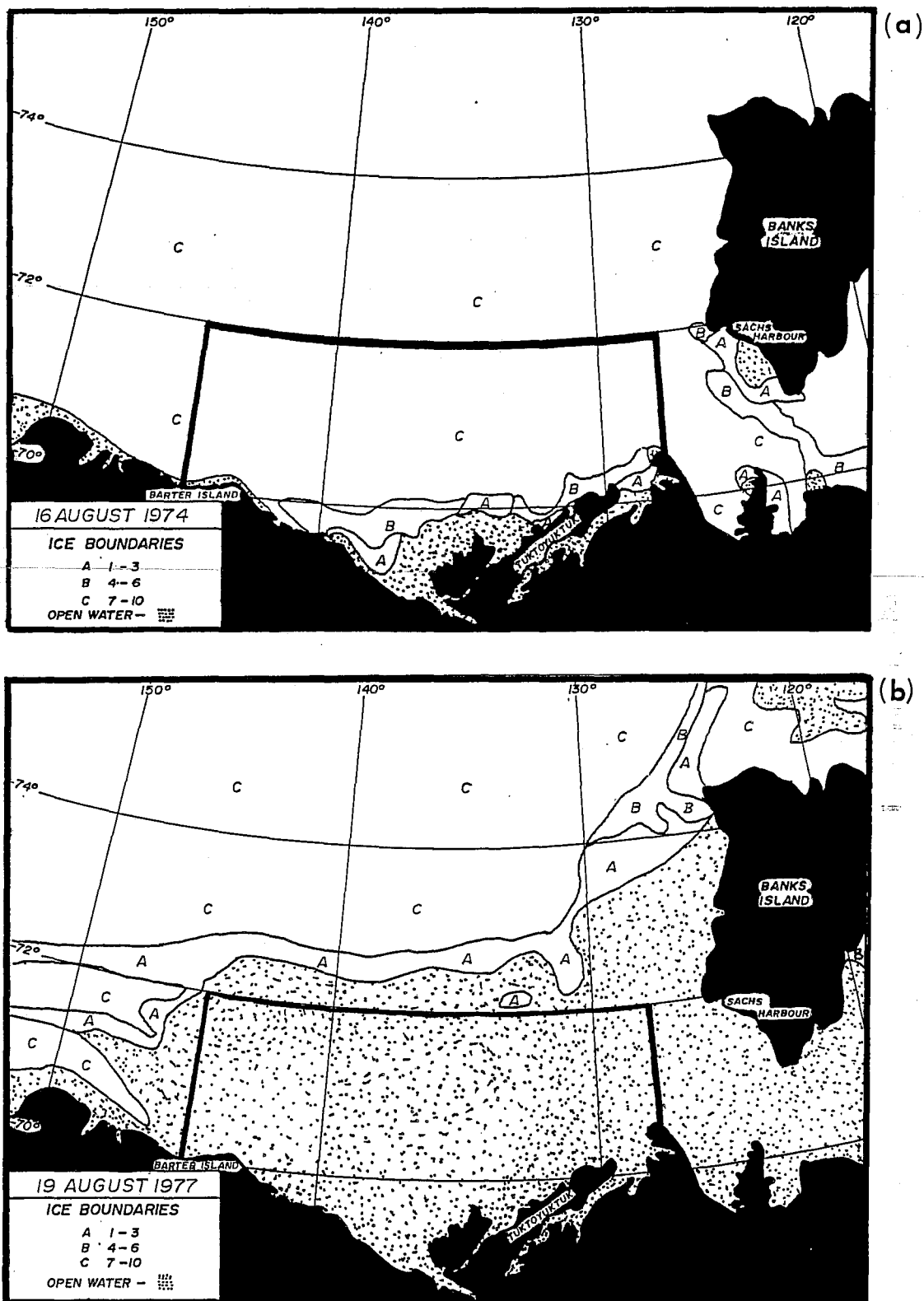


Figure 5: An example of the display of sea-ice concentrations for mid-July of (a) 1974, having the maximum sea-ice concentration; and (b) 1977, having the minimum sea-ice concentration. Also shown are the two separate areas ('continental shelf' and 'full area') in which the areas of open water and ice concentrations \leq seven-tenths were computed.

3.3 RIVER DISCHARGE DATA

Volume discharge measurements of the rivers draining into the Beaufort Sea were obtained only sporadically until the latter half of the 1960's, when continuous monitoring was initiated at selected gauging locations. For this study, we used river gauge data to 1988 on selected major rivers whose discharges enter the Beaufort Sea. The river run-off into the Southeastern Beaufort Sea is dominated by the very large volume discharge entering through the Mackenzie River Delta (Figure 6). The total Mackenzie River discharge can be accounted for almost entirely by the sum of three gauging sites: Mackenzie River above Arctic Red River (annual volume of $28.71 \times 10^9 \text{ m}^3$), Arctic Red River ($0.49 \times 10^9 \text{ m}^3$) and Peel River ($2.36 \times 10^9 \text{ m}^3$). In addition, land run-off enters the Beaufort Sea from the Yukon Coastline and to the east of the Mackenzie Delta through the Eskimo Lakes and Liverpool Bay. The Yukon coast land run-off was computed as $0.22 \times 10^9 \text{ m}^3$ as derived from the measured discharges of the two largest rivers, the First ($0.13 \times 10^9 \text{ m}^3$) and Babbage Rivers ($0.03 \times 10^9 \text{ m}^3$), which were scaled up according to the total drainage area. For the area east of the Mackenzie Delta, the total volume discharges is estimated as $0.90 \times 10^9 \text{ m}^3$, which was computed from the measured discharges of the Anderson River ($0.47 \times 10^9 \text{ m}^3$) as scaled up for total drainage area.

For the dominant (88%) Mackenzie River discharge entering the Mackenzie Delta from above Arctic Red River, we have chosen to use river gauge data from three sites. The primary site, Mackenzie River at Arctic Red River, is situated approximately 190 km from the river mouth and is upstream of the large delta region (Figure 6). Measurements from Mackenzie River at Arctic Red River, were available only for fourteen years: 1973 to 1984 and 1986-1987. To provide a measure of river discharge for a longer period, the measurements at Norman Wells (available from 1969 onwards) were also used. Norman Wells is situated approximately 550 km upstream of Arctic Red River. Based on comparisons using 1987 measurements, an empirical method was devised to estimate the flow at Arctic Red River (F_{ARR}) from the Norman Wells data (F_{NW}):

$$\begin{aligned} (F_{ARR})(T) &= 1.10 (F_{NW}) (T - 4) \text{ in May and June;} \\ (F_{ARR})(T) &= 1.05 (F_{NW}) (T - 4) \text{ in July and August;} \end{aligned}$$

where T is the time in days. Comparisons in two other years of simultaneous data collection indicate that this method is accurate to within 5%.

Plots of river discharge volumes from 1972 to 1986 inclusive, are presented in Appendix H.

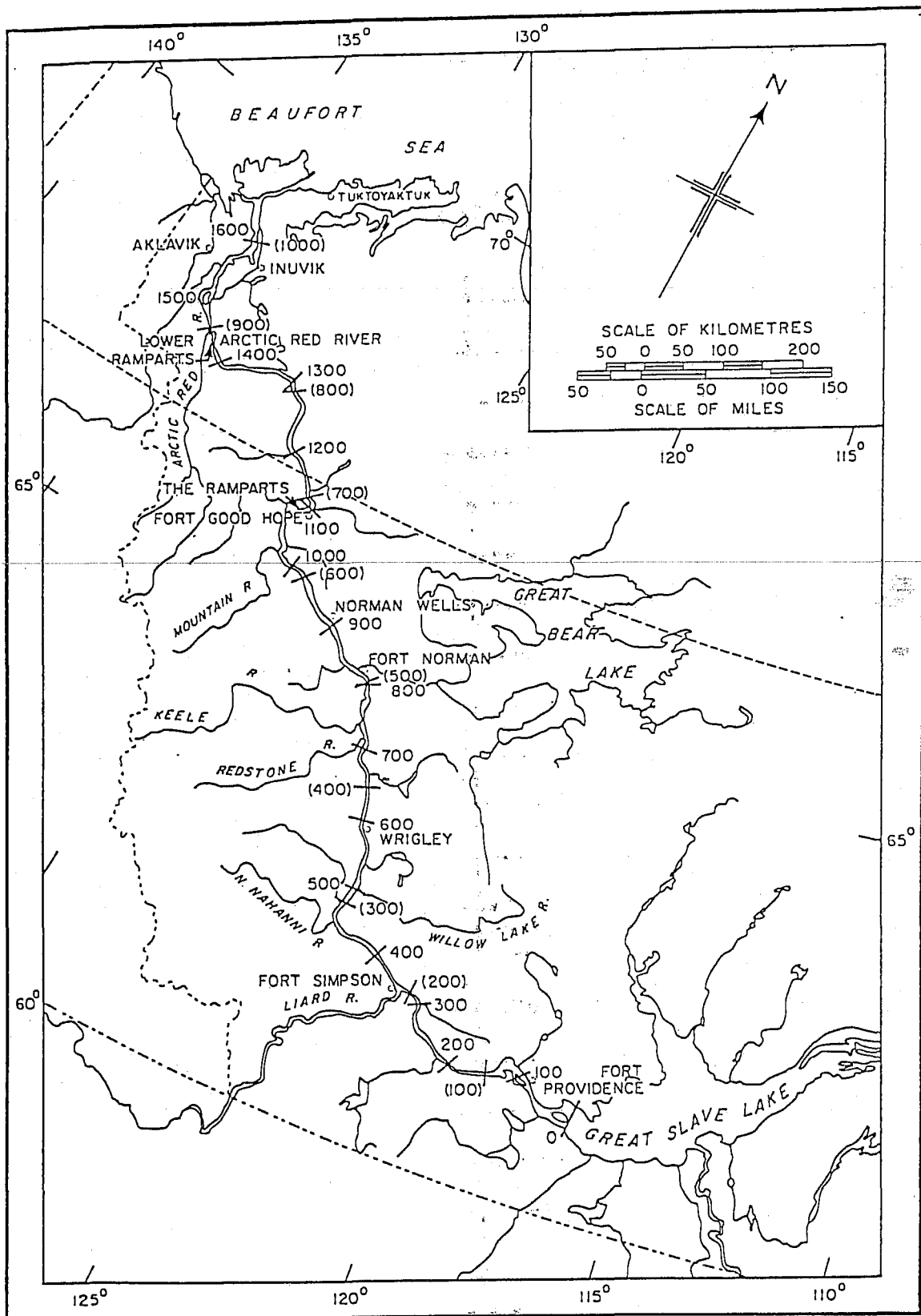


Figure 6: A map of the Mackenzie River drainage area. Note the river gauging sites at Arctic Red River, Inuvik and Norman Wells from which data were used in this study. The number along the Mackenzie River designate the distance from the head waters (in Great Slave Lake) in kilometers (and in miles).

4 RESULTS

4.1 INTERANNUAL VARIATIONS OF OCEANOGRAPHIC CONDITIONS

The year-to-year variations in oceanographic conditions during summer are displayed in the following figures:

- Fig. 7: temperature at 1 m;
- Fig. 8: salinity at 1 m;
- Fig. 9: heat integral over the upper 50 m of the water column;
- Fig. 10: freshwater integral over the upper 50 m of the water column

Estimates of these five oceanographic parameters were computed as means for five sub-regions of the study area described in Table 1 and shown as an inset map on Figures 7 to 10. The quantities were also computed for each of the three summer months, July, August and September. Some flexibility was permitted in assigning data sets to particular months: for example a data set spanning the period July 29 to August 11 would be assigned to the month of August even though the first three days of measurements were collected in July.

TABLE 1
Information for each of the five subregions used in computing
monthly mean values of oceanographic parameters

Region	Area (sq.km)	Approximate Depths (m)		
		Minimum	Median	Maximum
Mackenzie Bay/ Yukon Coast	6,200	0	25	100
Nearshore (Mackenzie Shelf)	14,300	0	10	25
Middle and Outer Shelf	41,400	15	50	300
Sub-total (Continental Shelf)	61,900			
Continental Slope	69,600	50	700	2,500
Amundsen Gulf (western entrance)	28,600	0	300	500

The year-to-year variations in oceanographic conditions during early spring are presented in Figure 11. The results were computed from any data collected in March and April, prior to the onset of the Mackenzie River freshet. Because of the few available data sets for this time of year, estimates were not derived for Amundsen Gulf or the Mackenzie Bay/Yukon sub-regions. No estimates were derived for the nearshore portion of the Mackenzie Shelf due to highly variable sampling within this region in terms of the relative proportion of measurements situated within, and outside of, the freshwater river plume water (situated beneath the sea-ice at this time of year).

The monthly mean values, represented as individual bars in Figures 7 to 11, were derived from sample sizes ranging from 1 to 51. Given the sparseness of the available data, caution must be applied in the interpretation of the results. As a guide to the reader, the results are coded in three categories. Monthly

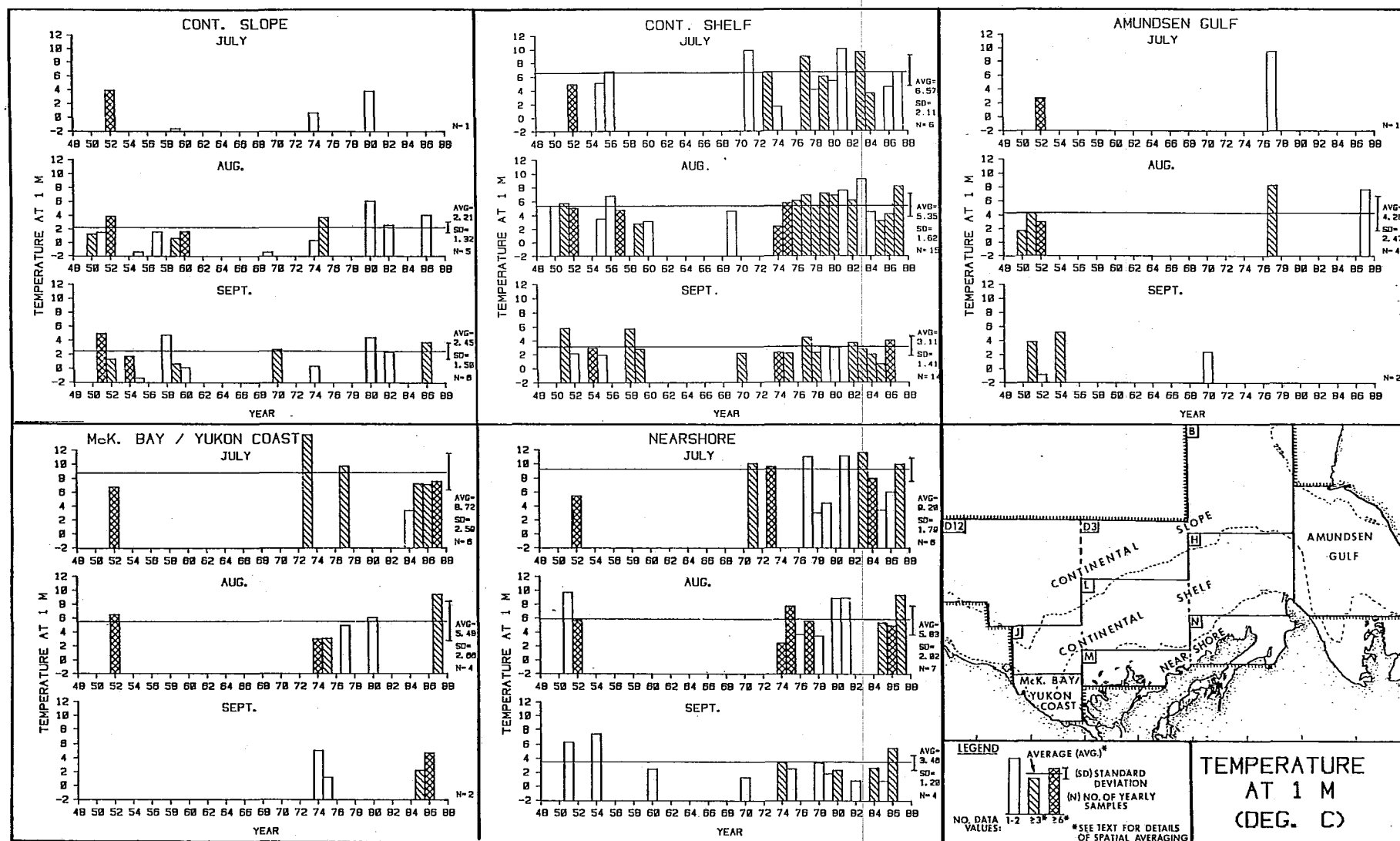


Figure 7: The monthly mean values of temperature at 1 m depth during July, August and September of each year in which data were available.

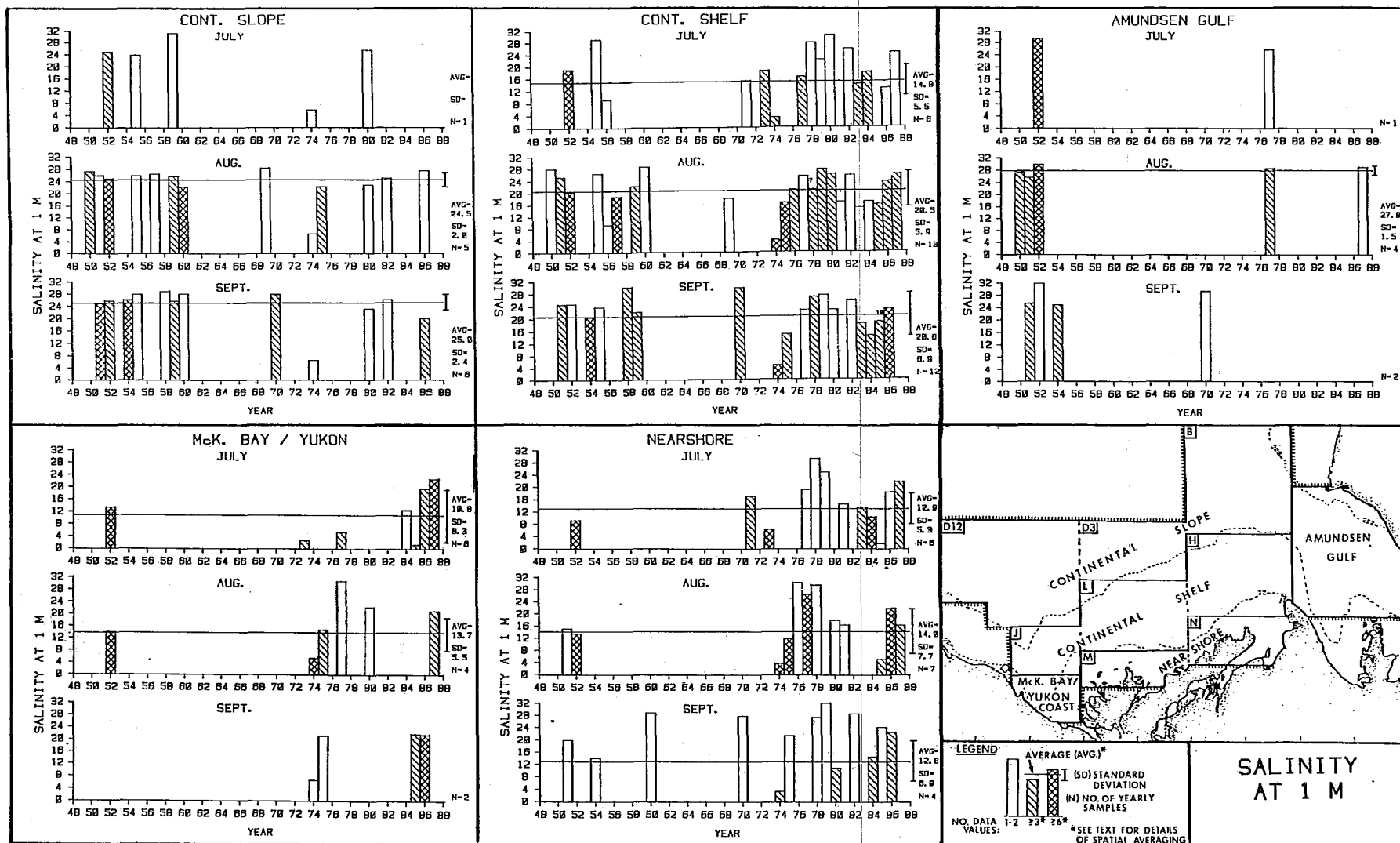


Figure 8: The monthly mean values of salinity at 1 m depth during July, August and September of each year in which data were available.

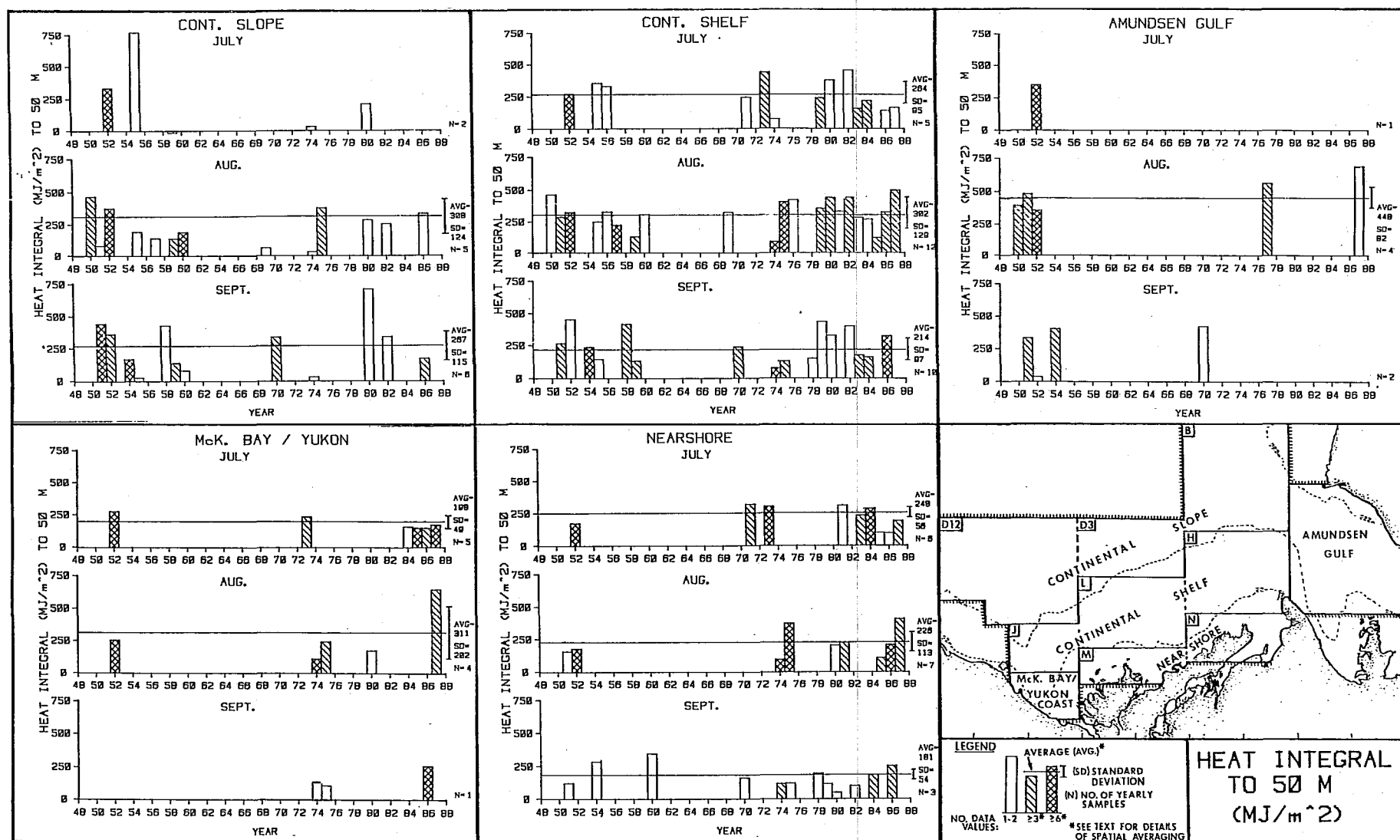


Figure 9: The monthly mean values of heat integral over the uppermost 50 m during July, August and September of each year in which data were available.

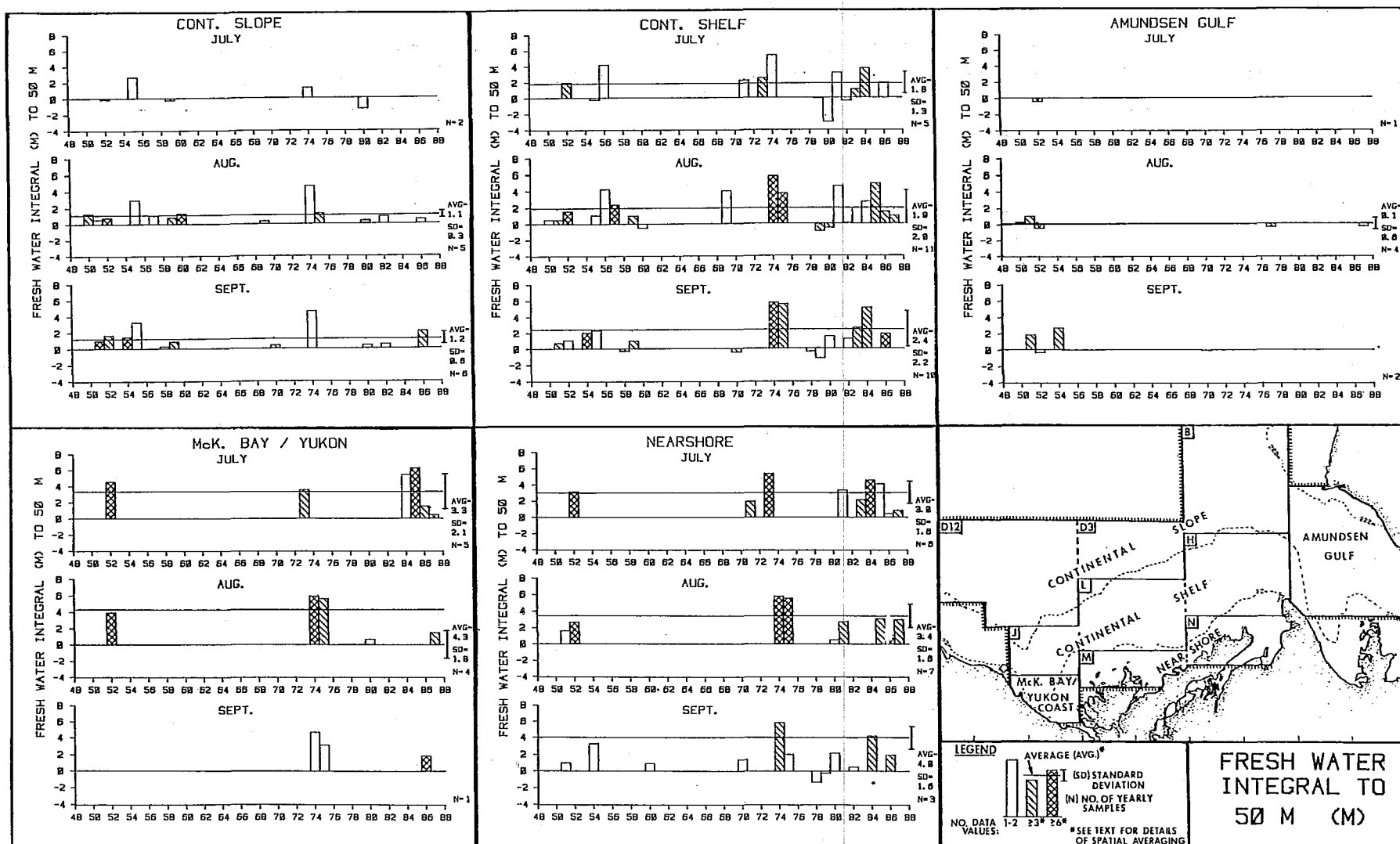


Figure 10: The monthly mean values of freshwater integral over the uppermost 50 m during July, August and September of each year in which data were available.

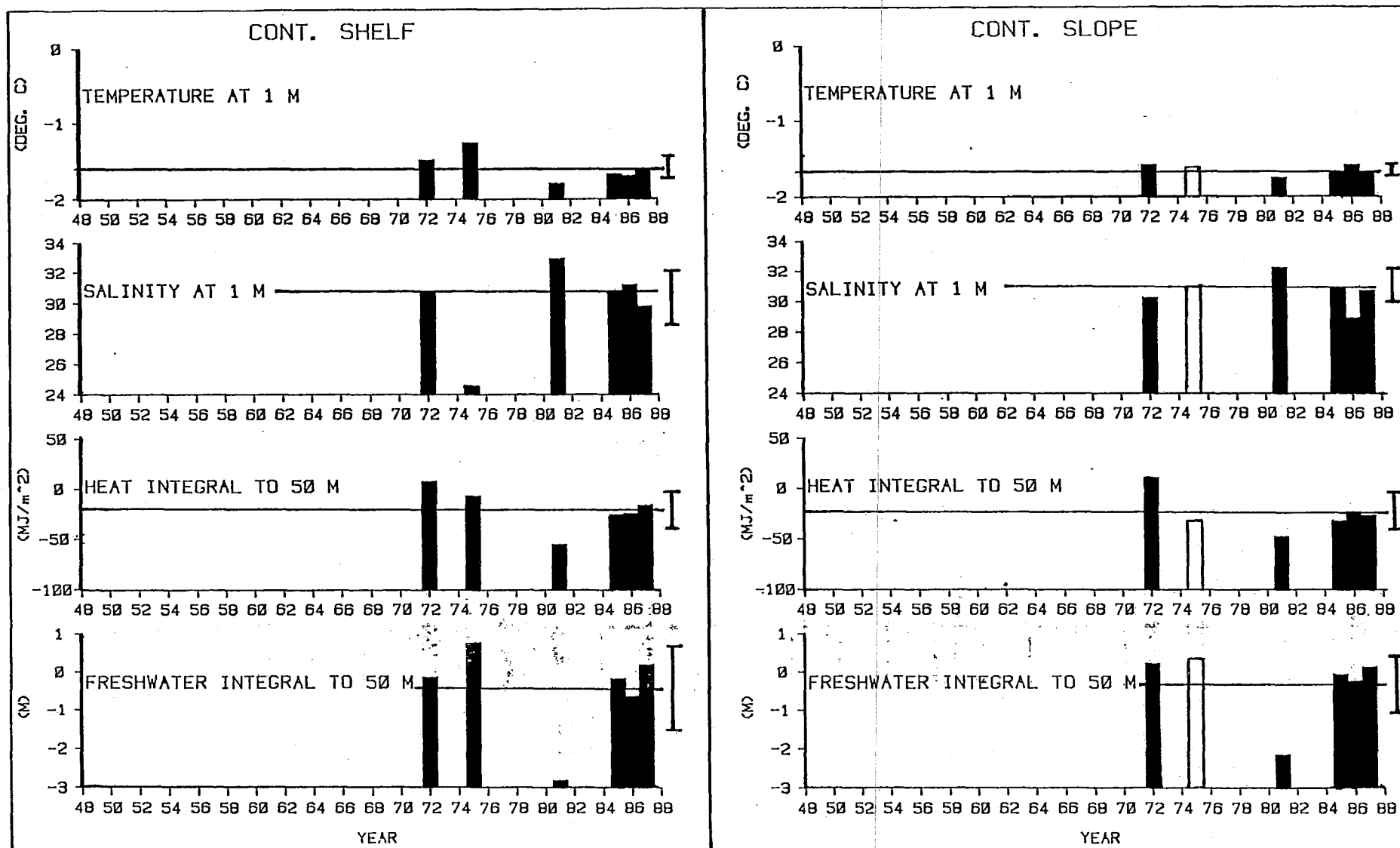


Figure 11: The monthly mean values of: temperature at 1 m; salinity at 1 m; heat integral: freshwater integral; for the March-April period of each year in which data were available. The results are displayed individually for the continental shelf and slope subregions.

estimates derived from only 1-2 samples are displayed as open bars. The most reliable monthly estimates, shown as double hatched bars, were computed from at least six data samples, with a minimum of two samples available in each sub-area (the continental shelf and slope regions are subdivided into three sub-areas, while the nearshore region has two sub-areas). An intermediate category is also used, displayed as single hatched bars; for this category, at least three data samples are required with a minimum of one sample available for two sub-areas, unless a total of six or more samples were obtained. In addition to the conditions listed above, estimates for sub-areas were not included if the data sampling locations were considered to be unrepresentative of the full sub-area. Note that even the monthly mean values shown as double-hatched bars may be based on as few as six samples, with the result that these computed values may not be fully representative of mean conditions over the large spatial and time scales of the derived quantities.

The number of monthly mean values available varied enormously with month and region. Over the period considered in this study (1950-1961; 1969-1988), the continental shelf subregion had the largest number of samples with 16 yearly estimates of temperature available for the month of August and 14 for September. Intermediate quantities of samples (12 - 16) were available for the continental shelf in July, the nearshore region (July to Sept.) and for the continental slope (August and September only). Fewer than 7 samples were available for: Mackenzie Bay/Yukon coastline, continental slope in July, the March-April period for all subregions, and Amundsen Gulf. Note that the quantities of samples given above are for temperature only; fewer samples are available for other quantities.

Long Term Means - Seasonal Variations

Long-term mean values were estimated for each month and region. In order to improve the reliability of the computed long-term mean, the least reliable monthly estimates (open bars) were not used in computing the long-term mean values. The long-term mean values are shown on Figures 7 to 11 as: solid lines when derived from six or more yearly estimates; or as dashed lines when derived from three to five estimates.

Surface Temperature and Salinity - Over the continental shelf (including the shallower inshore regions designated as Mackenzie Bay/Yukon and Nearshore), a generally consistent pattern of seasonal temperature variation is evident. Surface temperatures increase from near-freezing levels in March/April to maximum annual levels in July. The mean water temperatures are much warmer in inshore areas (9°C), than is the case over the middle and outer continental shelf (6.5°C) (Figure 12). By August, the mean surface temperatures are nearly identical throughout the complete shelf region (5.5°C), and they decrease further by September (3 to 3.5°C).

Temperatures in the continental slope zone are consistently lower through July and August, due presumably to its closer proximity to the Arctic Ocean ice pack. However, surface temperatures in Amundsen Gulf, available for the month of August, are larger and seem to be reasonably consistent with those measured on the eastern continental shelf (subregion H).

Surface salinity in shelf areas follows a somewhat different pattern from that of temperature during the summer months. In July, surface salinities attain

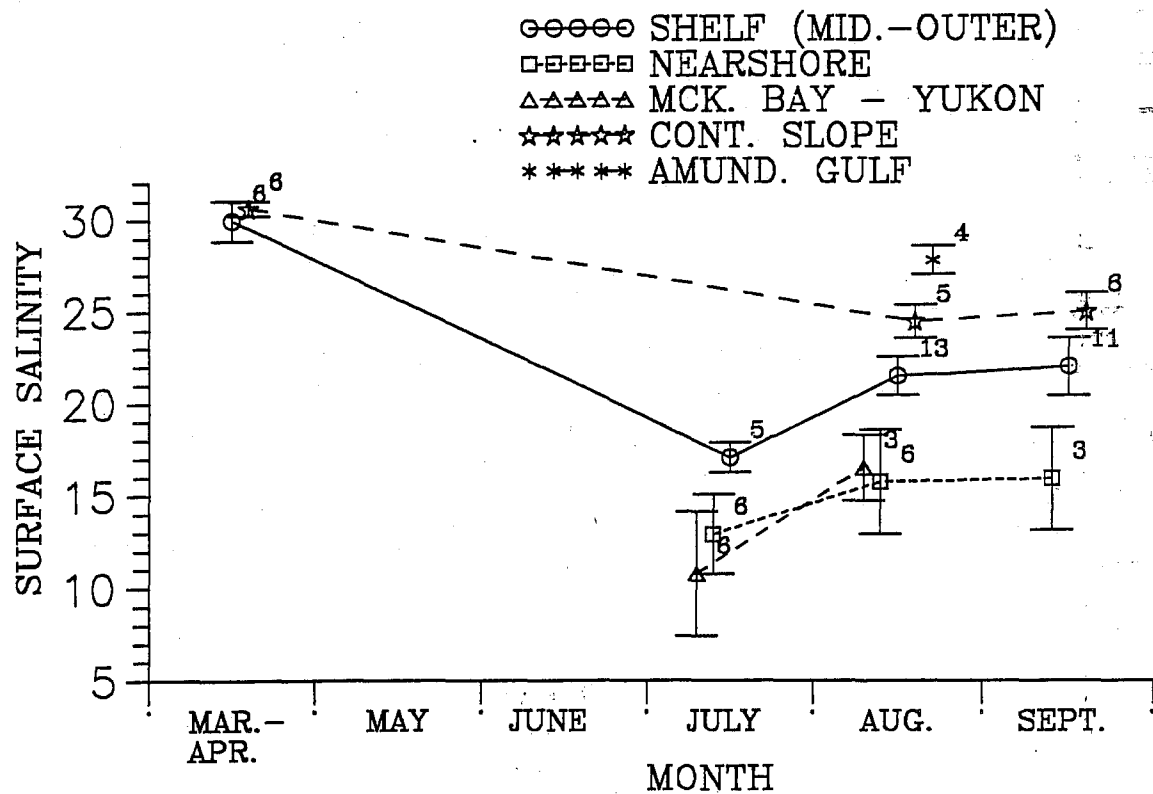
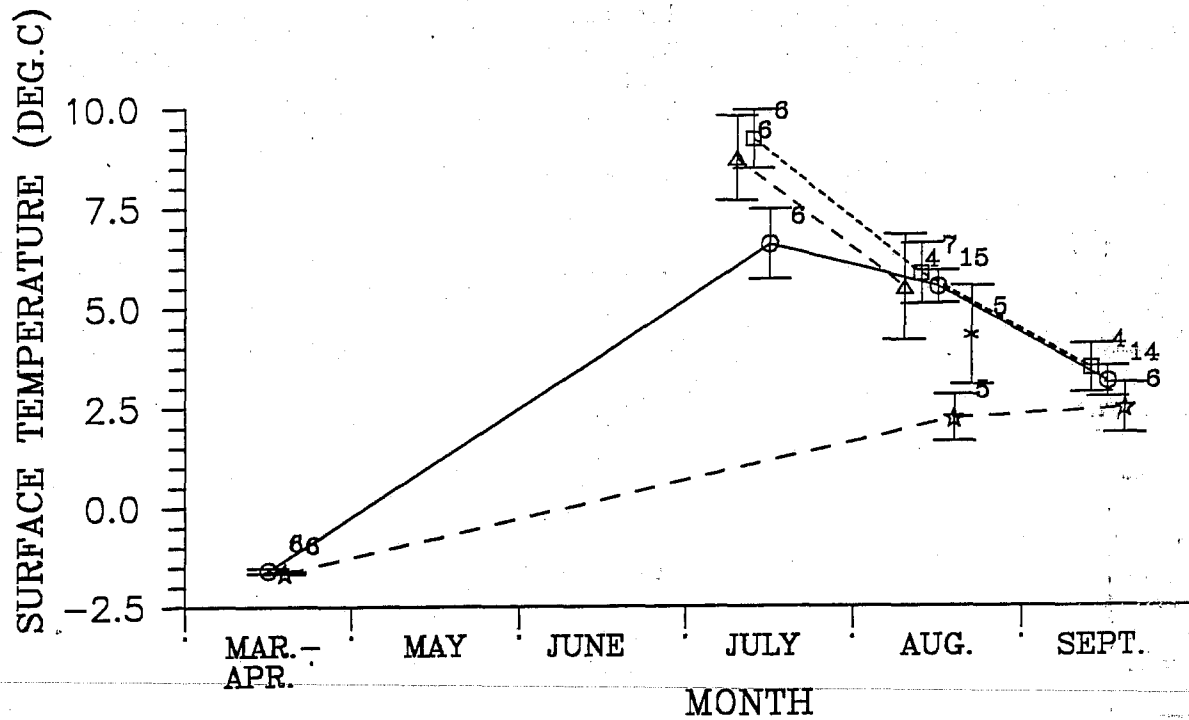


Figure 12: The mean monthly temperature and salinity values (at 1 m depth) averaged from those years where the available data are of the highest or intermediate reliability category (see text).

their lowest mean value of the year, greatly decreasing from the March- April level (>30) to 17 on the mid- and outer-shelf, and to even lower levels of 11 to 13 for the inner shelf. From July to August, surface salinities increase by approximately 3 to 4 in all parts of the continental shelf, followed by a much smaller increase (<1) from August to September. Note that summer salinity values for 1974 were excluded in computing the mean surface salinity because the very low values measured in this year significantly bias the computed means for those regions and summer months which include 1974 data. The extreme oceanographic conditions encountered in 1974 are discussed in more detail below in "Unusual and Extreme Occurrences".

The changes in surface salinity over the summer months differ from those of temperature in two key respects: (1) surface temperatures decrease throughout the summer, while surface salinities change little in the latter part of the summer as compared to the early summer; and (2) surface temperatures become more uniform in all regions by September, while surface salinities maintain distinct differences in September (reduced in inshore areas [16], as compared to the mid- and outer-shelf [22]). The above- mentioned spatial differences in surface salinity extend beyond the continental shelf: higher mean salinities (25) were computed over the continental slope (August to September) and even larger levels (28) occurred in Amundsen Gulf (data available from August only).

Heat and Freshwater Content (Upper 50 m) - The seasonal variations in the long-term mean heat and freshwater integral to 50 m depth (Figure 13) follow a similar pattern to that of surface temperature and salinity, although there are differences in the early summer period. From July to August, both integral quantities either remain constant or increase slightly. This pattern is in sharp contrast to surface temperature (and salinity) which decreased (increased) over the same period. (Recall that freshwater content varies in the opposite sense from salinity.)

Another interesting difference between surface and integral quantities occurs in the July heat content: in the inshore areas, the heat content is lower than that of the mid- to outer-continental shelf zone, while the surface temperatures were markedly higher in the inshore areas. This difference between heat content and surface temperature is due, at least in part, to the depths of the inshore areas being limited to 20 m or less, representing less than half of the 50 m integral depth limit used in computing heat content. Interestingly, the relative magnitude of freshwater content values is more consistent with surface salinity between the inshore and shelf areas. The better agreement between surface and integral salinity quantities, as compared to temperature, suggest that the relative contributions to the freshwater content (or negative salinity integral) from deeper waters exceeding 20 m are less important than is the case of temperature. Supporting evidence for this argument can be found in the presence of temperatures well in excess of the temperature integral reference level (-1.5°C) at the salinity integral reference level (31), as shown in Figure 14 for the years 1975 and 1986.

The seasonal patterns in the surface and integral quantities of temperature and salinity indicate important differences in the manner in which these quantities change over the summer. Temperatures in the upper water column have the following characteristics: (1) they attain maximum levels in July; (2) they are reasonably consistent over all parts of the continental shelf, and (3) they

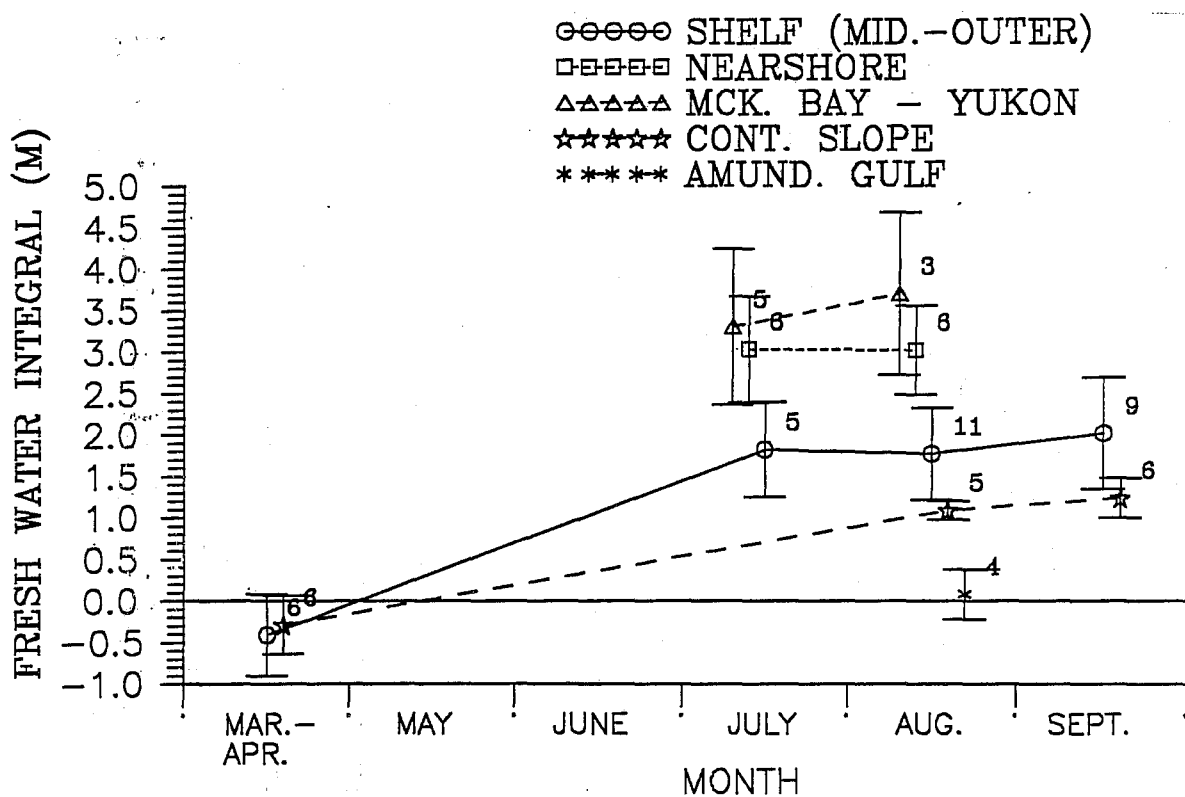
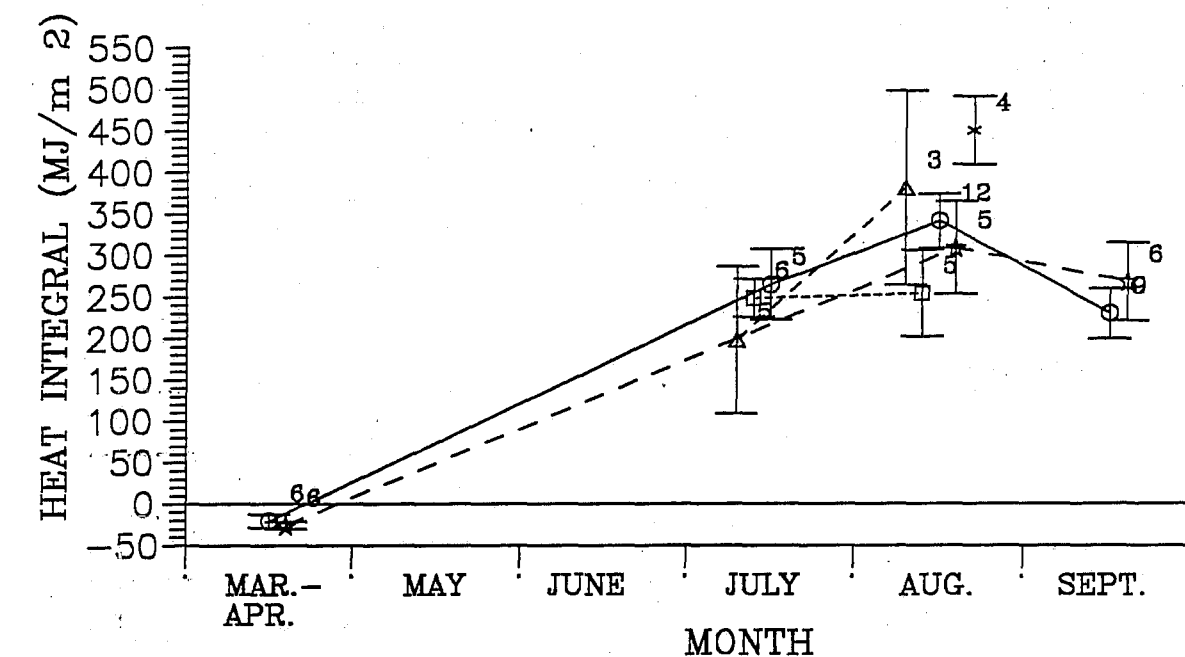


Figure 13: The mean monthly heat and freshwater integrals (over the uppermost 50 m) averaged from those years where the available data are of the highest or intermediate reliability category (see text).

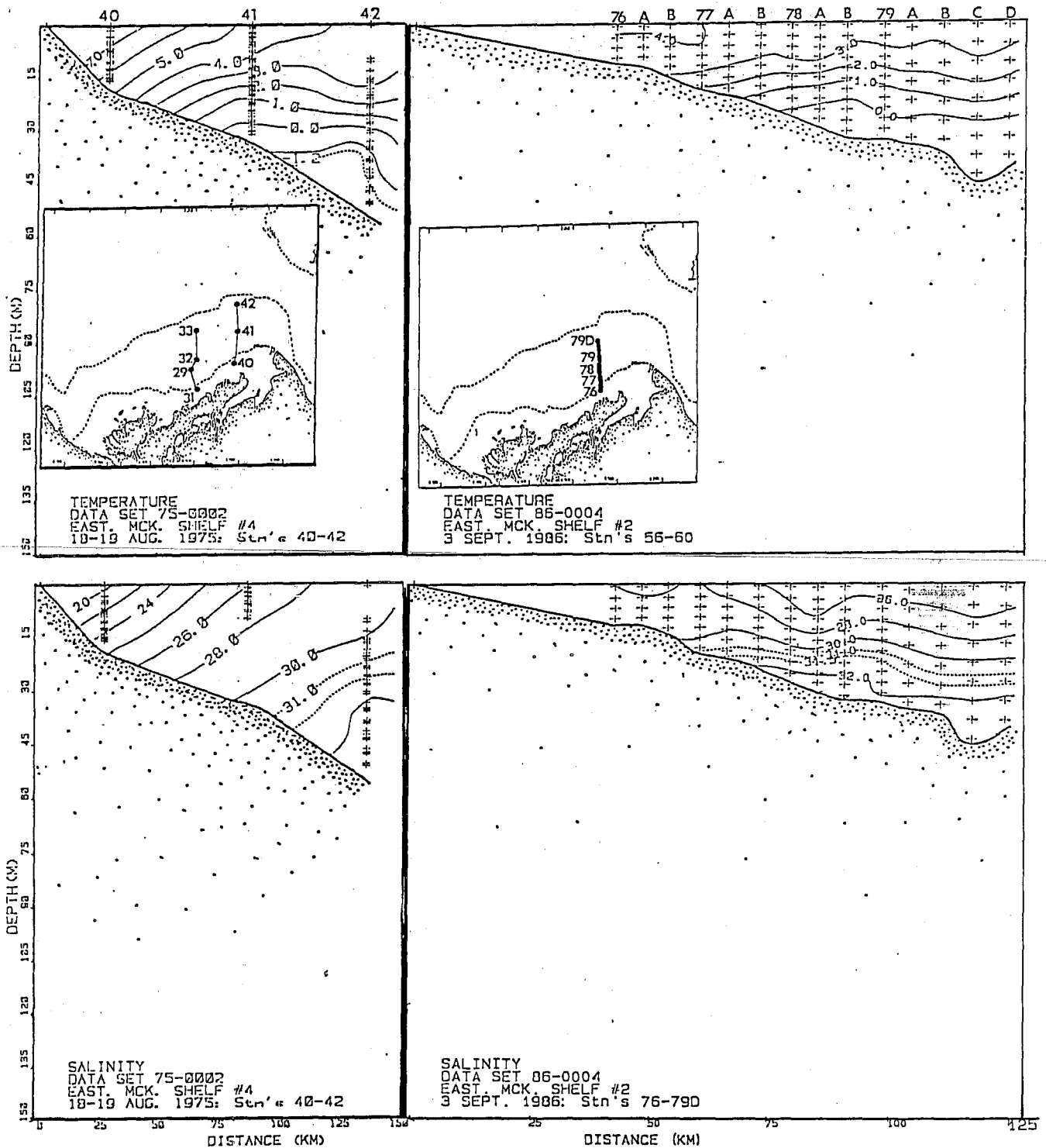


Figure 14: Two examples of vertical cross-sections of temperature and salinity (1975 and 1986) which reveal that at depths exceeding 25-30 m, contributions to the heat integral are positive, while contributions to the freshwater integral are small or negative.

decrease substantially in the late summer (August to September). These observations are consistent with the hypothesis that surface heat gained from the atmosphere controls the temperature and heat content of the upper water column (Tummers, 1980).

Salinity follows different patterns during the summer months: (1) although surface salinities attain their minimum levels in July, the integral quantity over the upper 50 m of the water column appears to change little throughout the whole summer; (2) salinities exhibit large spatial differences, increasing from coastal areas to the offshore regions (continental slope) and to the east (Amundsen Gulf); these spatial differences persist throughout the summer; (3) salinities decrease very little in the latter part of the summer, in sharp contrast to the substantial decrease in temperature during this period. The variations in long-term mean salinity over the summer months described above are consistent with reduced salinities in summer (as compared to winter and spring) due to a combination of the melting of the seasonal sea-ice cover and the large freshwater discharge from the Mackenzie River, beginning with the May/June freshet. The larger freshwater content in inshore regions is consistent with the influence of the Mackenzie discharge. The absence of a substantial salinity change during the summer months suggests that losses of freshwater, either through vertical exchanges at the surface or horizontal advection, is comparatively small during the summer.

A more comprehensive analysis of the temperature and salinity content of the upper water column is presented in Section 4.3 - "Heat and Freshwater Budget Considerations".

Extreme and Unusual Conditions - Using the individual monthly mean temperature and salinities, judged to be spatially representative (dashed bars in Figures 7 to 10), those years having unusually high or low values were examined. From those 25 years within the period 1950 to 1987 having at least some spatially representative measurements, several years emerge as having unusual temperature or salinity levels in some or all parts of the study area.

The most extreme event of the oceanographic record occurred in the summer of 1974. Surface temperature, surface salinity and heat content values attained record low levels ($2.4-2.9^{\circ}\text{C}$; $3.6-5.6$ [salinity]; $90-105 \text{ MJ/m}^2$) for August in the continental shelf, nearshore and Mackenzie Bay/Yukon zones, while freshwater content values attained their highest recorded levels ($5.7-5.9 \text{ m}$). The extreme oceanographic conditions of 1974 resulted from the worst summer ice conditions observed over the last 40 years: heavy Arctic Ocean pack-ice was situated over the continental shelf within 40 km of the coastline throughout July and most of August. Due to heavy sea-ice, the Mackenzie River plume was largely confined in a concentrated form to the limited area of open water, resulting in low salinity and large freshwater content. The low surface temperatures and heat contents experienced in 1974 resulted from much reduced levels of solar insolation in spring and summer due to the very limited area of open water (Tummers, 1980). This condition resulted in very little heat available to melt sea-ice on the continental shelf, which in combination with below normal easterly winds in August, led to a prolonged occurrence of sea-ice. The sea-ice cleared only in late August and early September, due to strong easterly winds.

In three other years, 1958, 1985 and 1987, oceanographic quantities were consistently at or near record levels:

- 1958: Very high temperatures accompanied by very high salinities occurred over the continental shelf during September. In all four parameters (temperature, heat content, salinity and freshwater content) the values were at or near record levels for September. (Unfortunately, no data are available during July or August of 1958.)
- 1985: Low temperatures and salinities occurred in the summer of 1985 over all portions of the continental shelf. These conditions persisted through to September, when the surface temperature reached the lowest levels recorded for the middle to outer portions of the continental shelf.
- 1987: Unusually high temperatures and high salinities prevailed through July and August (no observations were available for September). Record high levels of temperature and heat content occurred in August, 1987 for the nearshore and offshore portions of the Mackenzie Shelf.

Other years had unusually small or large values that were somewhat less extreme than 1958, 1974 1985 and 1987. These years include:

- 1951: High temperatures for the continental shelf and slope during September.
- 1959: Temperatures were unusually low during both August and September for the continental shelf and slope regions.
- 1970: Salinities were unusually high during September for both continental shelf and slope regions, and were comparable to the record levels of 1958. However, temperatures were near normal levels.
- 1975: Unusually low salinities occurred over the mid to outer shelf in both August and September. Temperatures were at near-normal levels, although low heat contents were measured on the continental shelf in September, in contrast to comparatively warm conditions in the nearshore experienced in August.
- 1984: Low surface salinities, and correspondingly high freshwater contents, characterized 1984 in the near, mid and outer continental shelf areas. Temperatures were below normal, but did not approach record levels.
- 1986: Unusually high temperatures and salinities occurred in August, and particularly in September, but the high values were largely confined to the nearshore portion of the continental shelf.

Interannual-Variability - A complete description of the year-to-year variability in oceanographic conditions in the summer months is made difficult by the absence of data for a substantial number of years during the period of interest, 1950-1987. In particular, there were no adequate data available in any region or month over the eight year period, 1961-1968. Nevertheless, some features of the interannual variability can be inferred for areas of comparatively intensive sampling, particularly: 1950-1960 for the continental

slope and shelf region; and 1972-1987 for the continental shelf and inshore regions.

Of the oceanographic quantities examined, surface layer salinities appear to exhibit the largest levels of interannual variability. Over the period 1974-1987, the surface salinity on the continental shelf shows some indication of an eight to nine year cycle.

Salinities were below average in 1974-1975, and again in 1983-1985, while generally above-average salinities occurred in 1977-1980 and again in 1986-1987. Salinities were also above average on the continental shelf in September 1970, but the available data are too limited for the period 1969-1972 to determine whether summer salinities were generally elevated during these years. In the 1950's, year-to-year patterns in summer surface salinities are more difficult to discern. There is some evidence that surface salinities reached above-normal levels during the period 1950 to 1952, and again during 1958 to 1959. The occurrence of maximum salinities appears to follow a roughly regular cycle with a periodicity of approximately 8 to 12 years. The amplitude of the interannual salinity variations is approximately ± 5 , representing about $\pm 25\%$ of the long-term mean values.

Surface salinities in the shallower waters of the nearshore and Mackenzie Bay/Yukon zones appear to have followed similar patterns to those described above for the continental shelf during the period 1974 to 1987. The summer salinity results for the continental slope are very sparse after 1960. During the period 1950-1960, the magnitude of year-to-year variations was low in comparison to other regions, with the highest August salinity occurring in 1950 (27.3) and the lowest in 1960 (22.9).

The year-to-year variability in freshwater content generally exhibits an inverse pattern of variation to that of salinity, as one would expect, although the number of available estimates is reduced. The amplitude of the freshwater variations is very large, amounting to approximately $\pm 50\%$ of the long-term mean value. (A noticeable exception is the August continental shelf zone data from 1981, in which a very high freshwater content was computed; this value is considered not to be representative of general conditions since the measurements were obtained in a very localized area [just north of Kugmallit Bay in the shallowest portion of the shelf zone]).

Temperatures, at both the 1 m level and the integral to 50 m depth (expressed as heat content), exhibit a smaller amplitude of interannual variability than with salinity. Similar tendencies between temperature and salinity do occur over the extended record of observations in the continental shelf, but are generally limited to years of extreme conditions. Abnormally low temperatures and salinities occurred in 1974 and again in 1985. Similarly, high temperatures coincided with high salinities in 1979 and 1987. The correspondence between temperature and salinity quantities is generally better for the integral quantities than for surface levels; the best correlations between heat and freshwater content occur in July and August on the continental shelf, in September on the continental slope (all negatively correlated), and in July in the nearshore zone (positively correlated).

Long-Term Trends in Oceanographic Properties - The interannual variations in oceanographic parameters compiled for this study (Figures 7-11) demonstrate the difficulty of detecting long-term changes in ocean properties associated with climatic processes, such as the 'greenhouse effect'. The relatively large amplitude of shorter-term variations in the ocean (occurring over time scales of the order of ten years or less) relative to the long-term mean, combined with the gaps in the data, has the effect of obscuring any long-term changes having amplitudes of less than 1 C. Based on long-term analyses of air-temperature in this region (Kelly et al., 1982), the expected amplitude of temperature changes at the surface would not be expected to exceed 1 C over the long-term (30 years or longer) time periods.

Temperature at Salinity = 31 - The sub-surface parameter, temperature at salinity of 31, suggests that the presence of warm subsurface water is highly variable from year to year (Figure 15). As one might expect, there is a good correspondence between temperature at S=31 and the heat integral (Figure 9), on both the continental slope and shelf. In the shallower waters of the nearshore zone, fewer samples of temperature at S=31 are available due to the limited depth.

Previous studies have revealed a warming from west to east over the continental shelf, based on analyses of data sets: 50-0001 (Mountain, 1974); 75-0002 (Macdonald et al., 1987); and 86-0004 (Fissel et al., 1987a). In the two later data sets, a marked increase in temperature at S=31 occurred to the east of 132°W.

The mean temperature at the salinity = 31 surface differs considerably among the various areas. Temperatures are lowest in inshore and continental shelf areas (<0°C) in August, somewhat higher over the continental slope (mean 0°C), and much larger in Amundsen Gulf (1.7°C). This spatial pattern is consistent with the results of previous analyses of data sets: 50-0001 (Mountain, 1974); 75-0002 (Macdonald et al., 1987) and 86-0004 (Fissel et al., 1987a) which revealed increasing temperatures toward the east.

An examination of mean temperatures at salinity = 31 within subregions of the shelf and slope areas (Figure 16) for all available data sets reveals that a pronounced positive easterly gradient occurred in 7 of the 10 years for which comparisons between subregions could be made. The two subareas adjacent to Amundsen (subregions B and H shown in map inset in Figure 15) had the largest mean values (0.4 and 0.8°C respectively in August), as well as the largest individual values (4°C in August 1975 - region H).

A tongue of comparatively warm water at or near the salinity=31 level is also found off the Alaskan continental shelf (Mountain, 1974; Hufford, 1975). This warm water core originates to the west in or near the Bering Sea and is advected eastward by the Beaufort Undercurrent (Aagaard, 1984), but its eastward advance is usually limited to 148 to 150°W. However, in some years the Bering Sea water has been observed further to the east in eastern Alaskan waters. Examples of the extended eastward advance of Bering Sea water into the Eastern Alaskan Shelf occurred in 1951 and 1986, as noted by Fissel et al., 1987a (Figure 17). In 1951, a minor subsurface core of warm waters is evident in the vertical temperature section off Herschel Canyon (appendix D, p. 263), while in

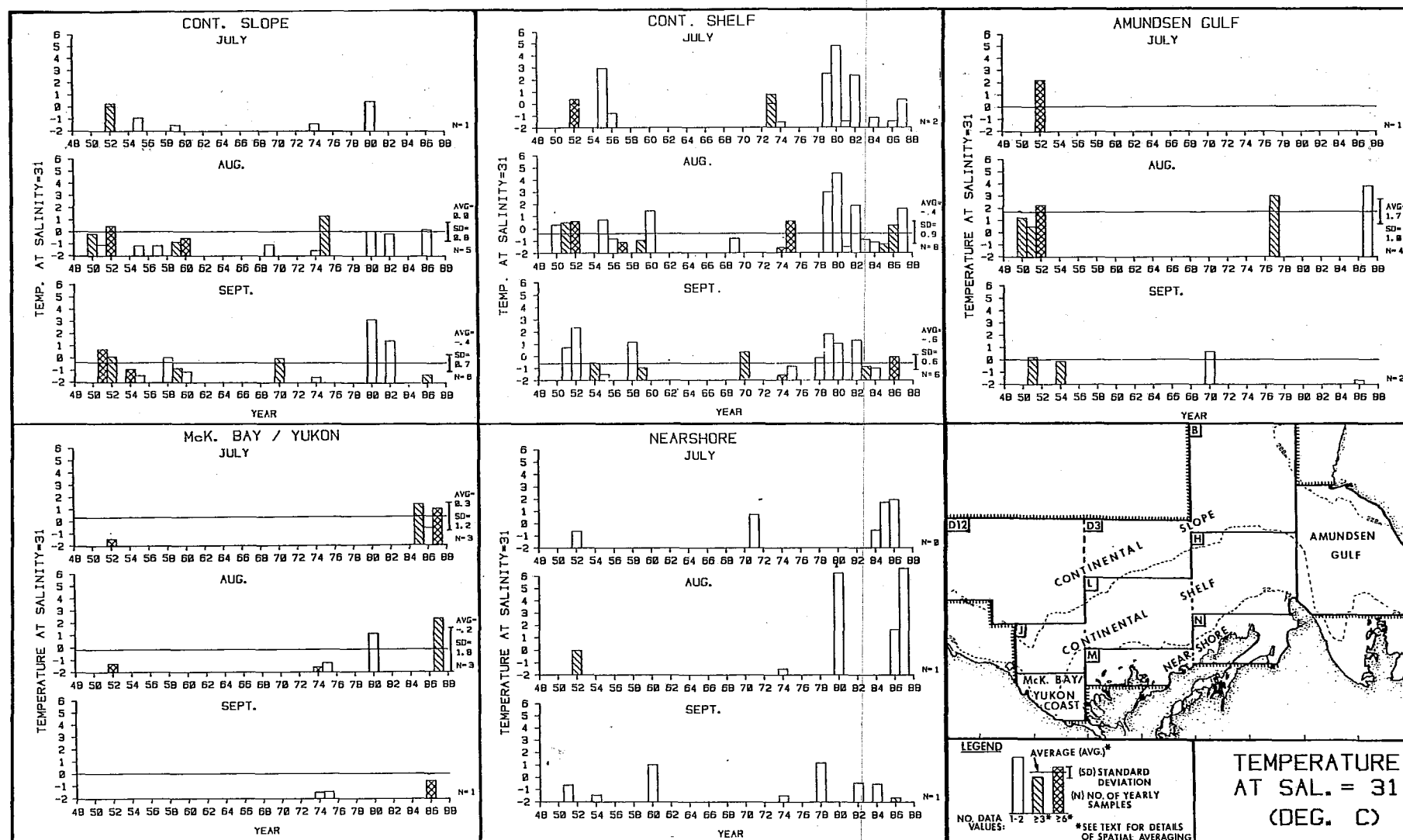


Figure 15: Monthly mean values of temperature at a salinity of 31. The results are displayed separately for five subregions of the study area.

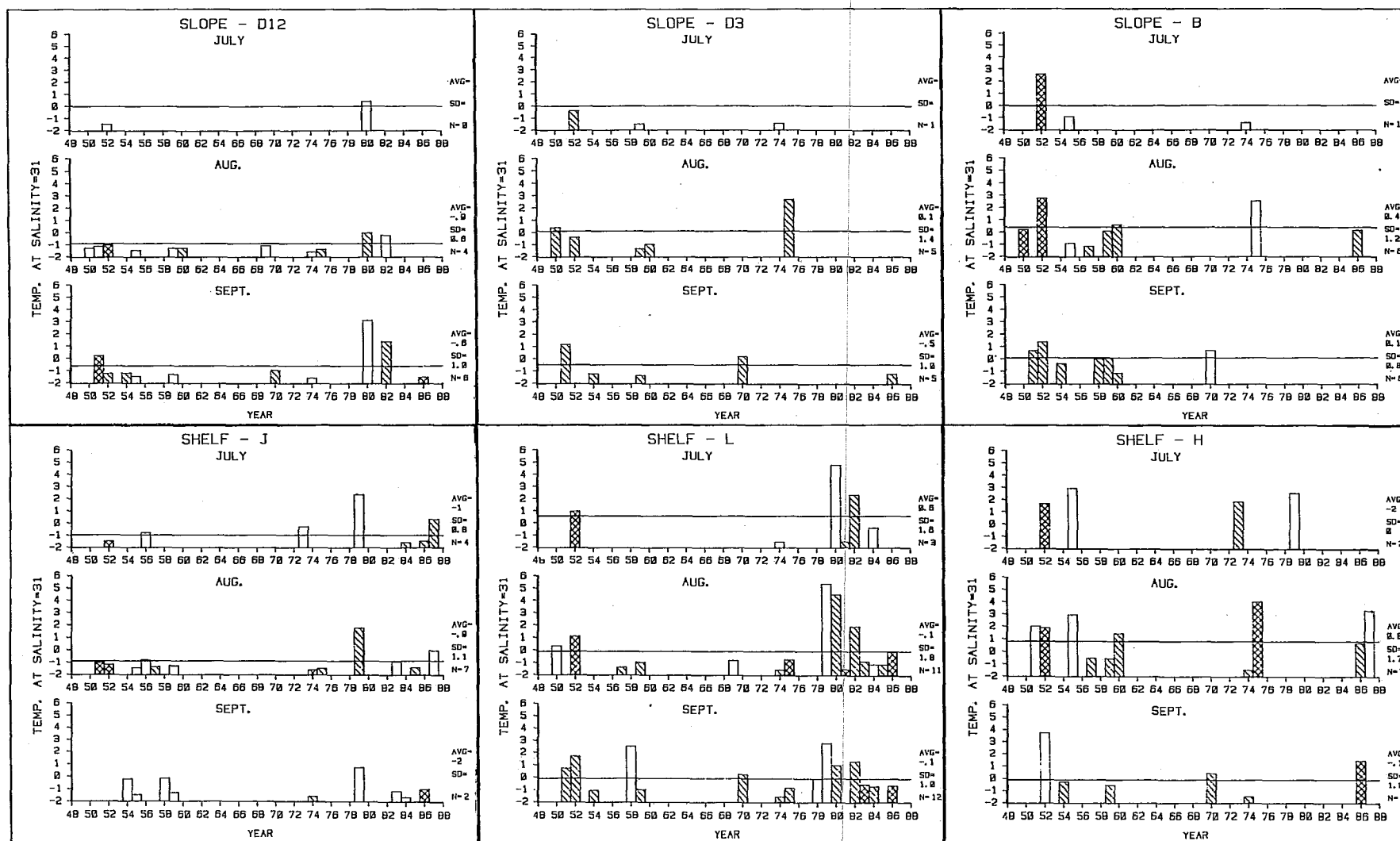


Figure 16: Monthly mean values of temperature at a salinity of 31. The results are presented for the portions of the continental shelf and slope subregions (shown in inset map of Figure 15).

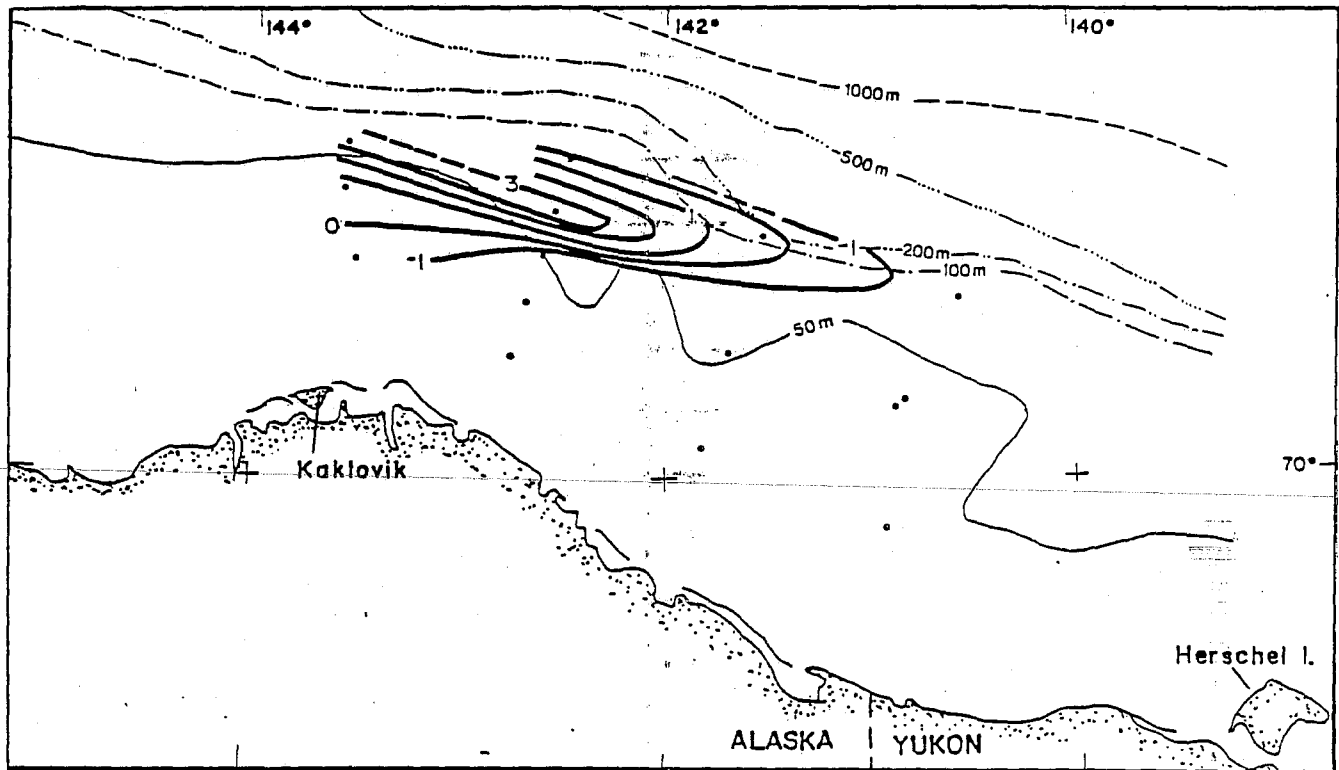


Figure 17: Maps of temperature and salinity over the eastern Alaskan continental shelf showing the presence of warm subsurface water of Bering Sea origin (from Fissel et al., 1987a).

1986 there was no evidence of Bering Sea water present in the Canadian sector of the Beaufort Sea.

Based on the temperature distributions at salinity=31, Bering Sea water appears to account for little of the heat observed at subsurface levels in the Canadian Beaufort Sea. Of much greater importance is the warming of surface waters in the Amundsen Gulf and eastern portions of the continental shelf and slope. In most years, these regions are exposed to greater solar insolation of the surface waters due to the early clearing of sea-ice, associated with the Cape Bathurst polynya (Smith and Rigby, 1981).

4.2 WIND, ICE AND RIVER DISCHARGES

Interannual Variations

Sea-Ice - Variations in sea-ice conditions are presented in Figure 18, as plots of the area with sea-ice concentrations less than 0.7 (hereafter referred to as "non-ice area") over the continental shelf and over the entire southeastern Beaufort Sea, including western Amundsen Gulf (see section 3.2 for full details on computation procedures). The reduced area of reduced ice cover varies by an order of magnitude between "good" (extensive areas of open water, eg. 1958, 1963, 1977 and 1987) and "bad" (extensive ice cover, eg. 1959, 1964, 1967, 1974 and 1985) ice years. Longer period variations appear to dominate the ice-free area in mid-August, while the mid-July conditions exhibit more variability between successive years. In mid-August, ice-free area reached maximum levels from 1977-1983, with lesser maximum levels occurring in 1986-1987, 1968-1972 and 1958-1963. For the mid-August data from 1954-1987, a cycle having period of approximately nine years is evident, similar to the long-term cycle noted previously for surface salinity.

The interannual variations of sea-ice extent in the southeastern Beaufort Sea appear to differ considerably (Figure 18b) from those examined over a much larger portion of the Western Arctic Ocean by Mysak and Manak (1989). The overall correlation between the two areas is statistically significant, but numerically low ($r=0.57$). Major deviations are noted in some years, such as 1974. This was a very bad year in the S.E. Beaufort Sea, but a moderate ice year in the larger area due to extensive retreat of sea-ice experienced in the Chukchi Sea. Mysak and Manak note an approximate 4-6 year cycle in sea-ice extent (from 1953-1984), which is a markedly shorter period than the 8-9 year cycle inferred in this study for the period 1954-1987. The differences noted between this study and that of Mysak and Manak (1989) underscore the importance of variability of sea-ice clearing patterns over regional areas in the peripheral portions of the Arctic Ocean.

Wind - The easterly wind component (Figure 19a), computed monthly from mid-May to mid-September, is highly variable both from year-to-year and between successive months within the same year. In the late spring and early summer, all years had a substantial easterly wind run (i.e. net displacement to the west), but in mid- and late-summer, the monthly wind run is more variable with occasional years having either a net westerly wind run or near-zero net displacement (eg. 1973, 1975, 1981-82, 1984-85). As noted in section 3.1 and Appendix F, individual wind events within each month can result in net displacements (typically 1500 to 4000 km, up to a maximum value of 13,000 km)

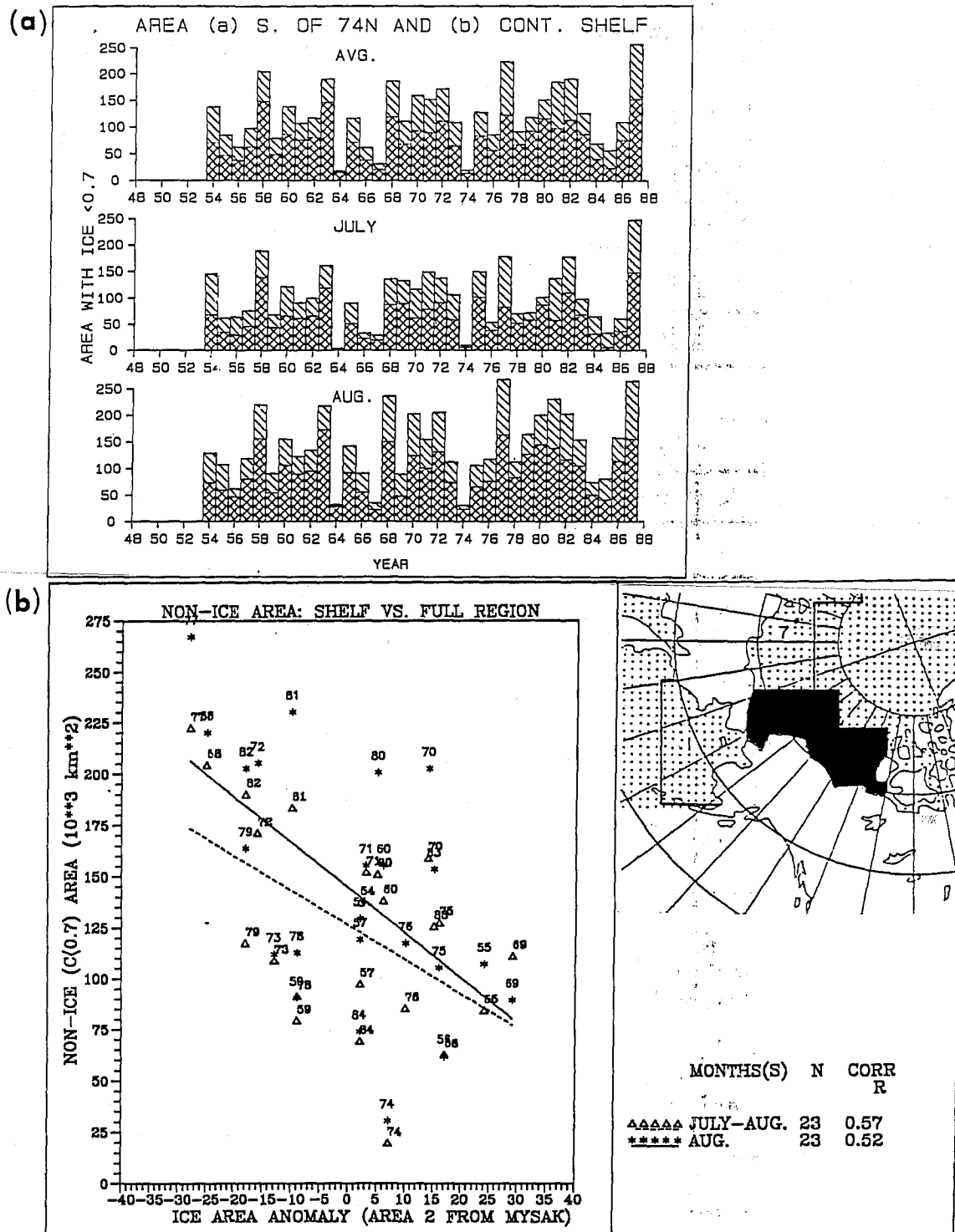


Figure 18: (a) The surface area, in thousands of km^2 , with ice cover of less than seven-tenths concentration for: (a) the S.E. Beaufort Sea; and (b) the portion of the S.E. Beaufort Sea spanning the continental shelf (regions are shown in Figure 5). The areas are plotted for mid-July, mid-August and the average of the two. (b) A scatter plot between the area of reduced ($C < 0.7$) ice concentration during August in the S.E. Beaufort Sea (this study) and the areal-ice extent of the much larger region (see inset) of Mysak and Manak (1989).

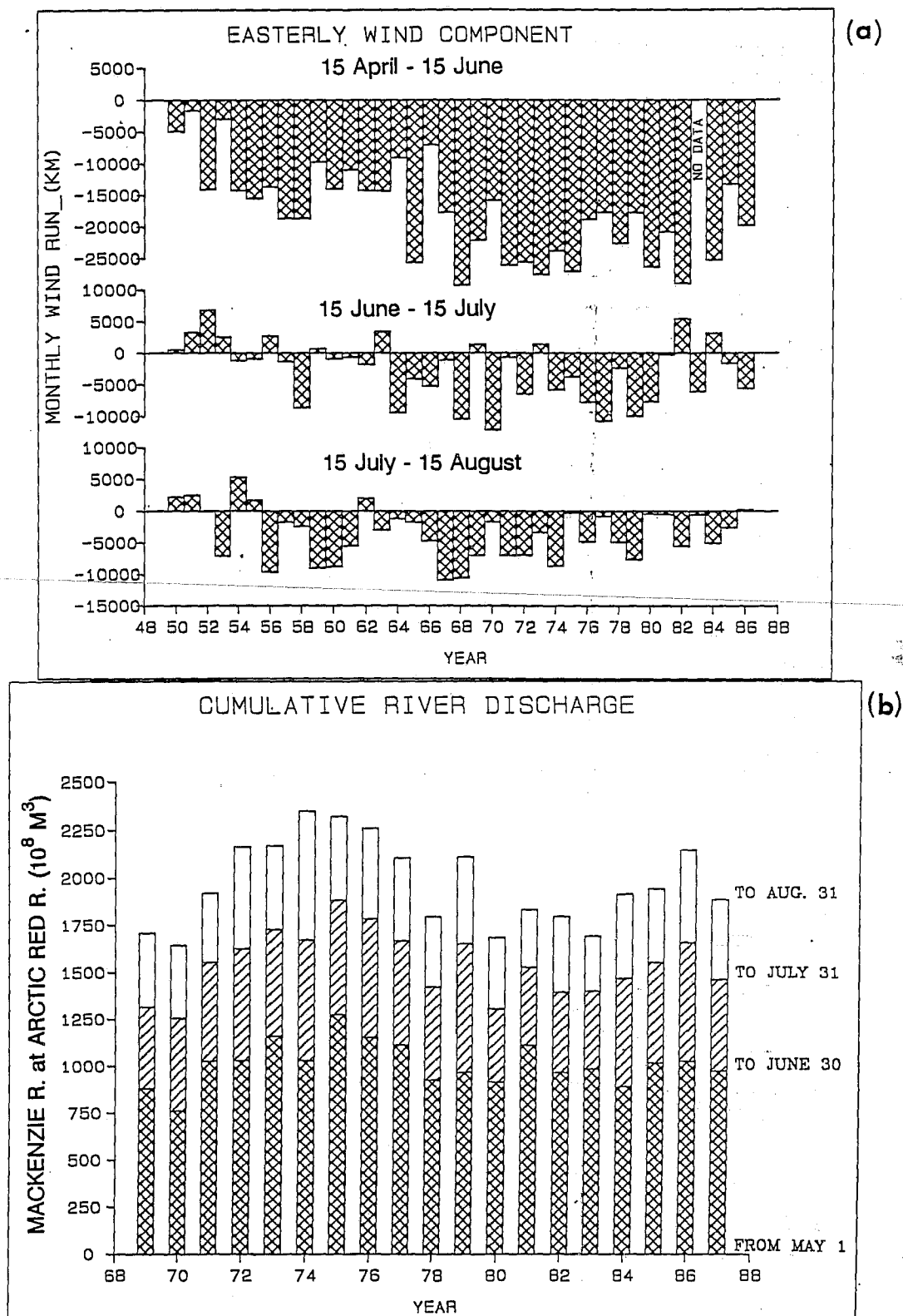


Figure 19: (a) The net wind displacement of the easterly wind component (in km) for April 15 to June 15, mid-June to mid-July and mid-July to mid-August, as computed from the marine geostrophic wind data. (b) The cumulative volume discharge of the Mackenzie River (at Arctic Red River) for May-June, July and August.

that approach in magnitude the computed mean wind run over a full month. As a result, caution must be exercised in using the monthly wind displacement as being fully representative of actual wind conditions. Reference to the history of individual wind events (Appendix F) may be required for some applications.

Mackenzie River Discharge - In comparison to the sea-ice and wind parameters, river discharge exhibits small year-to-year variations of $\pm 25\%$ in the cumulative discharge during the freshet period, May and June (Figure 19b). While year-to-year variations are somewhat larger for July and August (up to a factor of two), the cumulative discharge from May to August varied by less than 20% over the period 1968 to 1987. The largest cumulative discharges occurred from 1972 to 1977, with a secondary maximum in 1979 and 1986. Minimum levels were experienced from 1980 to 1983, 1969-1970 and 1978.

Wind vs. Sea-Ice Area - Comparisons of the easterly wind and ice free areas indicate that the ice free area of mid-July is not well correlated with the local cumulative winds experienced over the previous two month period. This lack of similarity in wind and ice-free area reflects the importance of other factors; including, for example: displacements in the Arctic polar pack ice resulting from large-scale, circumpolar wind patterns; and year-to-year variations in the effects of local melting in nearshore areas.

After breakup the situation changes; from mid-July to mid-August the changes in ice-free area are seen to be related to the cumulative easterly wind displacement over the same period (Figure 20). The linear regression between non-ice area and easterly wind displacement ($r=20$) indicates that a 10,000 km easterly wind run results in an average clearing of 65,000 km² of sea-ice from the continental shelf ice zone (Figure 5). This large area of ice clearing is equivalent to a 108 km offshore retreat of the ice edge over the full width (600 km) of the shelf zone: an average retreat rate of 3.6 km/d under monthly mean geostrophic winds of 333 km/d (3.9 m/s). Note, however, that the apparent relationship between easterly wind run and change in sea-ice coverage does not apply to several years, most notably 1969, 1975 and 1981. Nevertheless, the wind and ice-free area parameters are sufficiently decoupled that both quantities should be considered independently in examining oceanographic responses to external factors.

Comparison of Oceanographic Parameters with Wind, Ice and River Discharges

Scatter plots between oceanographic quantities (surface temperature and salinity, heat and freshwater content) with easterly wind displacement, non-ice area and river discharge were prepared for each summer month and for each of the five oceanographic regions. For many of the scatter plots, no significant correlation was evident. However, several of the plots were suggestive of a possible linkage between the oceanographic quantity and external parameter. These are described below, for each type of non-oceanographic parameter.

Non-Ice Area - Both temperature and salinity appear to be related to the extent of sea-ice clearing in the summer (Figures 21 to 24). The apparent coupling seems to be largest for the mid- and outer continental shelf, particularly for the monthly mean oceanographic parameters of August and September when regressed onto the August non-ice area. The corresponding results for July reveal low correlation levels for salinity, freshwater and heat

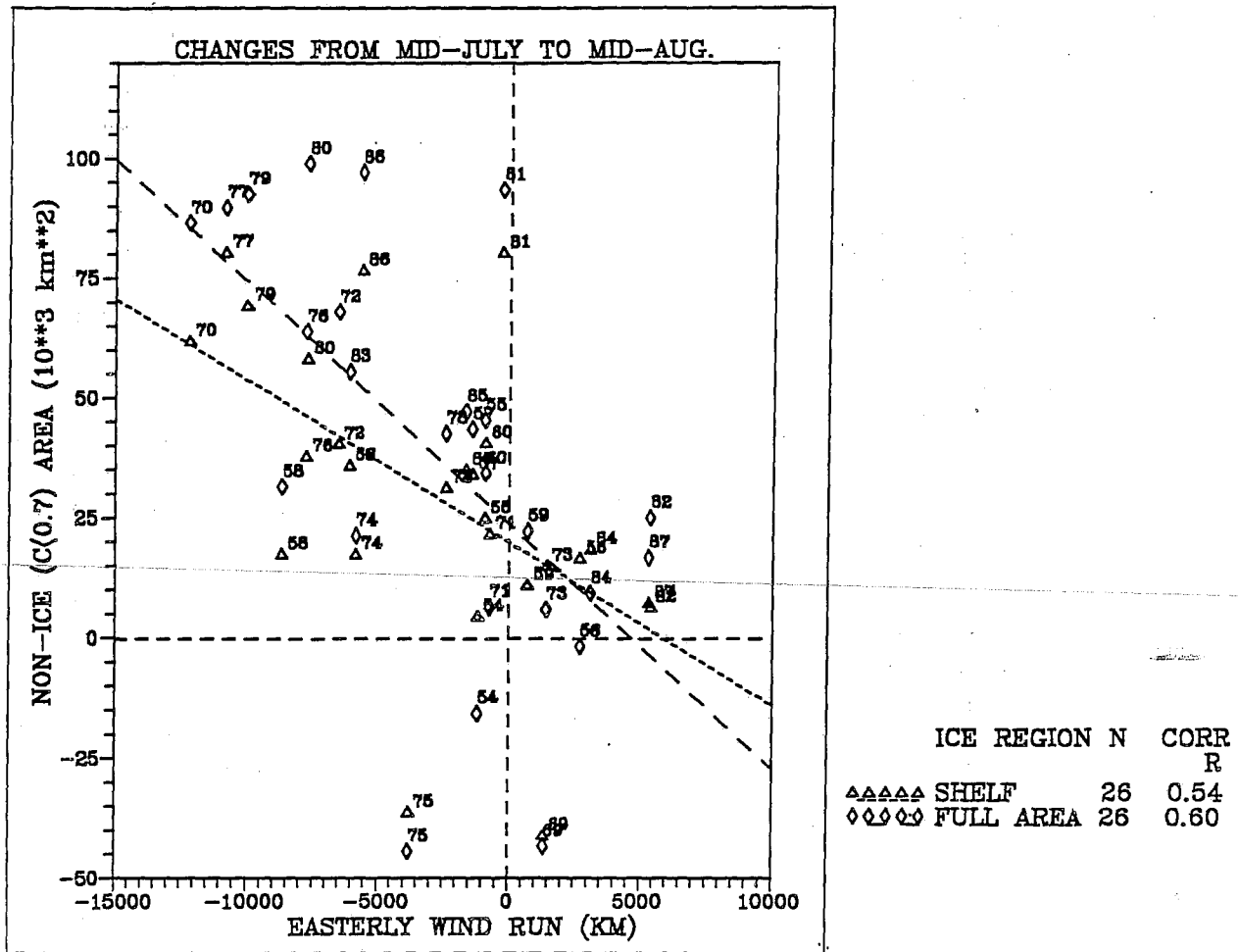


Figure 20: A scatter plot of the change in "non-ice area" (ice concentrations < 0.7) against the net easterly wind run from mid-July to mid-August.

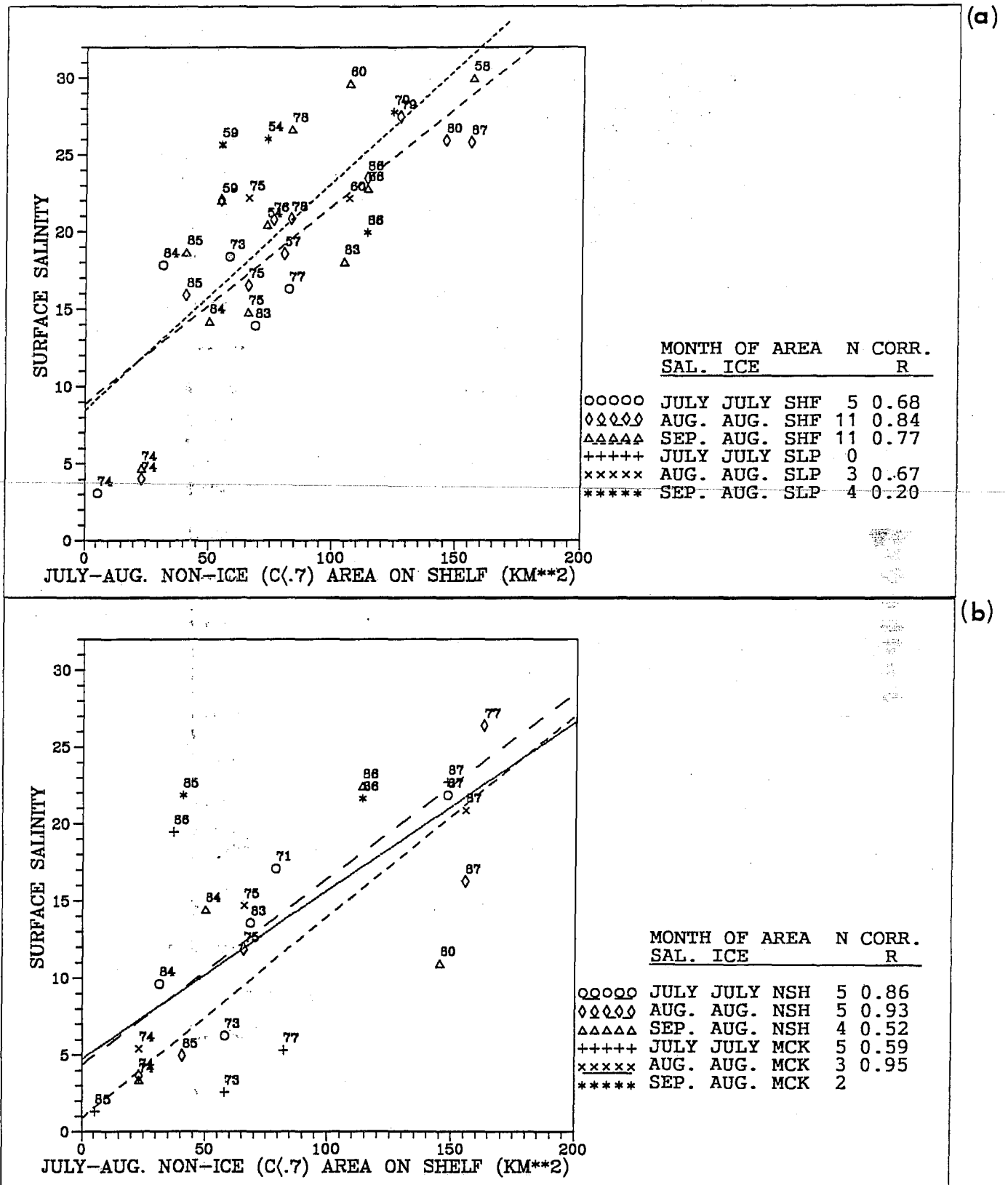


Figure 21: Scatter plot and linear regression results for salinity at 1 m versus area where ice concentration <0.7 for (a) continental shelf (shf) and slope (slp) subregions and, (b) nearshore Mackenzie shelf (nsh) and Mackenzie Bay/Yukon (mck) subregions.

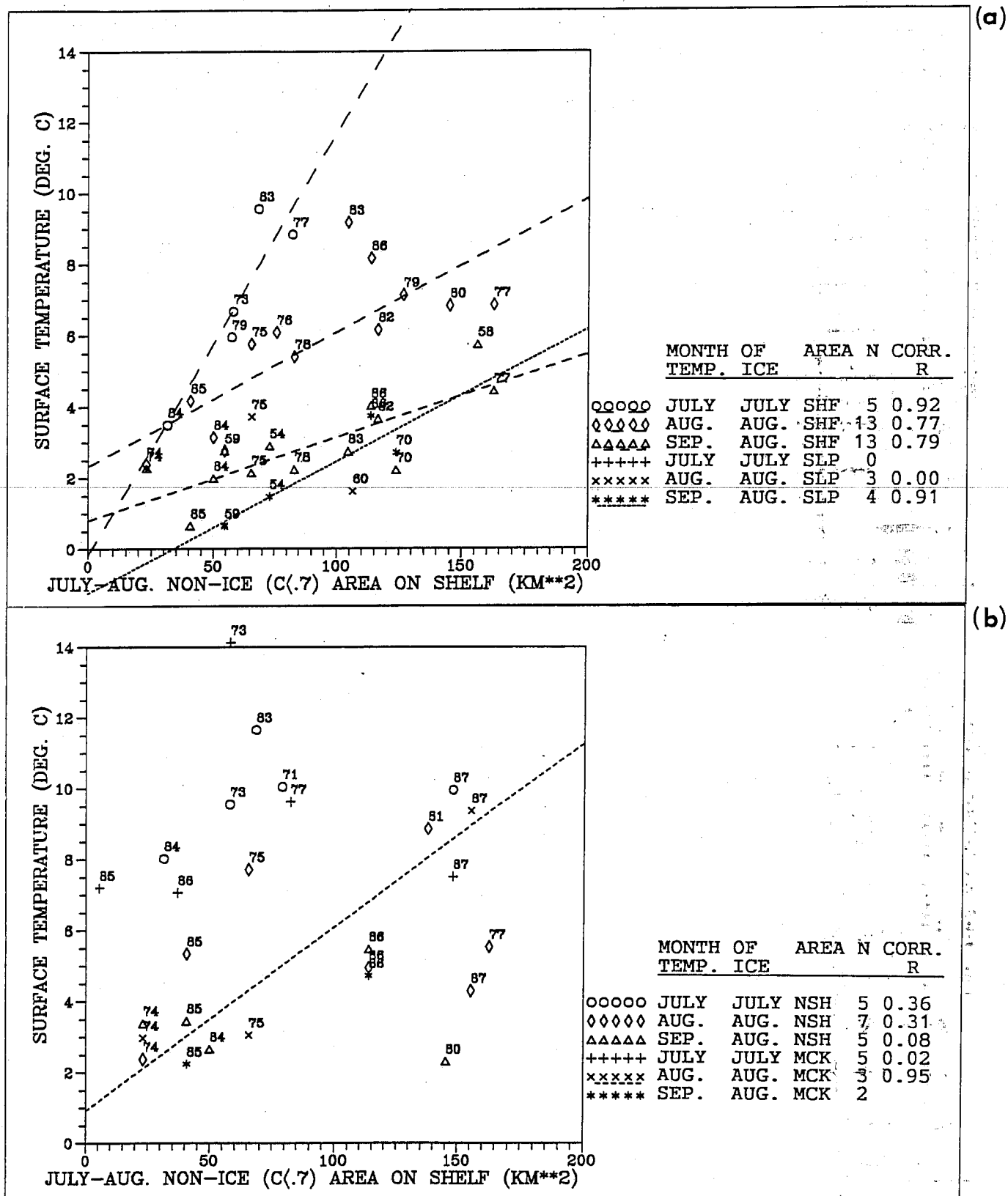


Figure 23: Scatter plot and linear regression results for temperature at 1 m versus area where ice concentration <0.7 for (a) continental shelf (shf) and slope (slp) subregions, and (b) nearshore Mackenzie shelf (nsh) and Mackenzie Bay/Yukon (mck) subregions.

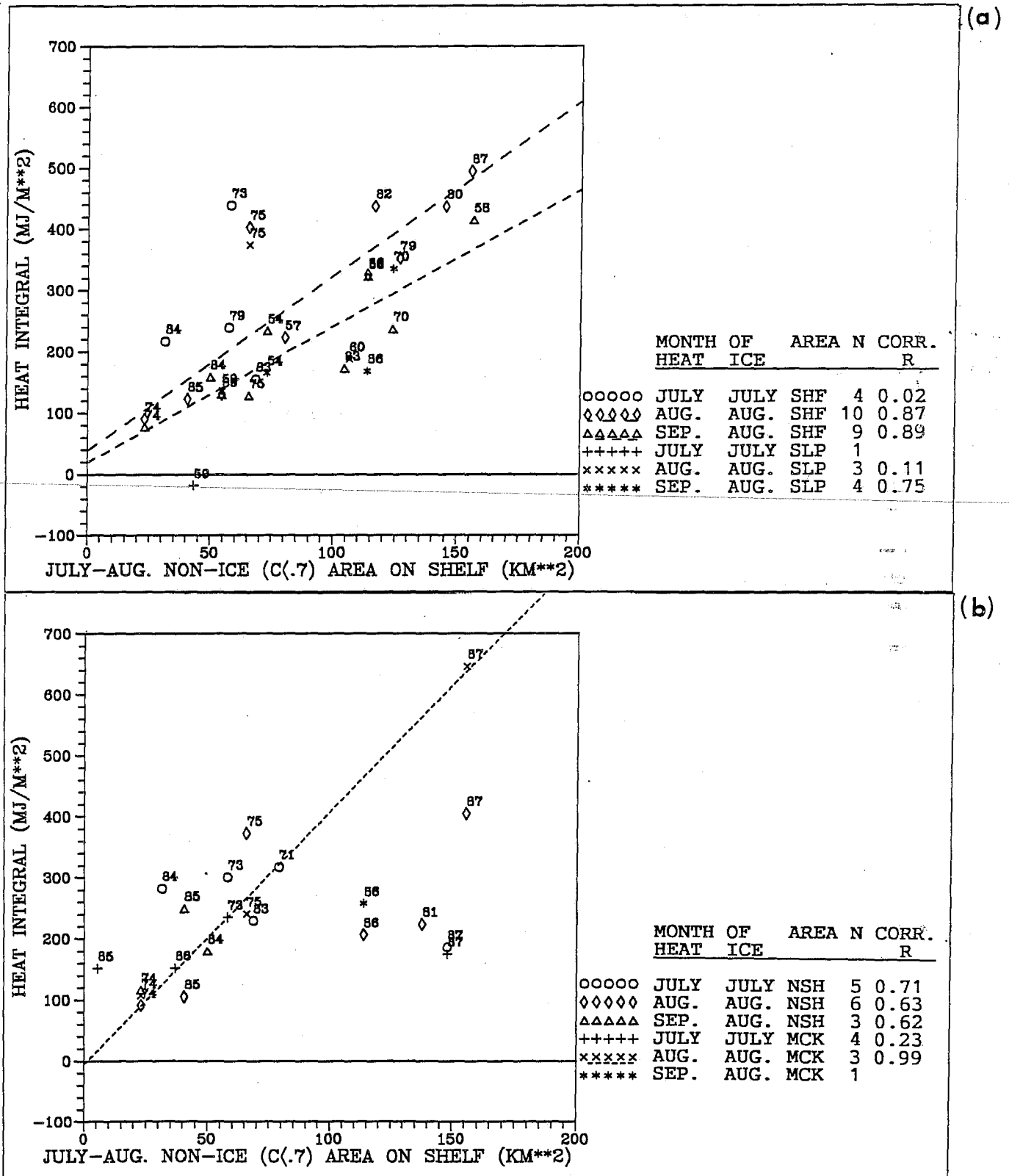


Figure 24: Scatter plot and linear regression results for heat content to 50 m versus area where ice concentration <0.7 for (a) continental shelf (shf) and slope (slp) subregions, and (b) nearshore Mackenzie shelf (nsh) and Mackenzie Bay/Yukon (mck) subregions.

integrals with only surface temperature attaining a statistically significant level ($r=0.92$).

The linear regression results of non-ice area consistently exceed statistical significance levels for both the surface and integral (freshwater) salinity parameters (Figures 21 and 22). These results are nearly identical for August and September on the continental shelf ($r=0.83$ and 0.77 , respectively). Extensive clearing of the sea-ice is associated with comparatively high surface salinities (>25) and low freshwater integral values (<1 m), with the converse of this statement holding true as well. Similar regression results for salinity on non-ice area were also computed for inshore areas, although the smaller sample sizes make the results less definitive.

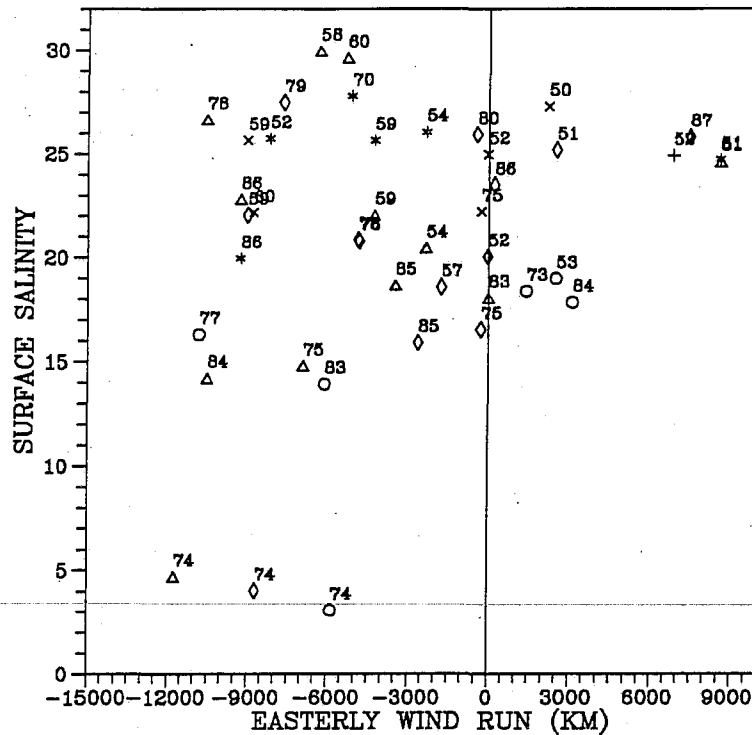
The surface and integral temperatures over the mid- and outer continental shelf also exhibit a general tendency to increase with sea-ice clearing. However, unlike the salinity parameters, this apparent correlation does not hold in inshore areas, but it does appear to be applicable in the continental slope, at least for September data versus August non-ice areas. Regression curves computed for temperature versus non-ice area exhibit large changes during the summer months (by comparison with salinity quantities), reflecting the progressive decrease in temperatures throughout the summer.

Sea-ice clearing appears to exert an important influence on oceanographic properties throughout the summer. There are two major ways in which sea-ice clearing could alter oceanographic properties: (1) the amount of sea-ice clearing is important in determining the vertical exchange between ocean and atmosphere, particularly the total amount of solar insolation reaching the ocean surface; and (2) sea-ice limits the horizontal exchange and dispersion of surface layer water properties. This latter effect of sea-ice clearing is expected to be more important for salinity than temperature. Fresh water tends to remain confined within the surface layer by buoyancy effects, and vertical exchanges through the sea-surface are smaller for salinity than for temperature. Further examination of the role of sea-ice in determining summer oceanographic properties is given in the next section concerning "Heat and Freshwater Budgets".

Winds - An examination of the scatter plots between oceanographic parameters and the monthly easterly wind run suggests there is little correspondence (Figures 25 to 28). For some months, and areas (9 out of 24), surface temperature and the heat integral (Figures 27 and 28) appear to be positively correlated with wind run. However, either the correlation coefficients are low (<0.8), or the sample size is very small ($N<6$). The positive correlation is unexpected, since the positive wind runs associated with westerly winds would be expected to reduce the ice-free surface area and thereby lead to reduced temperatures. However, in inshore areas, upwelling associated with easterly winds may be important. The occurrence of upwelling would be consistent with a positive correlation of temperature and wind run: negative winds (from the east) combined with low temperatures.

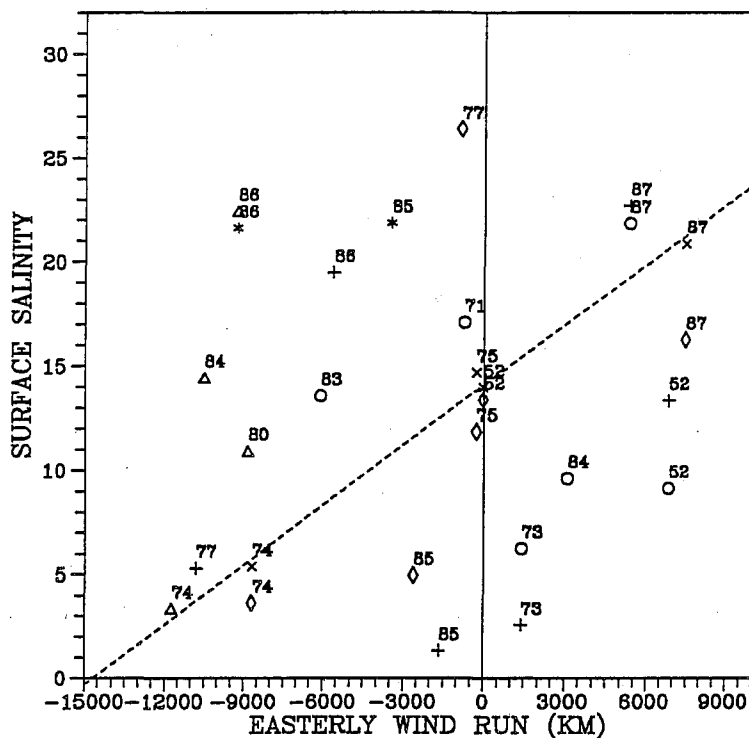
The surface salinity and freshwater integral exhibit even more scatter with monthly wind run (Figures 25 and 26). In offshore areas, there was no significant correlation with wind run, while in inshore regions, only three of the twelve combinations had statistically significant correlations. The cases with significant correlations were positively correlated for salinity and

(a)



	MONTH OF	AREA	N	CORR.
	SAL.	WIND		R
ooooo	JULY	MAY-JUL	SHF	6 0.22
ooooo	AUG.	JUL-AUG	SHF	13 0.16
aaaaa	SEP.	AUG-SEP	SHF	12 0.09
+++++	JULY	MAY-JUL	SLP	1
xxxxx	AUG.	JUL-AUG	SLP	5 0.12
*****	SEP.	AUG-SEP	SLP	6 0.05

(b)



	MONTH OF	AREA	N	CORR.
	SAL.	WIND		R
ooooo	JULY	MAY-JUL	NSH	6 0.04
ooooo	AUG.	JUL-AUG	NSH	6 0.53
aaaaa	SEP.	AUG-SEP	NSH	4 0.66
+++++	JULY	MAY-JUL	MCK	6 0.31
xxxxx	AUG.	JUL-AUG	MCK	4 0.99
*****	SEP.	AUG-SEP	MCK	2

Figure 25: Scatter plot and linear regression results for salinity at 1 m versus easterly wind run for (a) continental shelf (shf) and slope (slp) subregions, and (b) nearshore Mackenzie shelf (nsh) and Mackenzie Bay/Yukon (mck) subregions.

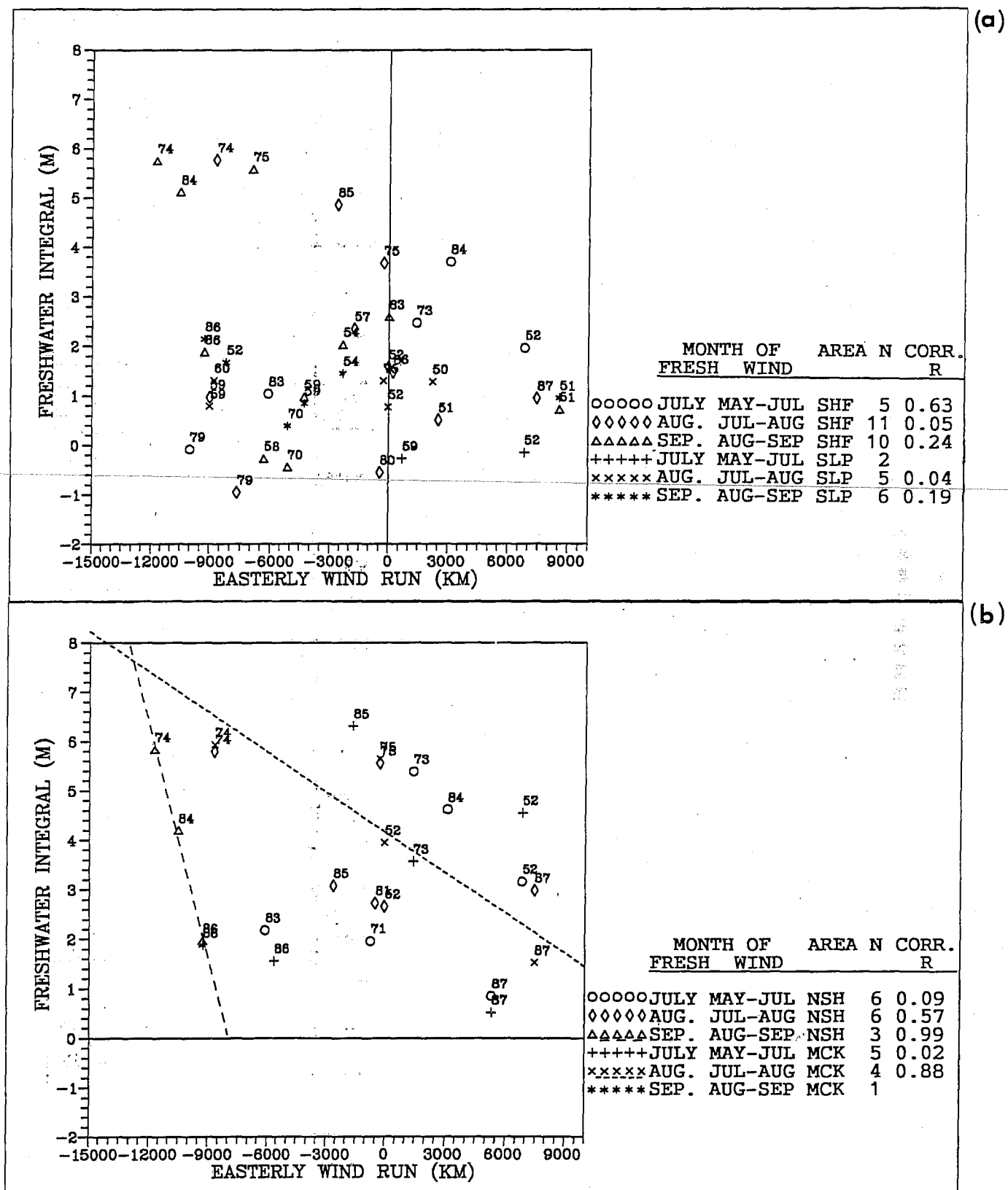
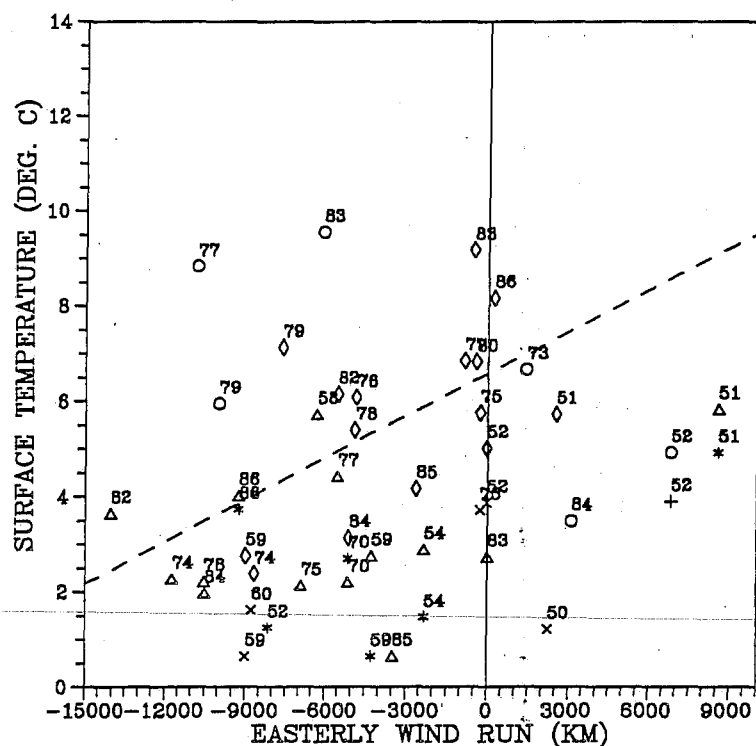


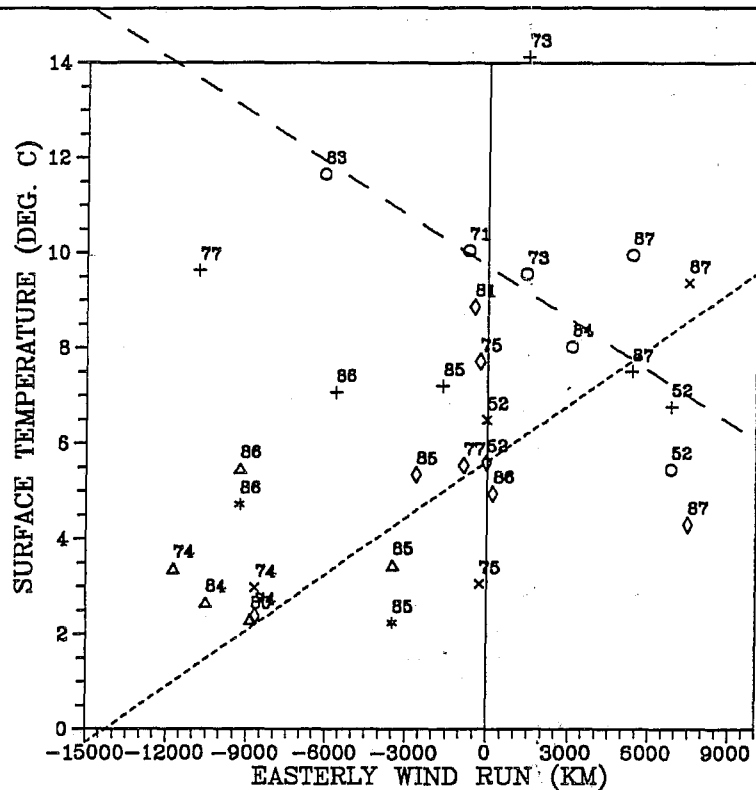
Figure 26: Scatter plot and linear regression results for freshwater content to 50 m versus easterly wind run for (a) continental shelf (shf) and slope (slp) subregions, and (b) nearshore Mackenzie shelf (nsh) and Mackenzie Bay/Yukon (mck) subregions.

(a)



	MONTH OF	AREA	N	CORR.
	TEMP	WIND		R
ooooo	JULY	MAY-JUL	SHF	6 0.67
ooooo	AUG.	JUL-AUG	SHF	15 0.55
ooooo	SEP.	AUG-SEP	SHF	14 0.33
+++++	JULY	MAY-JUL	SLP	1
xxxxx	AUG.	JUL-AUG	SLP	6 0.53
xxxxx	SEP.	AUG-SEP	SLP	6 0.53

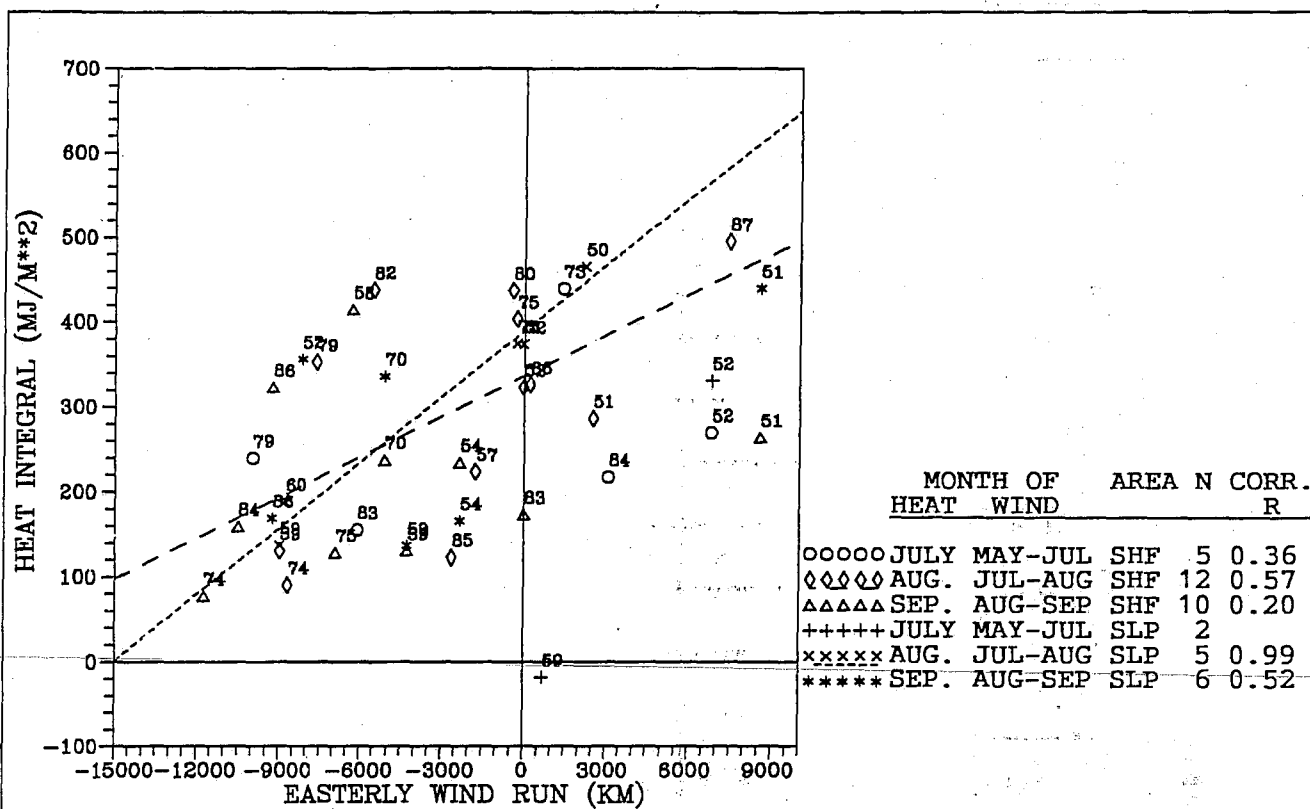
(b)



	MONTH OF	AREA	N	CORR.
	TEMP	WIND		R
ooooo	JULY	MAY-JUL	NSH	6 0.79
ooooo	AUG.	JUL-AUG	NSH	8 0.27
ooooo	SEP.	AUG-SEP	NSH	5 0.04
+++++	JULY	MAY-JUL	MCK	6 0.10
xxxxx	AUG.	JUL-AUG	MCK	4 0.85
xxxxx	SEP.	AUG-SEP	MCK	2

Figure 27: Scatter plot and linear regression results for temperature at 1 m versus easterly wind run for (a) continental shelf (shf) and slope (slp) subregions, and (b) nearshore Mackenzie shelf (nsh) and Mackenzie Bay/Yukon (mck) subregions.

(a)



(b)

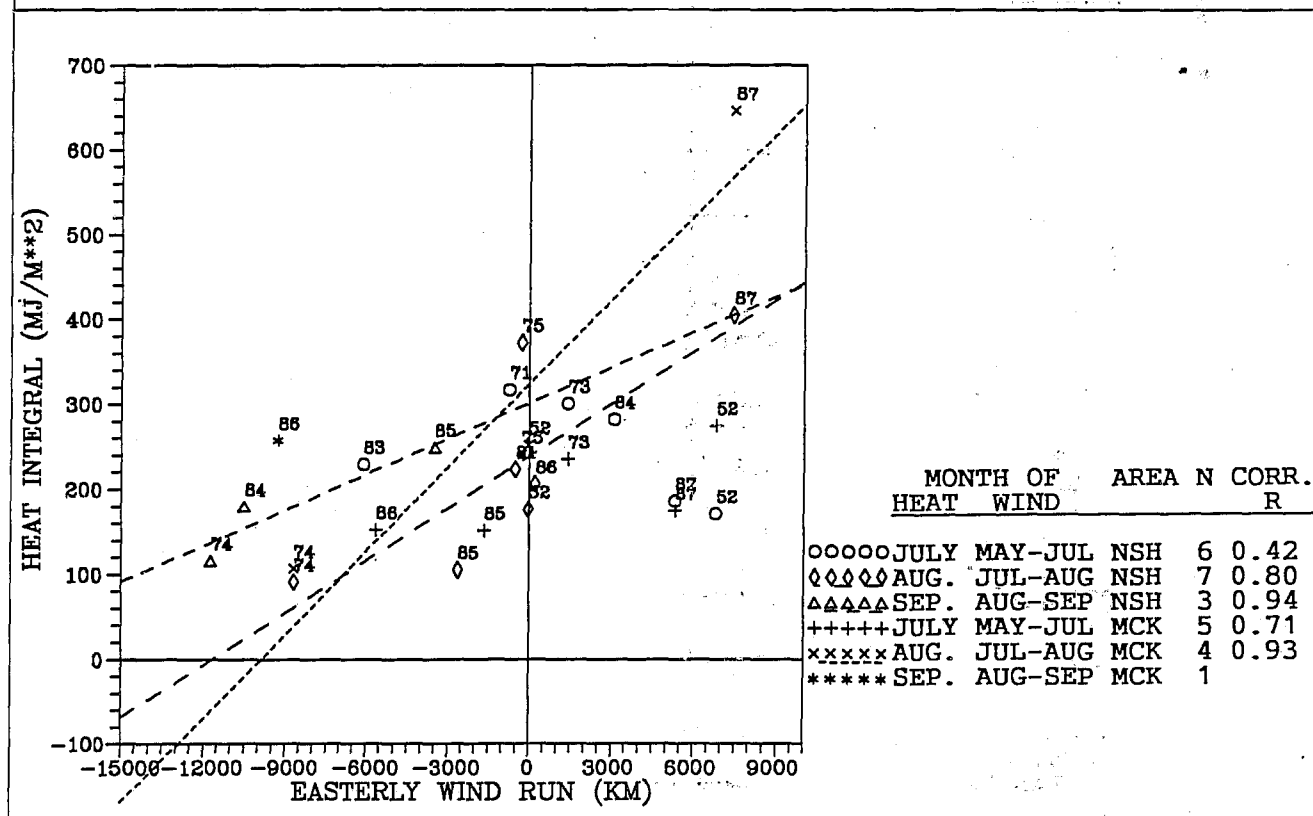


Figure 28: Scatter plot and linear regression results for heat content to 50 m, versus easterly wind run for (a) continental shelf (shf) and slope (slp) subregions, and (b) nearshore Mackenzie shelf (nsh) and Mackenzie Bay/Yukon (mck) subregions.

negatively correlated for freshwater integral. The results are opposite to those expected for wind-driven upwelling, and probably reflect the very low salinities of 1974, when monthly wind runs happened to be negative (i.e. winds from the east).

The apparent lack of coupling between oceanographic properties and winds does not necessarily imply the winds are unimportant in determining oceanographic distributions. Previous studies have revealed a reasonably good correlation between surface currents with winds (eg. Fissel and Birch, 1984) and surface water properties with winds (eg. Cameron, 1953; Thomson et al., 1986) in some summers. The low correlations determined in this study are likely the result of: (1) the larger effect of sea-ice clearing on oceanographic distributions, as discussed above, which are not simply related to local wind conditions; (2) the use of mean winds computed over an averaging interval much greater than the synoptic time scale of 3-10 days associated with individual wind events; and (3) computation of mean oceanographic parameters over large areas which may contain complex spatial features.

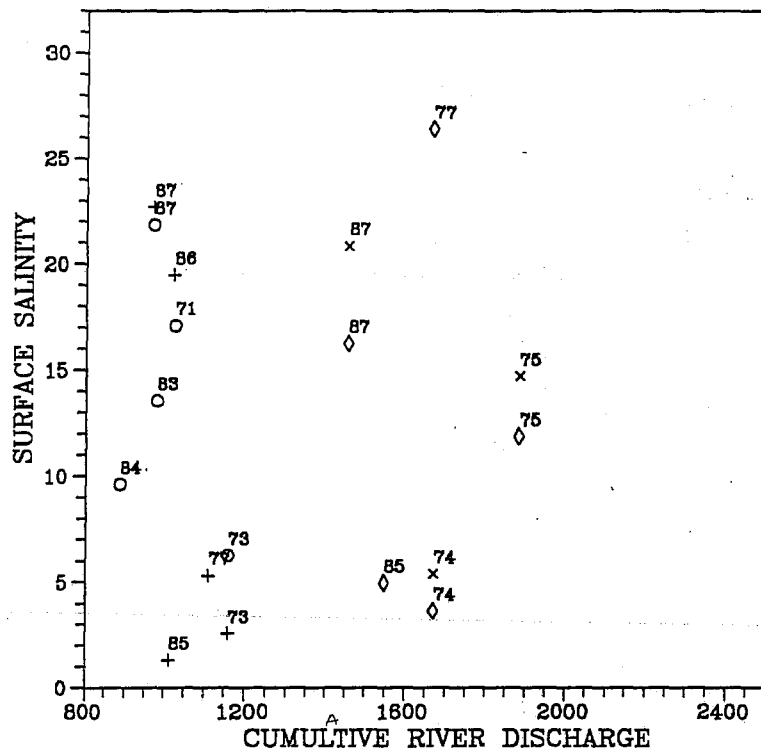
River Discharge - The monthly mean oceanographic properties appear to be unrelated to variations in Mackenzie River discharges in offshore regions. For the inshore areas (Figures 29 and 30), a small degree of coupling is suggested, with 3 of 16 possible combinations exhibiting statistically significant correlation results. The significant results include: positive correlations of surface temperature and heat integral in July with May to June river discharge in the Mackenzie Bay-Yukon inshore region, and a positive correlation between freshwater integral of July and the cumulative river discharge of May to June in the nearshore region. The correlation results suggest that cumulative river discharge may be important to oceanographic properties in inshore areas, but to a lesser degree than other influences, including the role of areal extent of sea-ice.

4.3 HEAT AND FRESHWATER BUDGET CONSIDERATIONS

Previous computations of the heat and freshwater (salt) budgets of the southeastern Beaufort Sea are limited to the analyses of 1974 and 1975, when an extensive set of summer oceanographic data were collected as part of the Beaufort Sea Project. Tummers (1980) computed a heat budget for both years while Thomas et al. (1986) examined the freshwater budget over the continental shelf for the same years. In this section, we will derive simplified heat and freshwater budget estimates for ten individual years, which have sufficient oceanographic sampling densities to permit such computations.

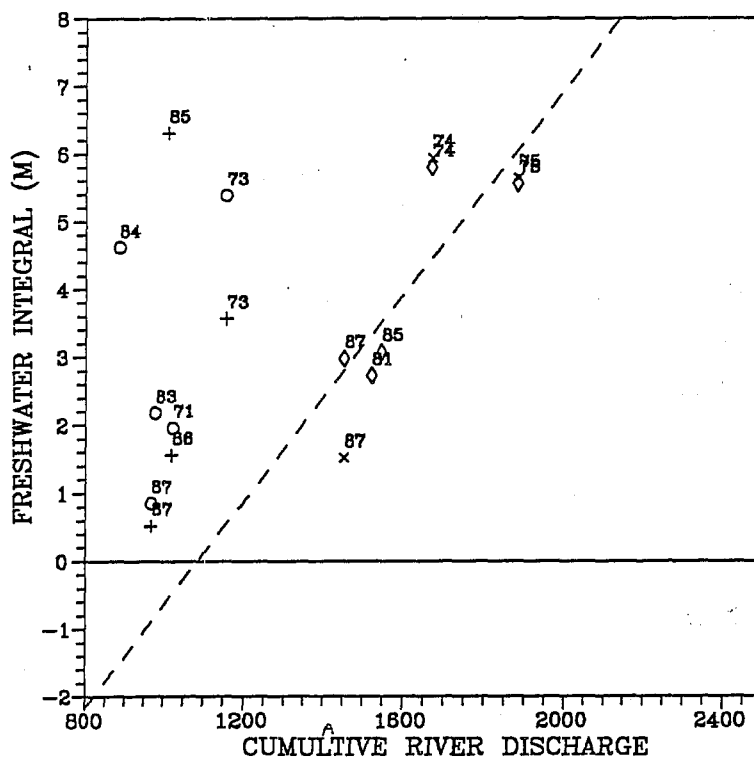
The freshwater budget estimates are considered first, since fewer physical quantities are involved and the resulting estimates are reasonably definitive. From the freshwater budget computations, the degree of advective exchanges between the shelf areas with adjoining regions can be roughly estimated. The more complex heat budget is then considered and the residual heat exchange needed to balance the budget is compared with the corresponding freshwater residual value.

(a)



MONTH OF SAL.	RIVER	AREA	N	CORR. R
ooooo	JULY	MAY-JUN	NSH	5 0.36
ooooo	AUG.	TO JULY	NSH	9 0.02
+++++	JULY	MAY-JUN	MCK	5 0.66
xxxxx	AUG.	TO JULY	MCK	3 0.40

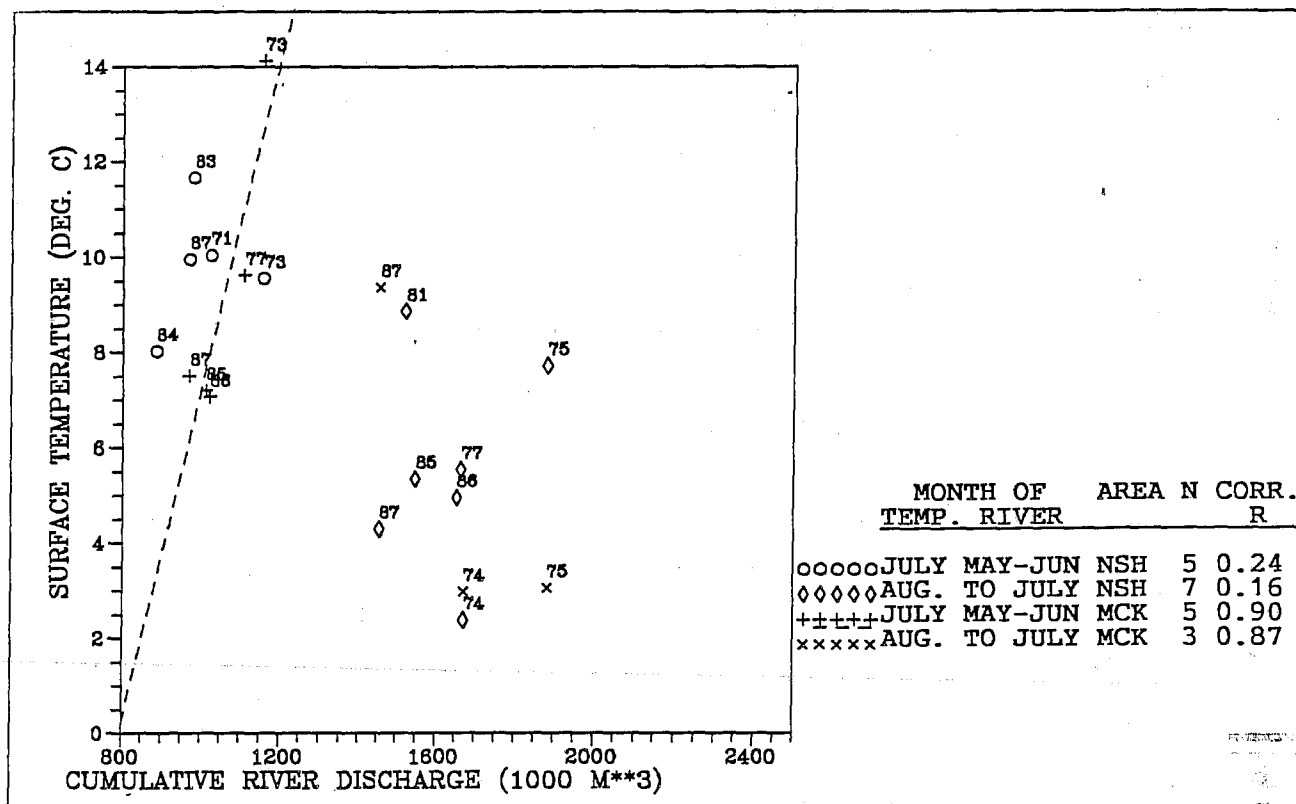
(b)



MONTH OF FRESH	RIVER	AREA	N	CORR. R
ooooo	JULY	MAY-JUN	NSH	5 0.33
ooooo	AUG.	TO JULY	NSH	5 0.84
+++++	JULY	MAY-JUN	MCK	0 0.28
xxxxx	AUG.	TO JULY	MCK	3 0.84

Figure 29: Scatter plot and linear regression results for (a) salinity at 1 m, and (b) freshwater content to 50 m versus Mackenzie River discharge for inshore areas: nearshore Mackenzie shelf (nsh) and Mackenzie Bay/Yukon (mck).

(a)



(b)

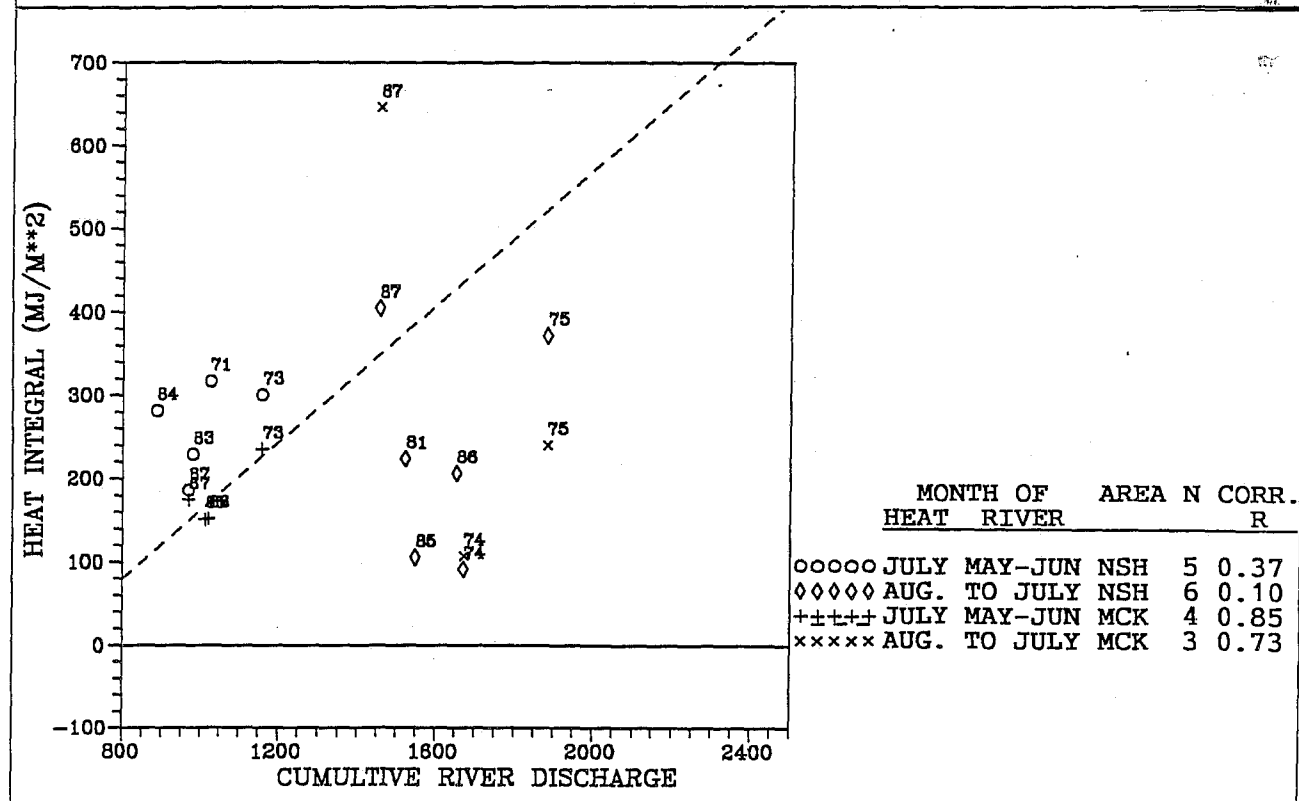


Figure 30: Scatter plot and linear regression results for (a) temperature at 1 m and (b) heat content to 50 m versus Mackenzie River discharge for inshore areas: nearshore Mackenzie shelf (nsh) and Mackenzie Bay/Yukon (mck).

Freshwater Budget

Freshwater budget computations were carried out over the continental shelf area of the Canadian Beaufort Sea (Figure 31) for the years having reasonably dense oceanographic sampling: 1970, 1973-1975, 1980, 1983-1987.

Examination of the exchanges of freshwater (or equivalently as salt) were also considered for the same ten years considered in the heat budget computations. An equality in the sum of freshwater fluxes and net storage in the ocean is represented as:

$$F_N + F_O + F_A - F_W = 0 \quad \text{where} \quad (\text{Eq. 4-1})$$

$$F_N = F_R + F_I + P - E \quad (\text{Eq. 4-2})$$

where:

F_N is the total freshwater input to the study area exclusive of advective exchanges within the ocean;

F_I is the gain of freshwater due to melting of sea-ice in place. It was assumed that the initial sea-ice thickness was 2 m with a mean salinity of seven (Nakawo and Sinha, 1981). F_I was estimated from changes in the monthly sea-ice charts, as contained in Appendix G (estimated uncertainty is $\pm 15\%$). More details on the computational procedure used to compute F_I are provided in Table 2 (see section on H_I , heat to melt sea-ice);

P is the mean precipitation, and E is the loss due to evaporation. The net value, $P-E$, was derived as one-half of the mean precipitation measured at Tuktoyaktuk, N.W.T. (estimated uncertainty of $\pm 50\%$);

F_R is the Mackenzie River discharge (Appendix H) from December 1, when inshore ice cover had stabilized, until the following summer, with an estimated uncertainty of $\pm 10\%$;

F_O is the freshwater stored in the upper layer during summer. Computational methods are defined in Section 2.6 and displayed in Appendix C. The estimated uncertainties, which vary with spatial sampling density, range from 12 to 40% about a median value of 27%.

F_W is the initial, pre-freshet volumes of fresh water storage in the ocean. Unfortunately, this quantity cannot be estimated due to the paucity of oceanographic data in winter and spring. (However, available oceanographic data in the mid- and offshore continental shelf and continental slope regions for March-April (Figure 6), suggest that in five of six years, interannual variability was small. In the other year (1981), the freshwater content was anomalously negative, presumably the result of extensive mixing and exchanges with more saline waters from the Arctic Ocean during the previous autumn.)

F_A represents the difference in the above terms, and can be attributed to horizontal advection of water and sea-ice out of the Beaufort shelf area through freshet to summer.

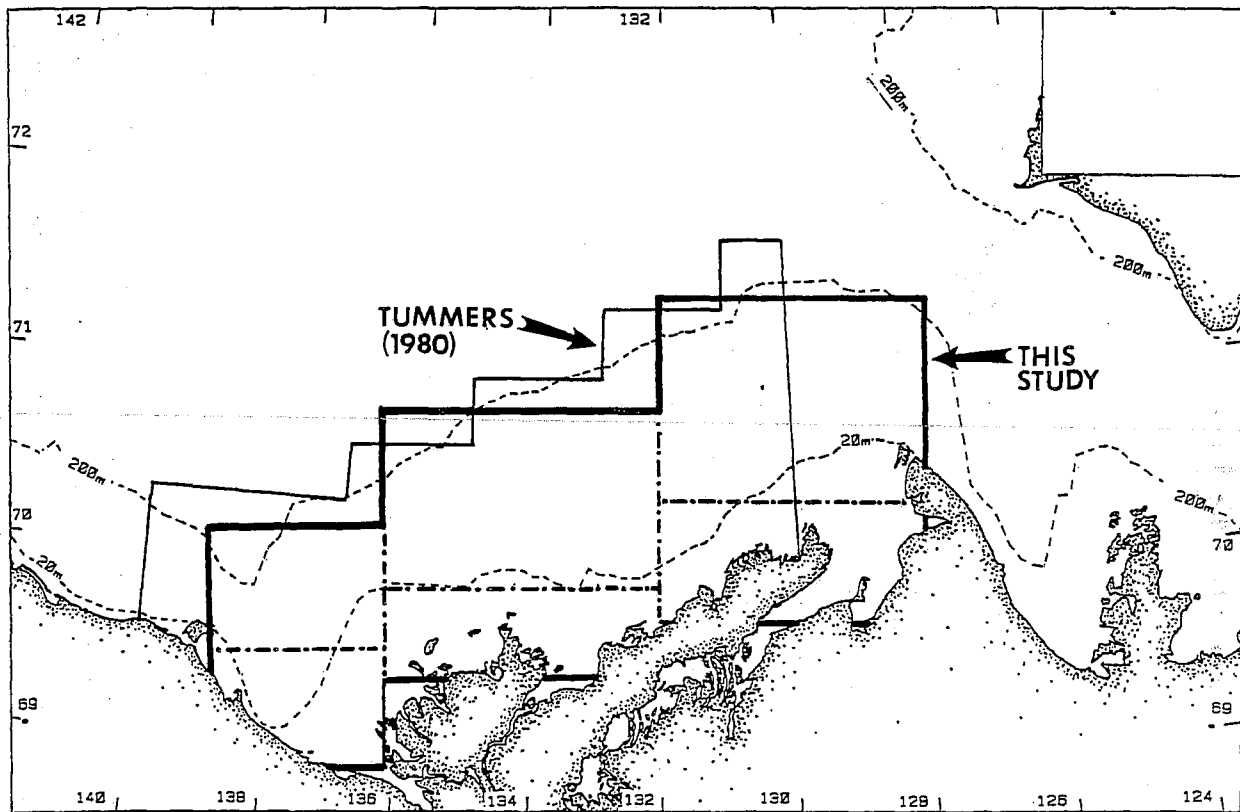


Figure 31: The area of the continental shelf ($61,950 \text{ km}^2$) for which the freshwater and heat budgets were computed.

In principle, our quantitative budget estimates are limited to computing $F_A - F_W$ as the residual term, since F_W cannot be quantitatively estimated from available data. In practice, F_W is expected to be small in most years; it could, however be important when $F_A - F_W$ is large and reflect a large fresh water deficit prior to spring freshet, such as was observed in 1981.

Seasonal Variations, May to August--Mackenzie River discharge represents the dominant source of freshwater input to the continental shelf, amounting to an average value of $25.1 \times 10^{10} \text{ m}^3$ from December (when newly formed sea-ice is sufficiently extensive to retain a freshwater layer beneath it) to August (Figure 32). If all of the freshwater remains over the continental shelf area ($61,900 \text{ km}^2$ as used in our budget computations), the accumulated River discharge is equivalent to a freshwater layer of 4.1 m in thickness.

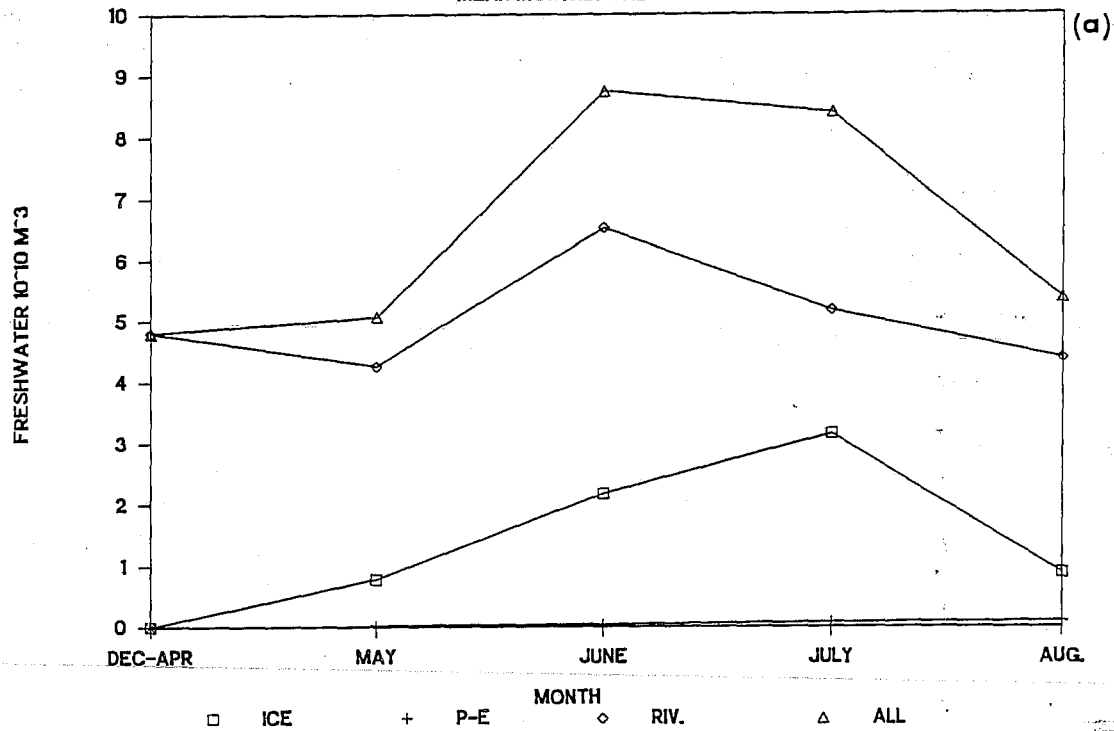
The only other significant source of freshwater is from sea-ice melt, since the excess of precipitation over evaporation is negligible ($<0.3 \times 10^{10} \text{ m}^3$, or an equivalent layer thickness of $<0.05 \text{ m}$). The contribution of freshwater from ice melt is more difficult to estimate, since some of the local sea-ice can be advected out of the study area before it melts or, conversely, sea-ice originating elsewhere can melt within the study area; if it is assumed that the melt of sea-ice is due to local sea-ice only, the total freshwater contribution from May to August is $7.0 \times 10^{10} \text{ m}^3$ (equivalent to a 1.1 m thick layer of freshwater) or approximately 32% of the River contribution. The interannual variability of the ice melt contribution is somewhat larger (30% vs. 20%) than that of River discharge over the four month period of May to August, and it is even larger in the monthly values (50-100% vs. 25-30%; Figure 33). The large interannual variability in sea-ice melt reflect the wide range in sea-ice coverage between: "good" ice years, when the continental shelf is nearly clear of sea-ice by August; and "bad" ice years (eg. 1974 and 1985), when sea-ice cover remains intact over much of the shelf (see section 4.2 Sea-Ice, for a more complete discussion).

Estimates of the storage of freshwater within the ocean were limited in number, ranging from one to two each year, between mid-July and mid-September. The ocean storage values vary enormously from year-to-year, as shown in Figure 34a. From mid-July to mid-August, the mean value is $14.7 \times 10^{10} \text{ m}^3$ (equivalent to 2.4 m layer thickness) with individual values varying from 0.8×10^{10} (1980) to 28.4 (1975). One month later, the range in estimated values remains large from $1.4 \times 10^{10} \text{ m}^3$ (1970) to 29.8×10^{10} (1984) about a mean value of $17.7 \times 10^{10} \text{ m}^3$ (equivalent to 2.9 m freshwater layer).

Advection of Freshwater--The portion of the total freshwater input (F_A) from the time of winter freeze-up through to summer is balanced by (a) $F_0 - F_W$, increased storage of freshwater in the study area and (b) F_A , export of freshwater from the study area. Thus estimates of freshwater advection from the study area can be derived from the estimated values F_N , F_0 and F_W . However, as noted above, the initial value of ocean freshwater storage in the ocean (F_W) cannot be derived in six of the ten years considered. For the other four years (1975, 1985, 1986 and 1987), estimates of F_W are available in the March-April period (Figure 11) over the middle and outer shelf and slope regions. In all these four years, the freshwater content appeared to fall within a narrow range of -0.5 to 0.7 m, as compared to 1981, a year with anomalously high salinities on the continental shelf. For most (six) of the 10 years considered (1970, 1973,

FRESHWATER INPUTS

MEAN MONTHLY VALUES



FRESHW - ALL INPUTS

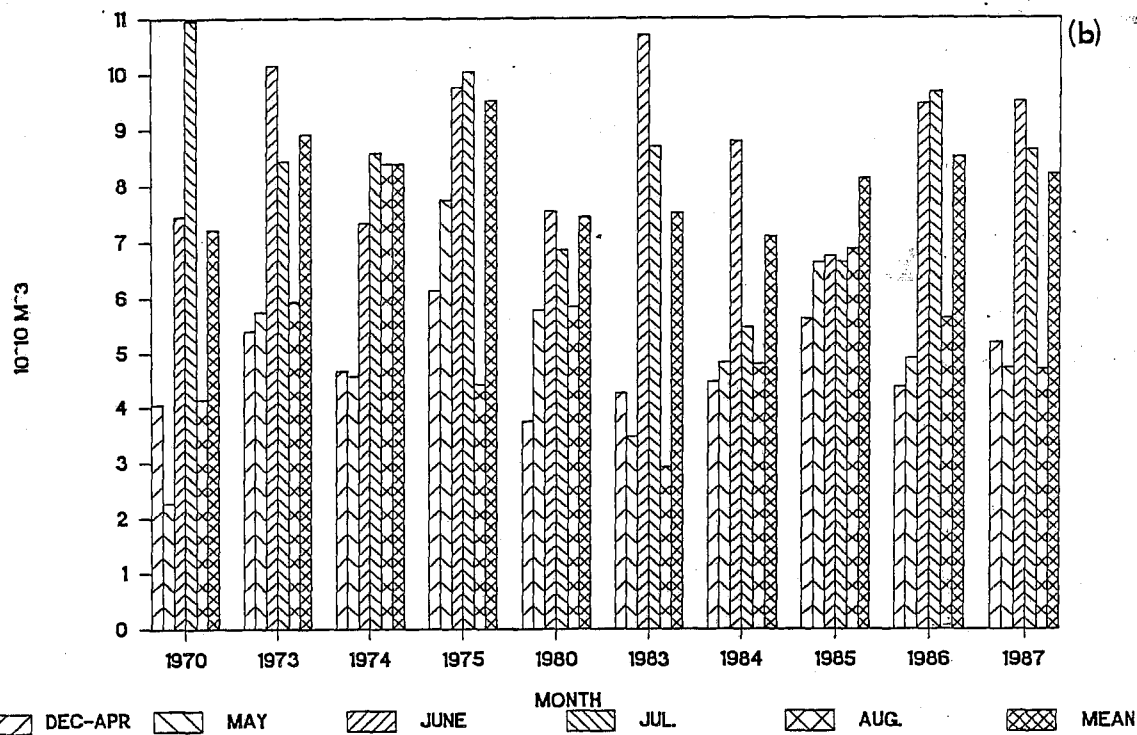


Figure 32: (a) The monthly mean values of freshwater input to the continental shelf including River discharges, melt of sea-ice in place, and the excess of precipitation over evaporation. The mean values are given for May, June, July and August, as well as the cumulative value for the five month period of December to April. (b) Total freshwater inputs to the continental shelf by individual years for the averaging periods shown in (a).

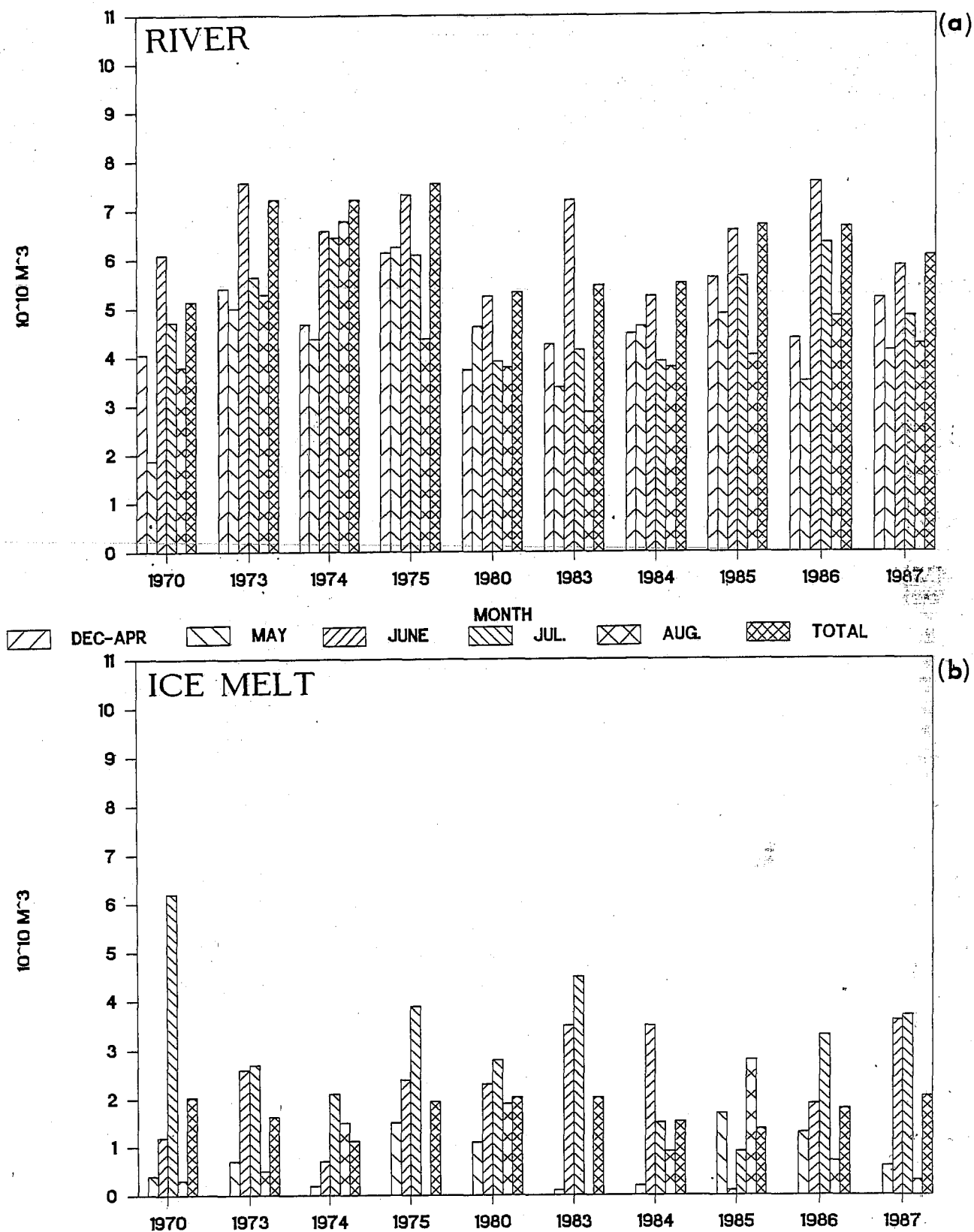


Figure 33: Freshwater input to the continental shelf resulting from (a) River discharge, and (b) ice melt by individual years for the months May, June, July, August as well as the five month averaging period: December-April.

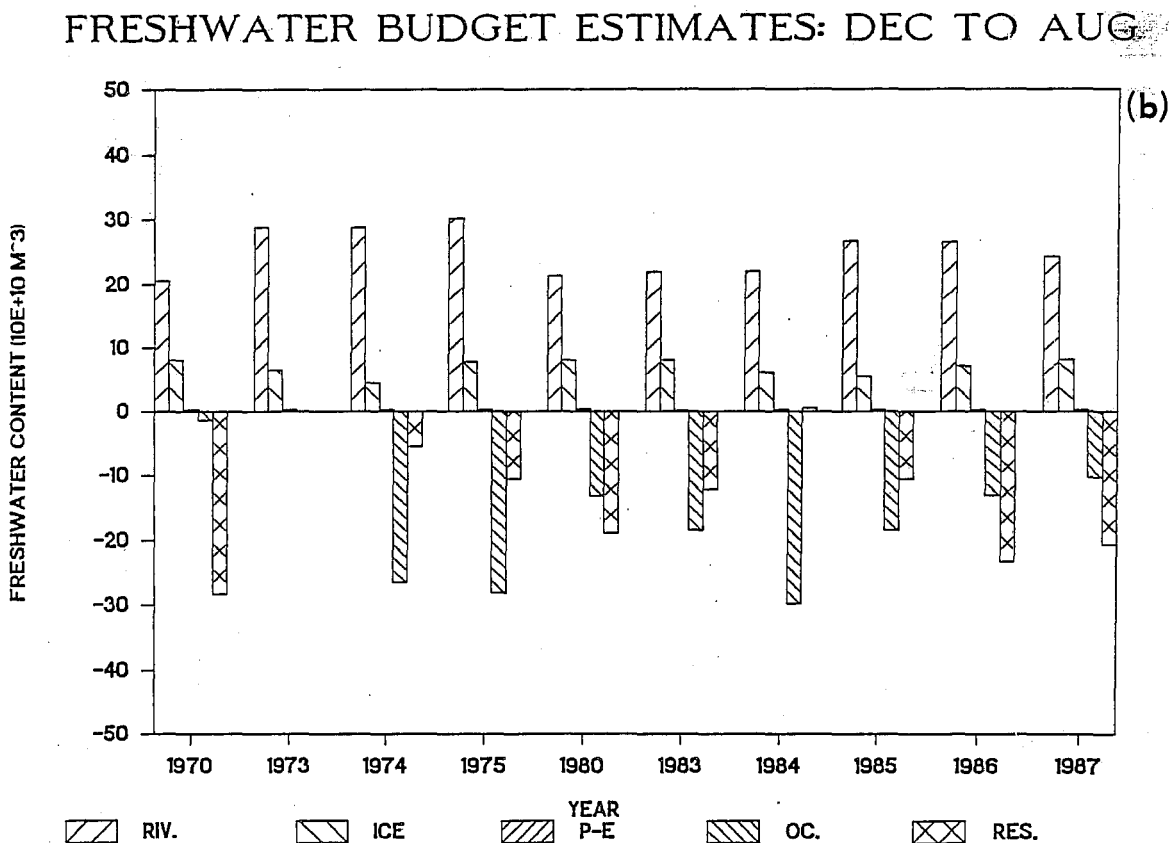
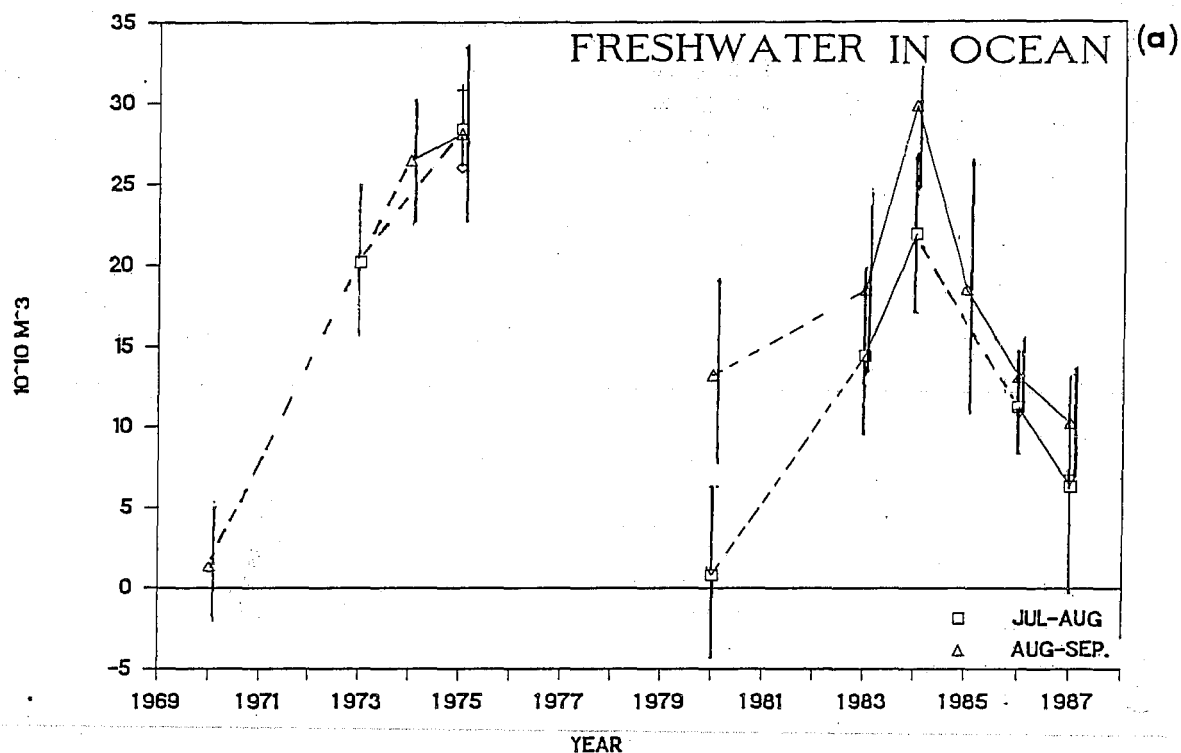


Figure 34: (a) Estimated freshwater stored in the continental shelf by year for the periods: (1) mid-July to mid-August, and (2) mid-August to mid-September. See the text for the method used to estimate the uncertainties shown as error bars. (b) The accumulated value of the freshwater budget terms over the period December to August, by individual years. The numbers displayed below the bars represent the estimated percentage uncertainty (of total freshwater input) in the ocean storage values for each year.

1974, 1980, 1983, 1984), we assume that the F_w was also small and near-normal. If this assumption is incorrect and the salinities were unusually high, as in 1981, the computed value of advection off the shelf (F_A) would be overestimated (i.e. too large) by a considerable amount ($12 \times 10^{10} \text{ m}^3$ in 1981).

Given the large interannual variability in ocean storage of freshwater over the continental shelf (Figure 34b), the residual losses of freshwater are correspondingly large. The estimated advective losses of freshwater from the continental shelf range from near zero in 1984 to an estimated $25 \times 10^{10} \text{ m}^3$ by mid-September of 1970. The large loss estimated for the summer of 1970 amounts to between 80 and 100% of the total freshwater input.

Using the approach outlined above, estimates of the proportion of the total freshwater input advected off the continental shelf are displayed in Figure 35a. Note the large magnitude of the error bars relative to the estimate of advective losses arising from sparse oceanographic sampling in each of the shelf subareas and the additional uncertainty in the six years where F_w cannot be estimated. Given the magnitude of the estimated uncertainties, the small negative percent losses computed in 1984 simply reflect very small advective losses in that year.

In four of the ten years considered (1973, 1974, 1975 and 1984), advective losses are comparatively small, amounting to less than 25% of the cumulative input. Three of the years (1970, 1980 and 1987) exhibit large advective losses likely exceeding 70% of the cumulative input, although the estimates from 1980 and 1987 have large uncertainties ($\pm 25\%$), due to poor spatial coverage of the available oceanographic observations. (For 1970 and 1980, the actual losses due to advection may be overestimated due to the absence of estimates for F_w .) For the remaining three years (1983, 1985 and 1986), the estimated losses have intermediate values, between 25 and 75% of the cumulative freshwater input. (The 1983 values are more uncertain due to lack of F_w estimates.) The estimate of advective losses for 1985 is also considered particularly uncertain, because of the extensive but broken sea-ice which covered the middle and outer portion of the Mackenzie Shelf, and impeded any data collection. The extent to which freshwater occupied this extensive area is not known.

Thomas et al. (1986) estimated the flushing time for freshwater on the continental shelf to be about four months, as computed from 1974 and 1975 measurements. In particular, they estimated an advective freshwater loss of $11.2 \times 10^{10} \text{ m}^3$ between the spring and summer of 1975, equivalent to 60% of the incoming river input over the same period. In this study, the estimated values of advective losses for this same year are somewhat smaller: $7.5 \times 10^{10} \text{ m}^3$ by mid-August and $10.5 \times 10^{10} \text{ m}^3$ in early September due to differences in the methods and assumptions used in estimating the freshwater terms associated with ice melt and ocean storage. Our results suggest that the flushing rates of freshwater from the continental shelf during the summer are highly variable from year to year, and could be significantly smaller in some years (eg. 1973-1975, 1984), and larger in others (1970, 1980, 1987), than the estimated values of Thomas et al. (1986).

The cause of the large interannual variations in advective losses of freshwater appear to be related, at least in part, to the extent of sea-ice clearing experienced during spring and summer. Regression analyses for all freshwater content in the ocean subregions on available ice data (Figure 22)

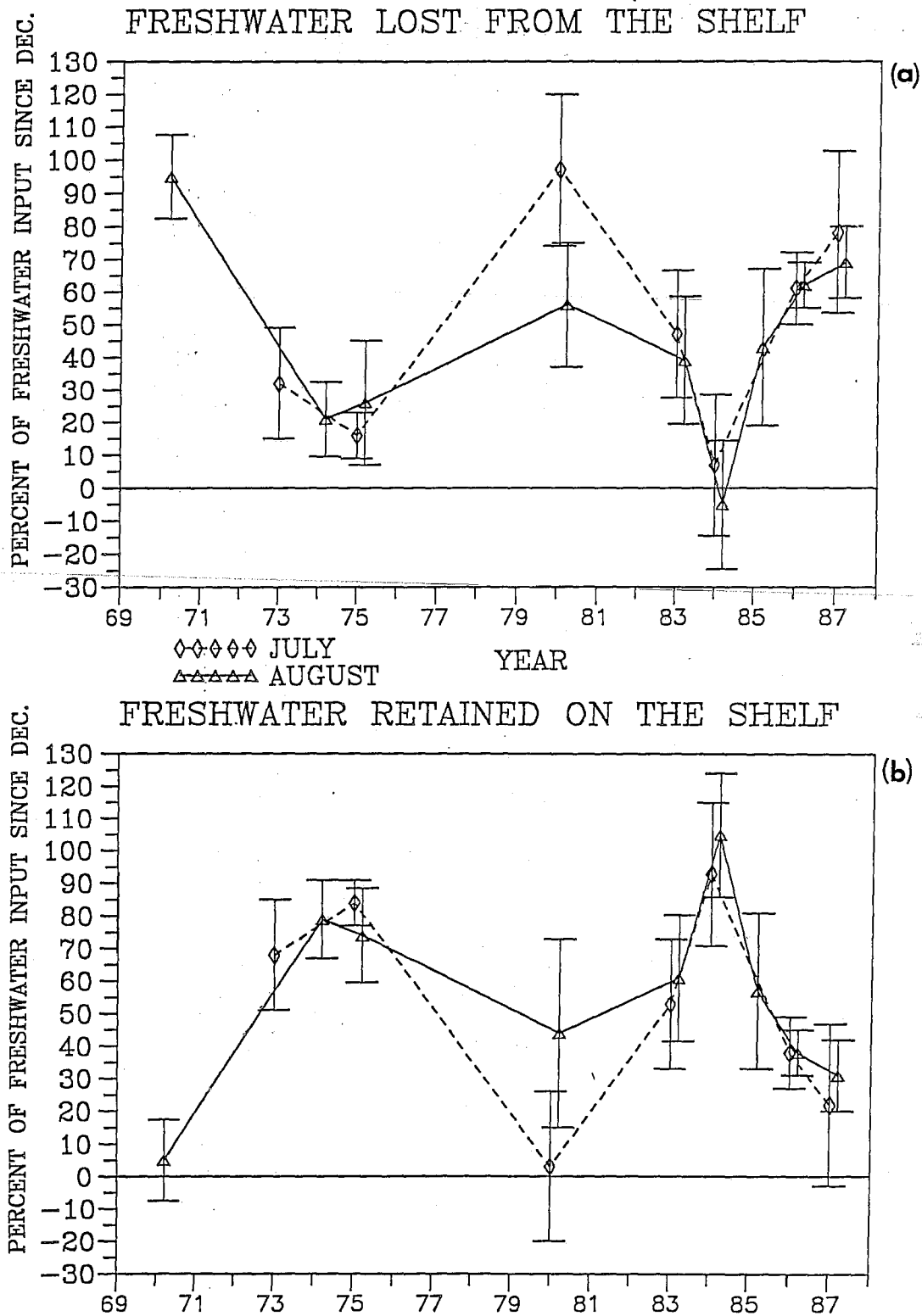


Figure 35: The computed values of (a) freshwater lost from the continental shelf and (b) freshwater retained on the continental shelf, as a percentage of total freshwater input. The values displayed represent the cumulative losses from the period beginning in December to either: mid-July to mid-August; or mid-August to mid-September.

revealed a significant negative correlation between freshwater and the area of open water and low sea-ice concentrations. These results suggest that extensive sea-ice cover would impede dispersal and advection of freshwater from the shelf into adjoining regions. This mechanism was clearly operative in the extreme ice year of 1974, and to a lesser extent in 1985 and 1984 when the clearing of sea-ice was limited. Conversely, of the three years for which there are large advective losses of freshwater, two of these years (1980 and 1987) were characterized by extensive clearing of the sea-ice in July and extending into August.

Even with the correspondence between advective losses of freshwater and open water areas evident for some years, there are other years (1970, 1973 and 1975) having moderate levels of open water area for which advective losses do not follow the same implied relationship to open water area. Wind-driven advection from the shelf may also be important, and the general wind pattern was compared to estimated advective losses:

Year	Loss of Freshwater	Open Water Area	Wind Run (10^3 km) (Jul 1-Aug 31)
1970	large	moderate	20, to W
1973	small	moderate	6, to W
1974	small	small	13, to W
1975	small	moderate	5, to W
1980	large	large	12, to W
1983	moderate	moderate	15, to W
1984	small	small	<1, to W
1985	small-moderate	small	4, to W
1986	moderate	moderate	13, to W
1987	large	large	-5, to E

The above comparisons to the wind observations indicate that the wind may be important in those years when the open water area is at intermediate levels. In 1970, the wind-driven advection was very large and directed westward, which may account for the large advective losses of freshwater computed in that year. In 1973 and 1975, the net wind run was relatively small, amounting to less than 30% of the 1970 level, which may account for the small advective losses of both these years.

These results suggest that clearing of sea-ice is the primary factor in controlling advection off the continental shelf. However, in years having intermediate levels of sea-ice clearing, the wind patterns and resulting surface layer advection may also affect the overall degree of advective losses during the summer months.

Heat Budget

The underlying calculations used in the heat budget of Tummers (1980) followed the general methods developed and previously applied by Maykut and Untersteiner (1971), Badgely (1966), Walmsley (1966) and Huyer and Barber (1970). Heat fluxes were calculated for the southeastern sector of the Beaufort Sea as delineated in Figure 31. An equality was assumed between the sum of fluxes and

net change in the energy stored in the sea-ice and water components of the studied system.

$$Q_A + Q_I + Q_R + Q_O + Q_N = 0 \quad \text{where} \quad (\text{Eq. 4-3})$$

$$Q_A = Q_S + Q_{AL} + Q_L + Q_E + Q_H \quad (\text{Eq. 4-4})$$

where:

Q_A is the surface energy balance, or net heat transferred through or from the atmosphere into the ocean;

Q_S represents the heat at the surface due to incident solar radiation;

Q_{AL} is the portion of Q_S lost due to reflection of short wave radiation from the surface (surface albedo);

Q_E represents the net latent heat exchange with the atmosphere. (Evaporation and melting represent losses and gains in the system energy respectively.);

Q_H is the net transfer of sensible heat between the sea and ice surface and the atmosphere;

Q_R is the heat input of the Mackenzie River;

Q_O represents the change in the heat content of the upper 50 m of the ocean;

Q_I represents the heat used to warm the ice and subsequently melt it in place;

Q_N represents the heat advected through oceanic boundaries, either by ocean currents or melting of imported sea-ice;

Q_L is the net long wave radiation lost from the surface.

Heat fluxes which result in transfer of heat into the ocean are positive and those which result in a loss of heat from the ocean are negative.

Calculation of the above fluxes was carried out for the study region from the May through August periods, which represents the time of year of substantial net transfer of heat to the ocean. Before and after this period, the ocean loses heat to the atmosphere.

To avoid the inherent difficulties in computing the atmospheric source terms (Q_S , Q_{AL} , Q_L , Q_E , Q_H) due to the paucity of suitable over-water measurements, estimated climatological means were used for the small Q_E and Q_H values, as derived from Burns (1973) and Tummers (1980). The much larger radiation flux value, consisting of net short wave radiation ($Q_S - Q_{AL}$) and net long wave radiation (Q_L), was estimated using available meteorological observations at two coastal locations: Tuktoyaktuk and Sachs Harbour, N.W.T. In all cases, the use of parameterizations or other assumptions was required to provide quantitative

Table 2

A summary of data sources, computational techniques and estimated uncertainties for quantities used in the heat budget computations.

Quantity and Data Sources	Algorithm	Estimated Uncertainty										
<p>Incident Solar Radiation (K_{in})</p> <p>R_{in} - incident solar radiation per unit area computed for the full study area</p> <p>R_{SH} - incident solar radiation per unit area measured at Sachs Harbour, N.W.T.</p> <p>C_{TK} - fractional cloud cover measured at Tuktoyaktuk, N.W.T.</p>	<p>$K_{in} = R_{in} * \text{Area}$; where</p> <p>$R_{in} = R_{SH} * (-0.6667 * C_{TK} + 1.3333)$</p> <p>The factor in parenthesis represents a reduction in solar radiation resulting from more cloudiness over marine areas in comparison with coastal measurement sites. To estimate these additional losses, a linear function of mean monthly cloud cover at Tuktoyaktuk was derived. The average reductions by month are:</p> <table><tr><td>May</td><td>0.91</td></tr><tr><td>June</td><td>0.92</td></tr><tr><td>July</td><td>0.86</td></tr><tr><td>August</td><td>0.85</td></tr></table>	May	0.91	June	0.92	July	0.86	August	0.85	<p>+/- 20 percent</p> <p>due primarily to the use of coastal measurements for estimation of marine conditions</p>		
May	0.91											
June	0.92											
July	0.86											
August	0.85											
<p>Solar Radiation Absorbed K_{net}</p> <p>Surface albedo (A) derived from tabulated values (Vowinkel and Orvig, 1970; Burns, 1973)</p>	<p>$K_{net} = R_{in} * \text{SUM} [(Area_i) * (1 - A_i)]$; for all i</p> <p>Surface albedo (A_i) values were assigned for the portion of the study area with open water ($A = 0.07$) and for the area covered by sea-ice:</p> <table><tr><td></td><td>A</td></tr><tr><td>May</td><td>0.69</td></tr><tr><td>June</td><td>0.50</td></tr><tr><td>July</td><td>0.35</td></tr><tr><td>August</td><td>0.40</td></tr></table>		A	May	0.69	June	0.50	July	0.35	August	0.40	<p>+/- 15 percent</p> <p>due to uncertainty in the albedo</p>
	A											
May	0.69											
June	0.50											
July	0.35											
August	0.40											
<p>Net Longwave Radiation (L-net)</p> <p>Q_b is the back radiation from the surface in the absence of cloud; taken to be constant at 95 W/m^2 (Pond and Emery, 1984); for the range of surface temperatures & humidities experienced from May to June, the actual value will be in the range of 90 to 105 W/m^2</p>	<p>$L_{net} = Q_b * (1 - 0.083 * C_K)$</p>	<p>+/- 20 percent</p> <p>due to uncertainties in actual cloud conditions over the full area and due to variation in Q_b from assumed constant value</p>										

Table 2, continued...

<p>Sensible Heat (H_s)</p> <p>Q_h is the sensible heat flux between the atmosphere and In this study, we used climatological mean values derived for the Beaufort Sea (Vowinckel and Orvig, 1970):</p> <table> <tr> <th>Month</th><th>Open Water (kJ/m²)[‡]</th><th>Sea-Ice (kJ/m²)[‡]</th></tr> <tr> <td>May</td><td>-6.9</td><td>-3.6</td></tr> <tr> <td>June</td><td>0.8</td><td>-0.8</td></tr> <tr> <td>July</td><td>-1.7</td><td>0.8</td></tr> <tr> <td>August</td><td>-3.6</td><td>-0.6</td></tr> </table>	Month	Open Water (kJ/m ²) [‡]	Sea-Ice (kJ/m ²) [‡]	May	-6.9	-3.6	June	0.8	-0.8	July	-1.7	0.8	August	-3.6	-0.6	$H_s = \text{SUM}(Q_{h_ice} * \text{Area}_{ice} + Q_{h_water} * \text{Area}_{water});$ <p>for all months, May to August</p>	<p>+/- 15 percent</p> <p>due to use of climatological and monthly mean values of sensible fluxes.</p>
Month	Open Water (kJ/m ²) [‡]	Sea-Ice (kJ/m ²) [‡]															
May	-6.9	-3.6															
June	0.8	-0.8															
July	-1.7	0.8															
August	-3.6	-0.6															
<p>Latent Heat (H_e)</p> <p>Q_e is the latent heat flux between the atmosphere and ocean. In this study, we used climatological mean values derived for the Beaufort Sea (Vowinckel and Orvig, 1970):</p> <table> <tr> <th>Month</th><th>Open Water (kJ/m²)[‡]</th><th>Sea-Ice (kJ/m²)[‡]</th></tr> <tr> <td>May</td><td>-5.4</td><td>-1.7</td></tr> <tr> <td>June</td><td>1.7</td><td>-1.7</td></tr> <tr> <td>July</td><td>-2.2</td><td>-2.5</td></tr> <tr> <td>August</td><td>-0.8</td><td>-0.4</td></tr> </table>	Month	Open Water (kJ/m ²) [‡]	Sea-Ice (kJ/m ²) [‡]	May	-5.4	-1.7	June	1.7	-1.7	July	-2.2	-2.5	August	-0.8	-0.4	$H_e = \text{SUM}(Q_{e_ice} * \text{Area}_{ice} + Q_{e_water} * \text{Area}_{water});$ <p>for all months, May to August inclusive</p>	<p>+/- 15 percent</p> <p>due to use of climatological and monthly mean values of sensible fluxes.</p>
Month	Open Water (kJ/m ²) [‡]	Sea-Ice (kJ/m ²) [‡]															
May	-5.4	-1.7															
June	1.7	-1.7															
July	-2.2	-2.5															
August	-0.8	-0.4															
<p>River Heat (H_r)</p> <p>R is the monthly total volume discharge measured at gauging sites on the MacKenzie River (section 3.3);</p> <p>T_r is the climatological mean temperature measured in the river delta (see Figure 4.3-2):</p> <table> <tr> <th>Month/dates</th><th>1-15</th><th>16-end</th></tr> <tr> <td>May</td><td>1</td><td>2</td></tr> <tr> <td>June</td><td>6</td><td>12</td></tr> <tr> <td>July</td><td>17</td><td>17</td></tr> <tr> <td>August</td><td>16</td><td>14</td></tr> </table> <p>rho is the density of the river water (1000 kg/m³);</p> <p>C_p is the specific heat of water taken as 4211 J/kg/deg.C</p>	Month/dates	1-15	16-end	May	1	2	June	6	12	July	17	17	August	16	14	$H_r = \rho * C_p * \text{SUM}[R * (T_r - (-1.5))];$ <p>for each half-month from May to August, inclusive.</p>	<p>+/- 20 percent</p> <p>due to uncertainties associated with the use of climatological temperatures</p>
Month/dates	1-15	16-end															
May	1	2															
June	6	12															
July	17	17															
August	16	14															

[‡] a negative sign denotes heat transfer from the ocean to the atmosphere.

Table 2, continued...

<p>Heat to melt ice in place (H_i)</p> <p>T is the mean ice thickness, 1.8m</p> <p>ρ_{ice} is mean density of sea-ice, 900 kg/m³</p> <p>h_f is the heat of fusion required melt sea-ice, 3.31E+5 J/kg/m²</p> <p>$area_{i_1}$ is the area covered with sea-ice of category i at month-end</p> <p>$area_{i_0}$ is the area covered with sea-ice of category i at the beginning of the month</p>	$H_i = \rho_{ice} * T * h_f * \text{SUM}[conc_i * (area_{i_1} - area_{i_0})]$ <p>for $conc_i$ categories:</p> <table> <tr> <th>category</th><th>range in mean tenths</th><th>$conc_i$</th></tr> <tr> <td>A+B</td><td>1-6</td><td>0.35 (all months)</td></tr> <tr> <td>C</td><td>7-10</td><td>0.97 (May)</td></tr> <tr> <td></td><td></td><td>0.92 (June)</td></tr> <tr> <td></td><td></td><td>0.87 (July)</td></tr> <tr> <td></td><td></td><td>0.82 (Aug.)</td></tr> </table> <p>N.B. $H_i = 0$ if overall ice concentration increases</p>	category	range in mean tenths	$conc_i$	A+B	1-6	0.35 (all months)	C	7-10	0.97 (May)			0.92 (June)			0.87 (July)			0.82 (Aug.)	<p>+/- 15 percent</p> <p>due to uncertainties in observations of sea-ice coverage and mean thickness.</p> <p>This estimated uncertainty does not include heat lost or gained associated with the melting of sea-ice that is advected into or out of the study area.</p>
category	range in mean tenths	$conc_i$																		
A+B	1-6	0.35 (all months)																		
C	7-10	0.97 (May)																		
		0.92 (June)																		
		0.87 (July)																		
		0.82 (Aug.)																		
<p>Heat to warm (or cool) the upper 50 m of the ocean</p>	<p>Computed as the area-weighted sum of the heat content in each subarea (Table 1) using the method described in section 2.6.</p> <p>Two additional adjustments were made:</p> <p>(1) where the ocean surface was covered by high concentrations of sea-ice (7-10 tenths), the heat content was assumed to be zero (i.e. mean temperature of -1.5 C beneath the sea-ice;</p> <p>(2) the heat content of the upper 1 m of the water column was computed and included in the total. To do this, the mean measured temperature a 1 m was assumed to extend to the surface.</p>	<p>+/- 10 percent</p> <p>due to a combination of uncertainties:</p> <ul style="list-style-type: none"> - insufficient time and spatial sampling; - measurement uncertainties in each individual profile; - in most profiles, the sampling does not extend to the sea-bed; - estimated area of heavy sea-ice concentration, and the zero heat content beneath sea-ice; - neglect of heat content in shallow nearshore areas where water depths were so small as to preclude sampling in most oceanographic surveys. 																		

estimates of the heat budget term. For the largest term (incident solar radiation term Q_S), two versions were applied. In the first, the direct measurements at Sachs Harbour were assumed to be representative of the full study area. In the second version, the effect of increased cloudiness experienced over marine areas was simulated through application of an additional factor, derived as a linear function of measured cloudiness at Tuktoyaktuk. This additional factor results in a mean reduction of 15% in Q_S , which likely still overestimates the actual net radiation, given the 30% reductions inferred from the results of Tummers (1980) in comparisons of solar radiation measured at Sachs Harbour with computed values using ship-based observations (used by Tummers only in August).

For all other terms, a single method of computation was applied in heat budget calculations. Further details on data sources, computational techniques and estimated uncertainties of the heat budget are provided in Table 2.

The non-atmospheric quantities (Q_I , Q_R and Q_0) were computed using available river discharge, ice concentration and oceanographic measurements tabulated for this study. To compute heat input from the Mackenzie River, mean River temperatures compiled from several years of observations in Figure 36 (Marko et al., 1983) were applied. The heat used to warm the ocean (Q_0) was computed using all available summer oceanographic data for each individual year, with the initial value in spring (taken as May 1 prior to freshet) being assumed to be zero. The spring oceanographic observations (Figure 11) suggest that this assumption will introduce uncertainties of approximately 10% or less in comparison with the summertime values of ocean heat content. Further details on computational methods, along with estimated uncertainties, are given in Table 2.

Finally, the residual form of all the above terms, taken to be Q_I (heat due to ice advection) by Tummers, was redefined for this study. Tummers (1980) assumed that "residual currents [were] weak and therefore cause little heat advection when compared to the river's heat input...". Given the results of freshwater budget computations, indicating considerable advection from the continental shelf in some years, this assumption appears suspect. Therefore, in this study, Q_I is considered to include all horizontal advective exchanges involving both water and ice (other than heat due to river discharge already estimated as Q_R).

Uncertainties in Estimated Heat Budget Terms--Prior to considering the heat budget results, the substantial uncertainties inherent in the computations should be considered (Figure 37). Due to paucity of direct observations, most terms were estimated through approximate parameterizations leading to considerable uncertainties (Table 2). The five terms representing individual components of vertical heat exchanges between the ocean and atmosphere (Q_S , A_{AL} , Q_L , Q_E , Q_H) had estimated uncertainties ranging from 15 to 21%. Using standard error estimation techniques (based on the ten-year mean magnitudes of each term), the uncertainty in Q_A (the net heat transferred from or through the atmosphere into the ocean) is much larger, with an estimated value of $\pm 49\%$. Since it is likely that the errors in each term are not independent, the actual cumulative uncertainty may be smaller.

The uncertainty in the estimated net transfer of heat to the ocean, Q_T (excluding advection through ocean boundaries), amounts to $\pm 78\%$, with the inclusion of the uncertainties in heat due to river input and in-place ice melt.

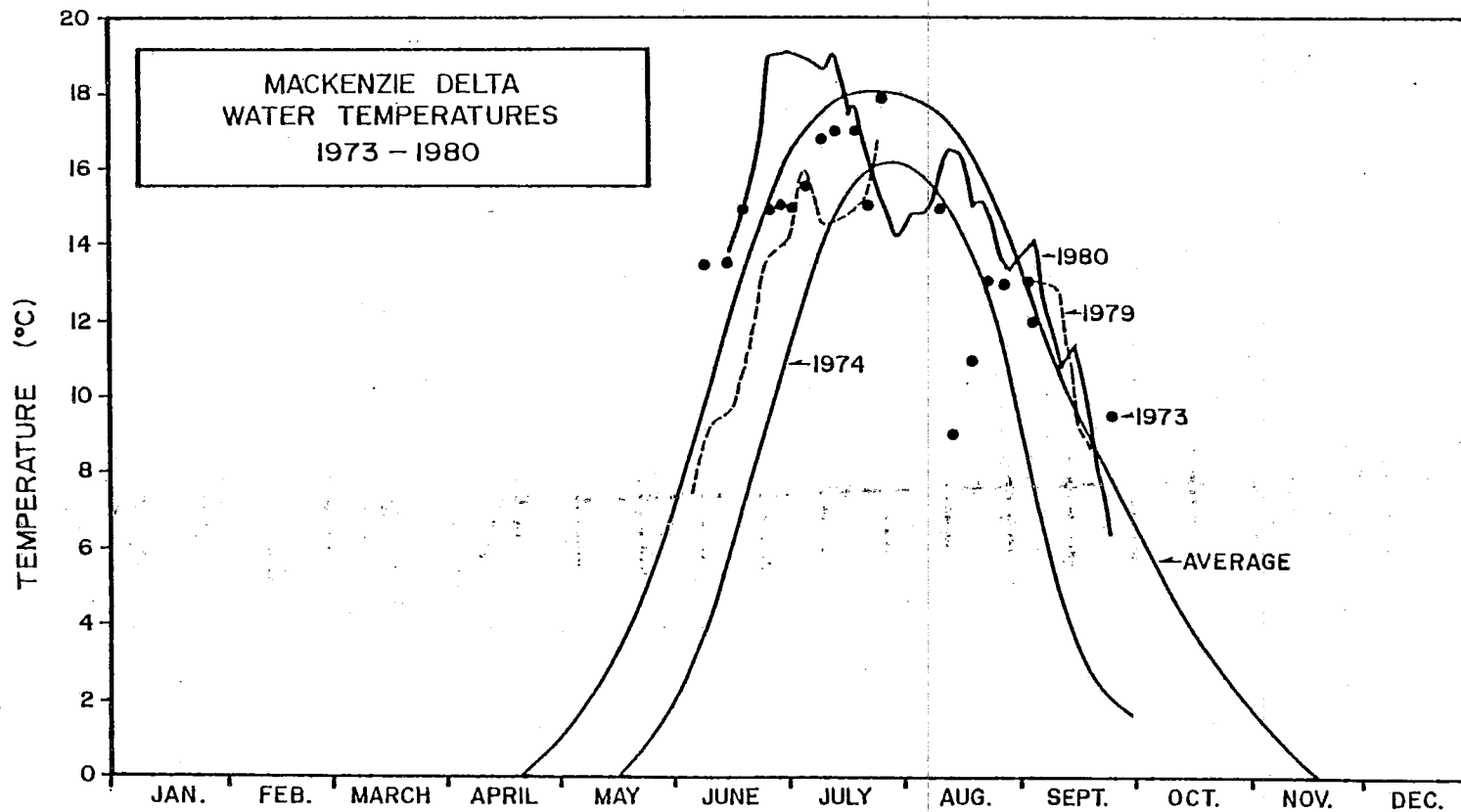


Figure 36: Water temperature measurement data for the Mackenzie River near Arctic Red River (Davies, 1975; B.C. Hydro, unpubl. data) and at points in the Mackenzie Delta. The included average temperature versus time curve is used in the heat budget computations (From Marko et. al., 1983).

EST. ERRORS IN HEAT BUDGET TERMS

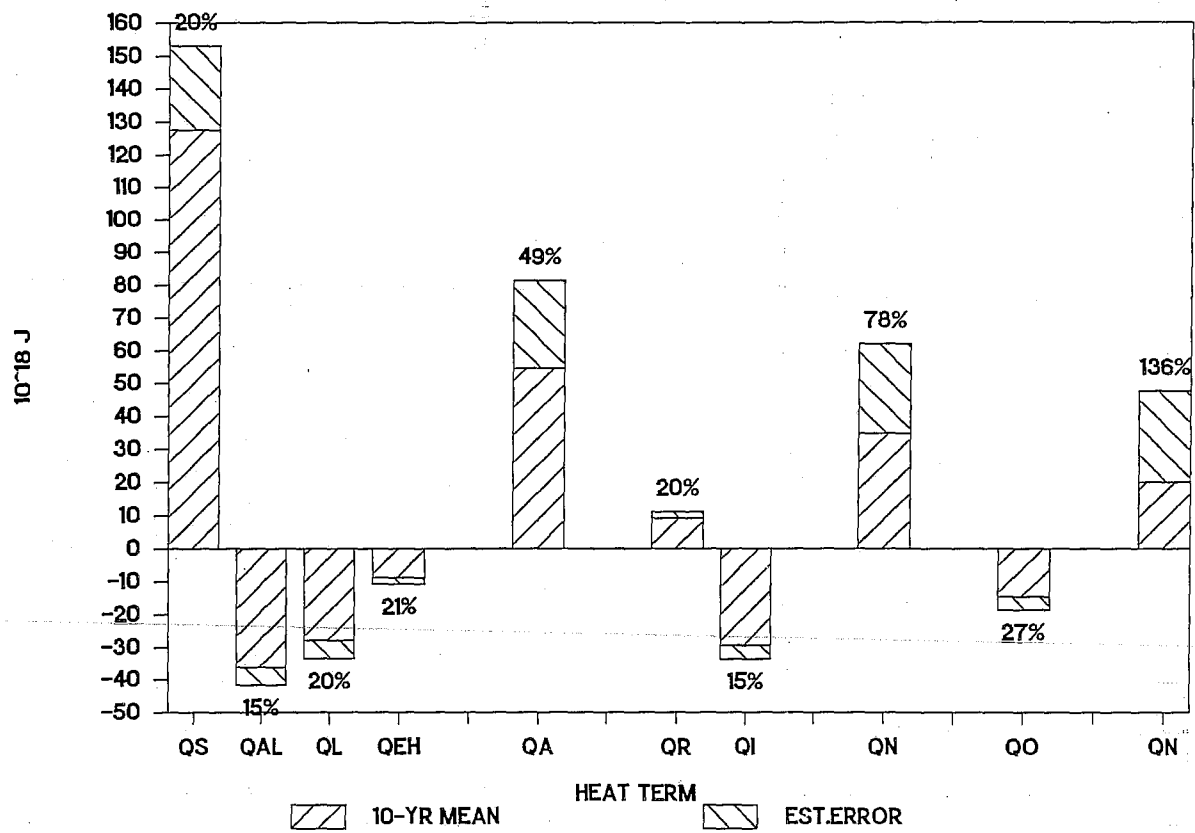


Figure 37: The long-term mean (computed over ten years) values of the heat budget terms, accumulated over the period May-August, along with the estimated uncertainty.

The uncertainties in the oceanic heat storage (Q_0) are highly variable (12 to 40% about a median value of 27%), according to the spatial sampling density available for each period of observations. For the residual heat term (Q_N), the resulting combination of oceanic heat with the net transfer of heat to the ocean (Q_T) leads to an estimated uncertainty of $\pm 136\%$ in Q_N . Given this large uncertainty, the residual term is essentially meaningless.

Atmospheric Heat Fluxes--The vertical heat exchanges between the atmosphere and ocean, or surface energy balance, are dominated by the net solar radiation from May to August (Figure 38). The incoming solar radiation is largest in May and decreases through the summer months. However, losses due to reflection from the extensive sea-ice cover in May and June result in the peak levels of the absorbed solar radiation being shifted to July, with an average value of 29.3×10^{18} J (25.5×10^{18} J in the version simulating increased marine cloudiness). Losses due to long wave net radiation and latent and sensible heat fluxes further reduce the net vertical heat exchanges to maximum monthly levels of 21.0×10^{18} J in July (17.1×10^{18} J including estimated marine cloudiness). A comparison of the atmospheric heat fluxes computed in this study reveals reasonably good agreement with those of previous heat budget studies in the Canadian Arctic (Figure 39).

The interannual variations in the surface energy balance from May to August (Figure 40) amount to approximately $\pm 25\%$ of the ten-year mean value of 54.7×10^{18} J (44.5×10^{18} J with increased marine cloudiness). The largest atmospheric heat input occurred in 1987 (65.0 or 55.7×10^{18} J) while the smallest value (42.5 or 34.0×10^{18} J) occurred in 1974. The net heat exchanged depends on a wide variety of factors, with the most important being the incoming solar radiation, although the level of interannual variability is comparatively small at $\pm 12\%$. The variations in surface albedo associated with good (eg. 1987) and bad (eg. 1974) ice years are also important, having a comparatively larger degree of interannual variability.

A comparison of the atmospheric heat gained by the ocean as computed in this study and the results of Tummers (1980) reveals a systematic difference of 15 to 34% in the computations. Tummers (1980) estimates the total heat gained from the atmosphere as 49.8×10^{18} J in 1974 (and 69.1×10^{18} J in 1975). The corresponding results from this study are: 42.5×10^{18} J in 1974 and 58.7×10^{18} J in 1975 (34.0×10^{18} J in 1974 and 43.9×10^{18} J in 1975, using the simulated increase in marine cloudiness).

Some differences between this study and Tummers (1980) may arise from differences in computational techniques:

- (1) the study area of Tummers is smaller (stated to be $46,794 \text{ km}^2$ on p. 32, although his map of (p. 194) indicates the area to be approximately $54,750 \text{ km}^2$). Our study area measures $61,950 \text{ km}^2$;
- (2) Tummers' (1980) computations are derived for the period May 1 to August 15, or 16 days less than the period used in this study (May 1 to August 31);
- (3) Tummers (1980) computed incident solar radiation using marine cloud observations when available (August); while in this study, two versions of computing incident solar radiation were used: (1) using solar radiation at

ATMOSPHERIC HEAT TERMS

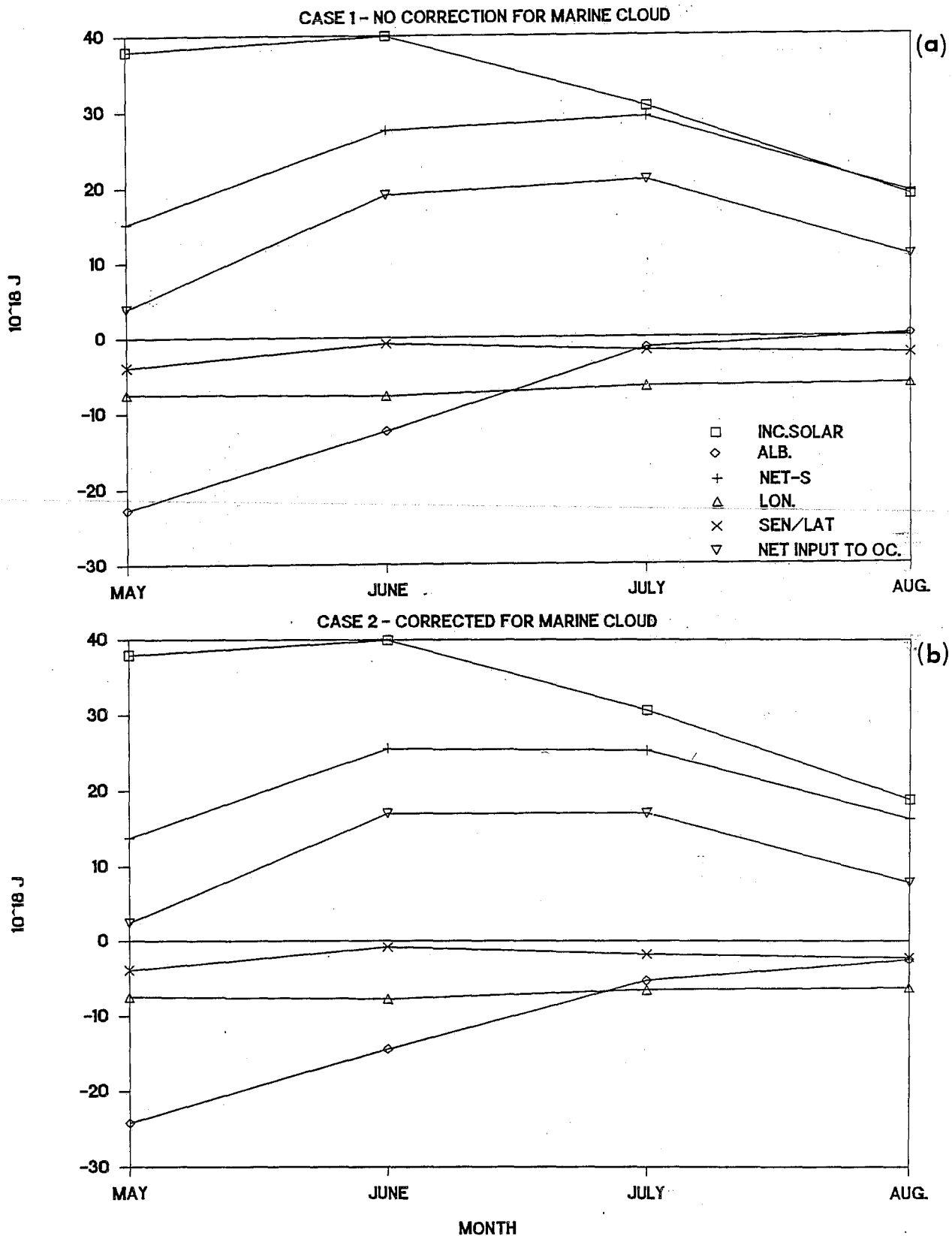
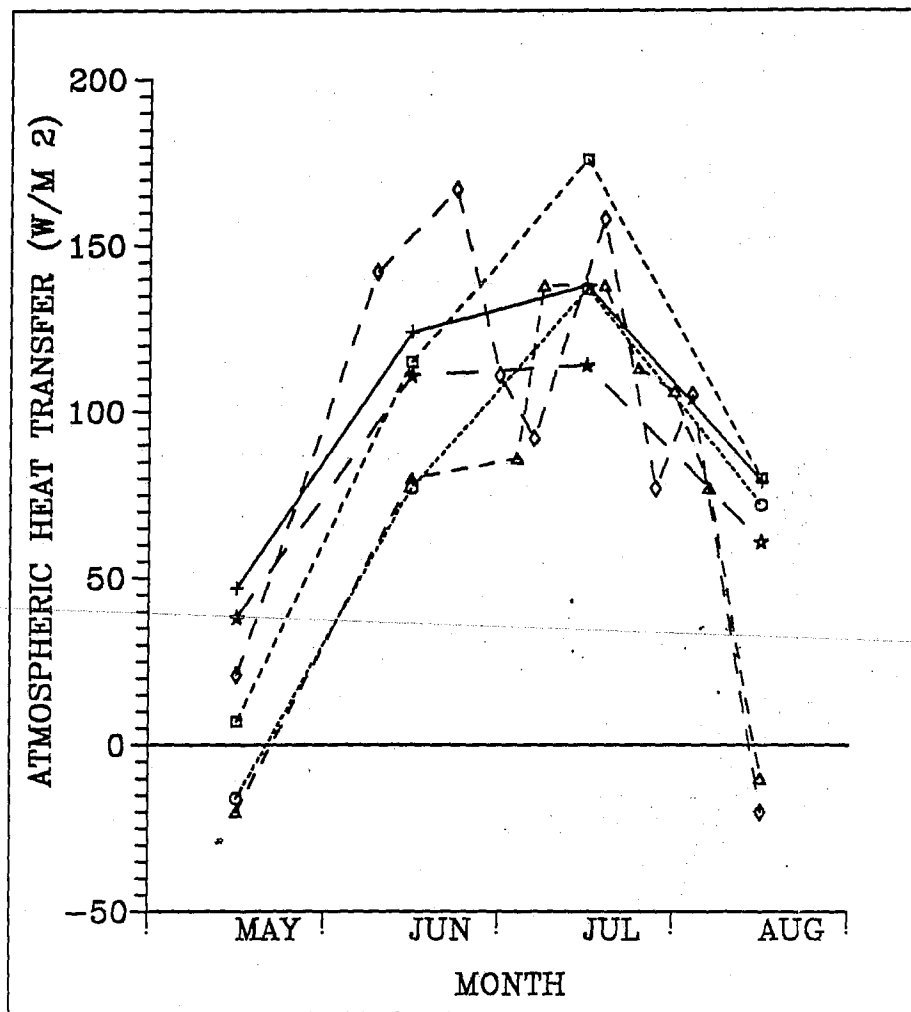


Figure 38: The long-term monthly means for all terms related to exchange of heat from the atmosphere computed with incident solar radiation determined (a) case 1 - from Sachs Harbour direct measurements and (b) case 2 - including an additional factor to simulate losses due to increased cloudiness over the ocean.



○○○○○ BAFFIN BAY (1919-1942): WALMSLEY
 ■■■■■ BARROW STRAIT (1962): HUYER AND BARBER
 ▲▲▲▲▲ BEAUFORT SEA (1974): TUMMERS
 ◇◇◇◇◇ BEAUFORT SEA (1975): TUMMERS
 ***** BEAUFORT SEA (1970-1987): THIS STUDY - CASE 2
 +++++ BEAUFORT SEA (1970-1987): THIS STUDY - CASE 1

Figure 39: A comparison of heat fluxes from this study with those of previous heat budget studies in the Canadian Arctic.

NET ATMOSPHERIC HEAT TRANSFER

CASE 1: NO CORRECTION FOR MARINE CLOUDS

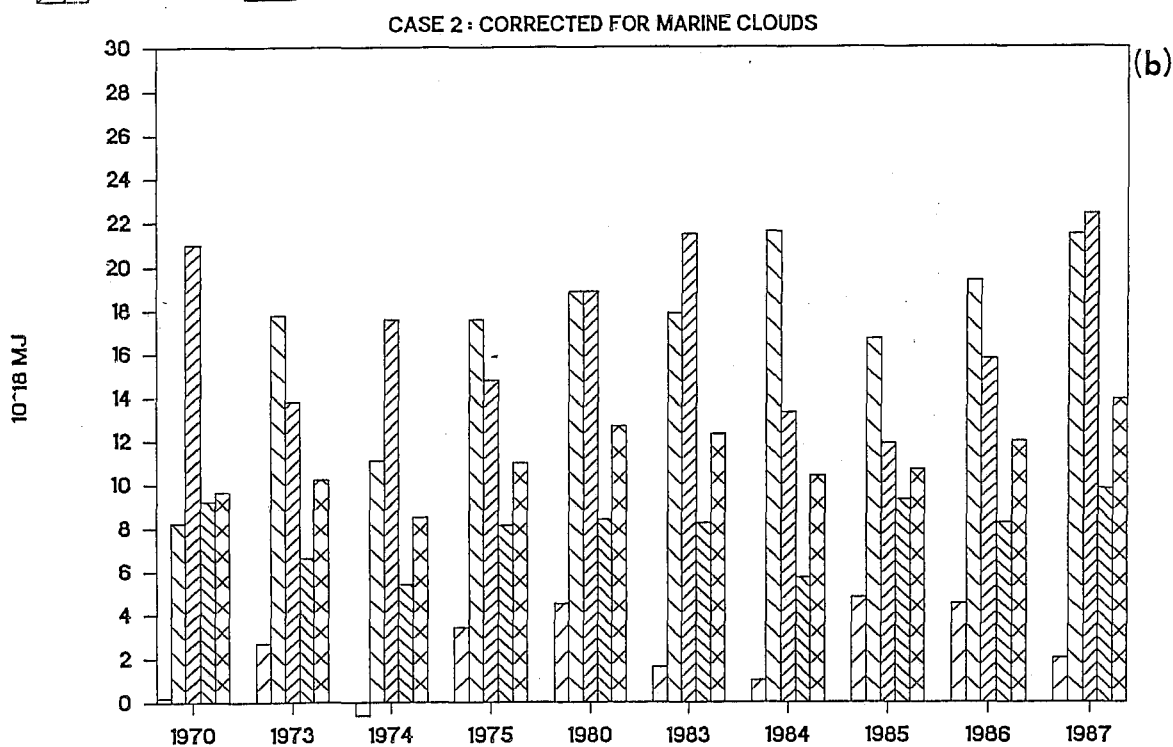
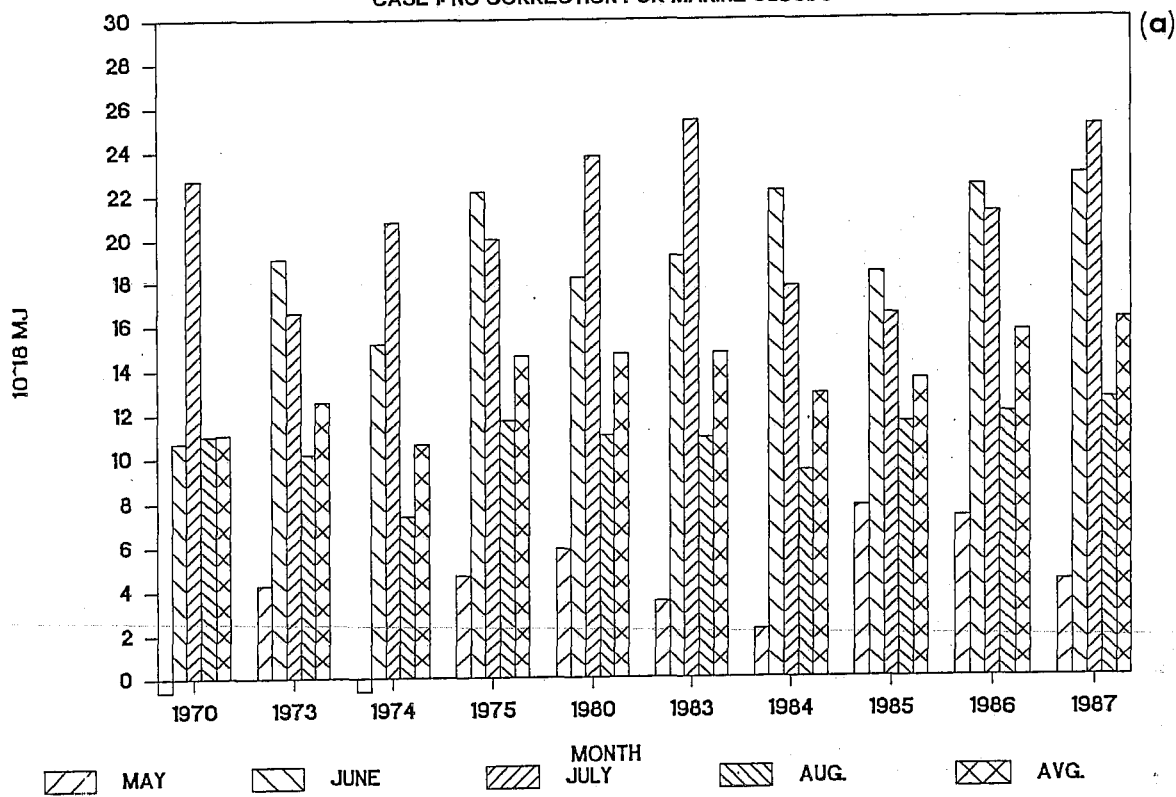


Figure 40: The monthly mean values of net surface heat transferred to the ocean (Q_A) by individual years for May, June, July, August and the average of these four months (a) without, and (b) with the additional simulation for effects of marine cloudiness.

Sachs Harbour, and (2) a reduced version of this using an equation to simulate increased marine cloudiness.

However, all of the above-cited differences in computational methods would have the effect of reducing the atmospheric heat values computed by Tummers (1980), while his results are larger than those of this study. The cause of the larger results given by Tummers (1980) remains unclear.

Ice Melt and River Heat Fluxes--The heat lost to melting sea-ice and the heat gained from the Mackenzie River represent two other physical mechanisms through which heat is exchanged with the ocean (Figure 41a). Of these, ice melt represents the largest heat transfer, amounting to an average of 29.3×10^{18} J, or more than half (54-65%) of the heat gained from the atmosphere. However, the interannual variability in heat due to melt ice (Figures 41 and 42) is relatively larger (+35%) than the combined atmospheric (+25%) terms. Like the atmospheric heat fluxes, heat exchanged due to ice melt is largest in July.

Heat gained from the Mackenzie River discharge is smaller (9.4×10^{18} J), amounting to 17-21% of the mean heat transferred from the atmosphere. The relative level of interannual variability is comparable to that of the atmospheric heat fluxes. Note that although the river heat is smaller by comparison to the net atmospheric input, it still represents about one-half of the net heat input to the ocean due external sources (atmospheric, ice and river).

Combining atmospheric, ice melt and river contributions, the net heat transferred to the ocean has an average value of 34.8×10^{18} J (24.6×10^{18} including the simulated loss of solar radiation due to marine cloudiness). Note that the estimated uncertainties in this value are large at +78% due to the combination of many individual terms, each with uncertainties of 15-20%.

The largest heat transfers occur in June, with only modestly smaller values in July and August. Interannual variations in the net heat are characterized by comparatively small levels (+20%) for nine of the ten years considered (Figures 41 and 42). The year 1970 has an anomalously small level of net heat transferred to the ocean, due to a combination of large heat losses to ice melt and a small atmospheric heat input.

Oceanic Heat Storage--Estimates of heat storage in the ocean are presented over two intervals, mid-July to mid-August and one month later (Figure 43) for those years having sufficient observations. For all years, except 1987, the ocean heat content decreases markedly from late July (20.3×10^{18} J) to late August (12.2×10^{18} J). In 1987, the trend was reversed, with heat storage increasing from 14.9 to 33.9×10^{18} J; the latter value was the largest oceanic heat storage value over the ten years of available observations.

The ocean heat storage exhibits only a moderate correlation with Q_A , the net heat transfer received through the ocean surface (Figure 44a) with $r=0.7$ ($r^2=0.5$) over the ten years of heat budget computations. (Note the higher correlation for the reduced atmospheric heat values computed with simulated losses due to marine cloudiness.) Years having the large surface heat transfer (1986 and 1987) have correspondingly large ocean heat contents, while years of small surface heat inputs generally have lower ocean heat storage levels. However,

HEAT BUDGET ESTIMATES: MAY TO AUG.

CASE 1: NO CORRECTION FOR MARINE CLOUDS

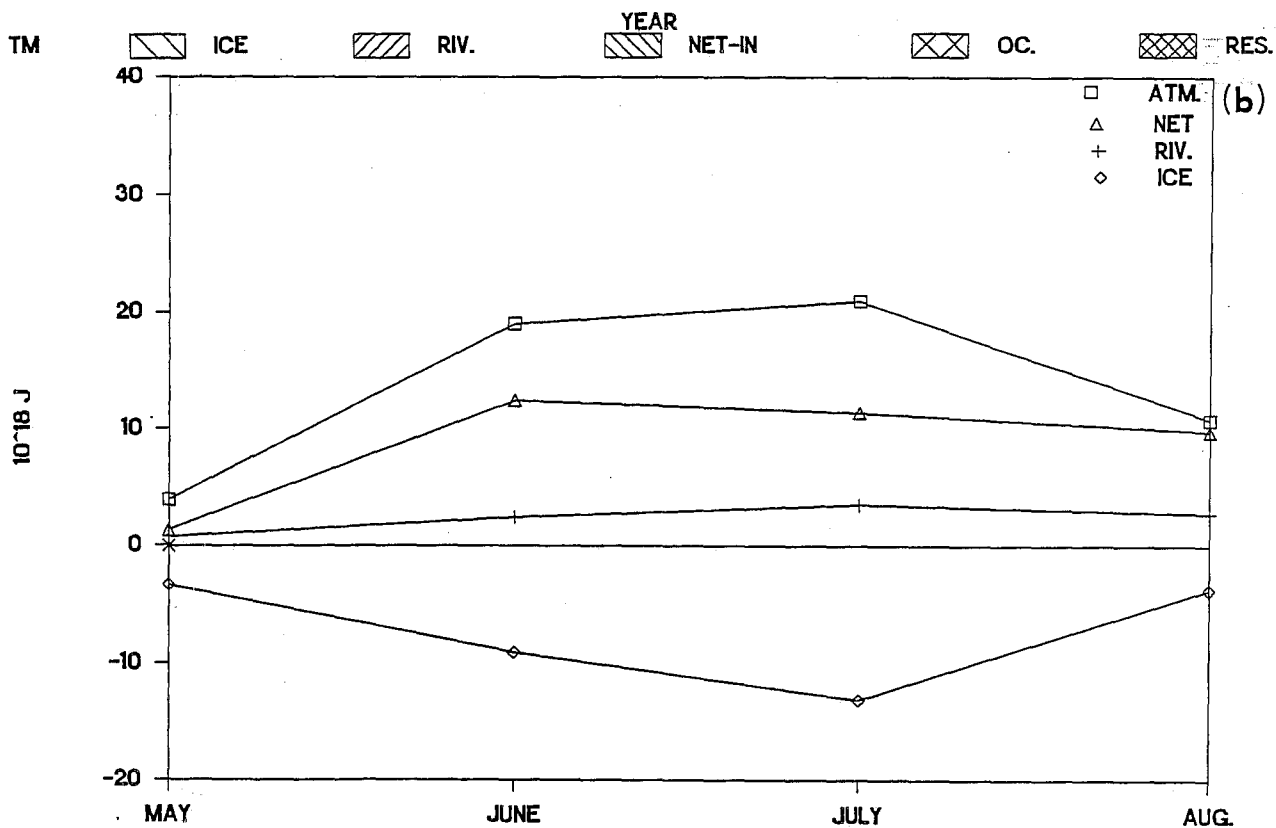
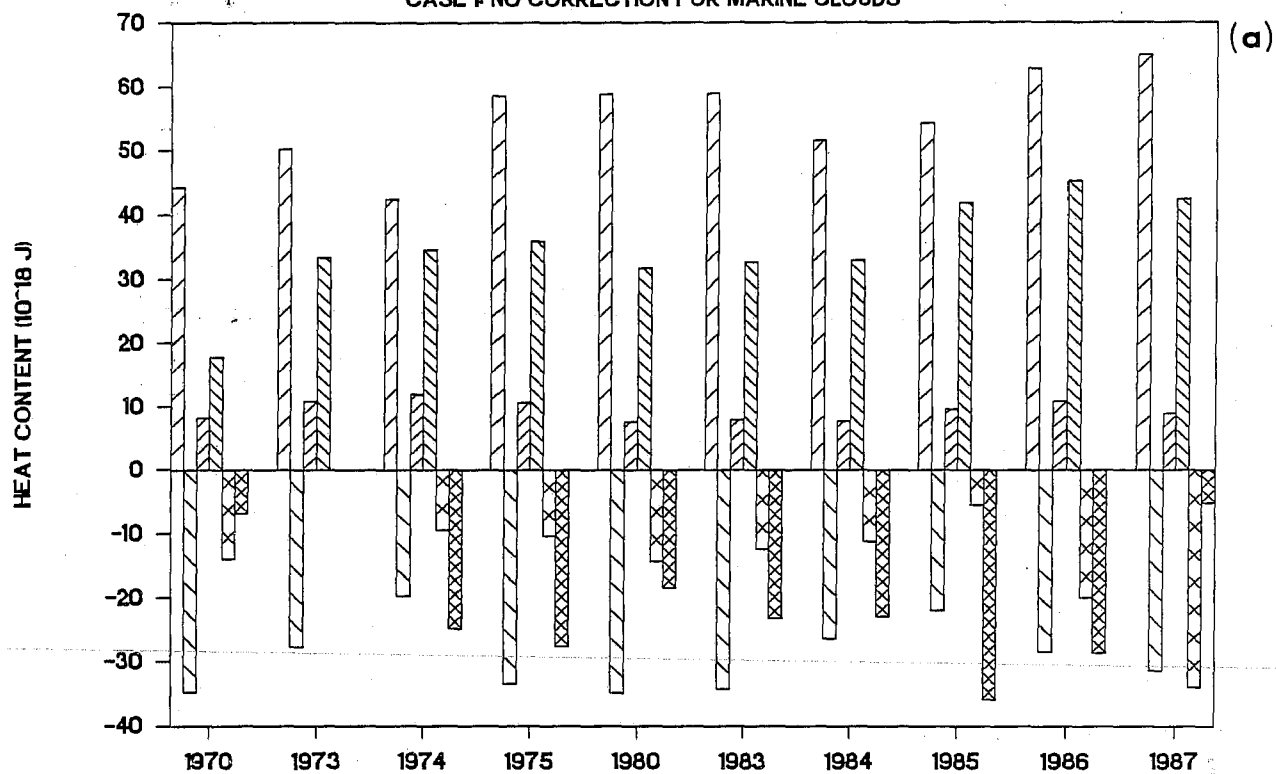


Figure 41: The surface heat transfer, river input, ice melt and the net input to the ocean (for case 1 net radiation) displayed as: (a) long-term mean values, by individual months; and (b) values from May to August by individual years.

HEAT BUDGET ESTIMATES: MAY TO AUG.

CASE 2: CORRECTION FOR MARINE CLOUDS

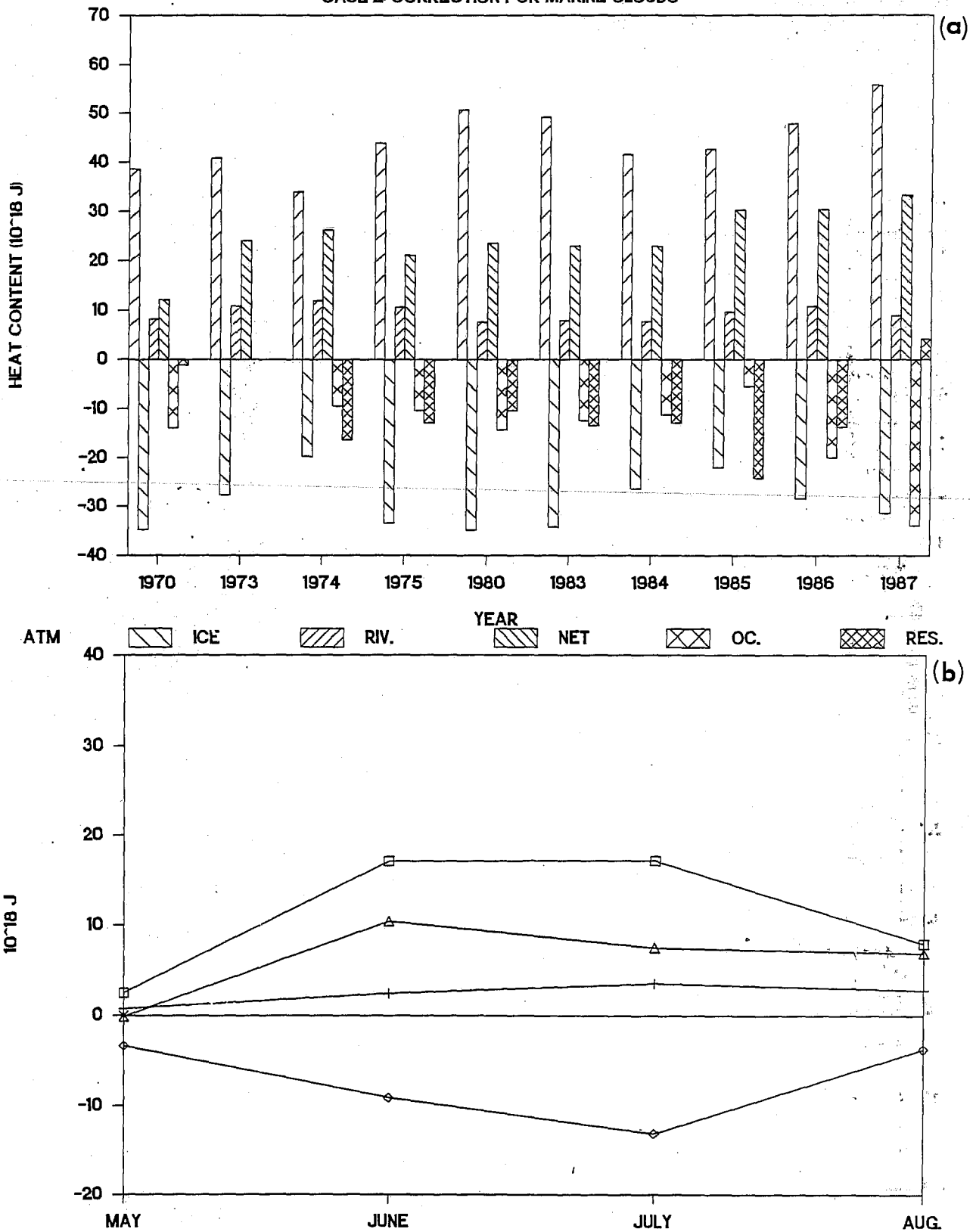


Figure 42: The surface heat transfer, river input, ice melt and the net input to the ocean (for case 2 net radiation) displayed as: (a) long-term mean values, by individual months; and (b) values from May to August by individual years.

HEAT STORED IN OCEAN

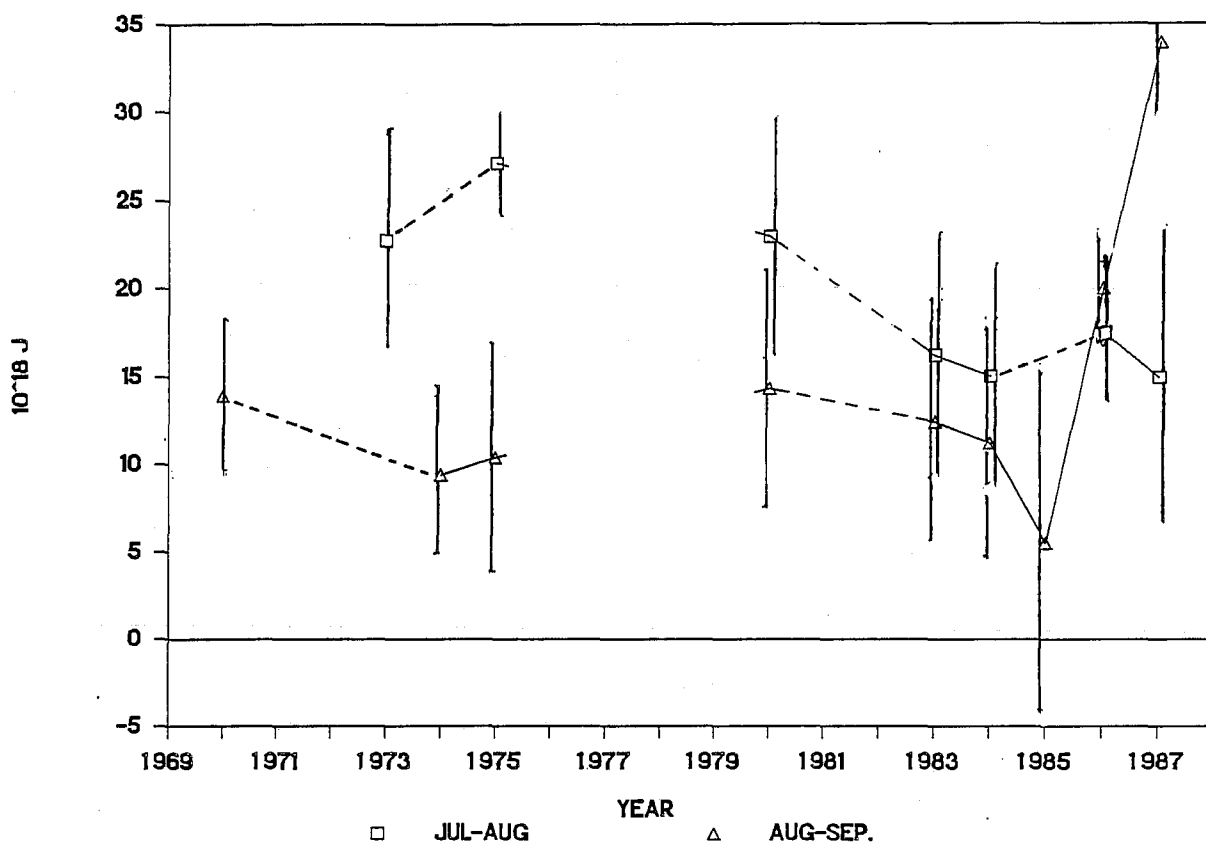
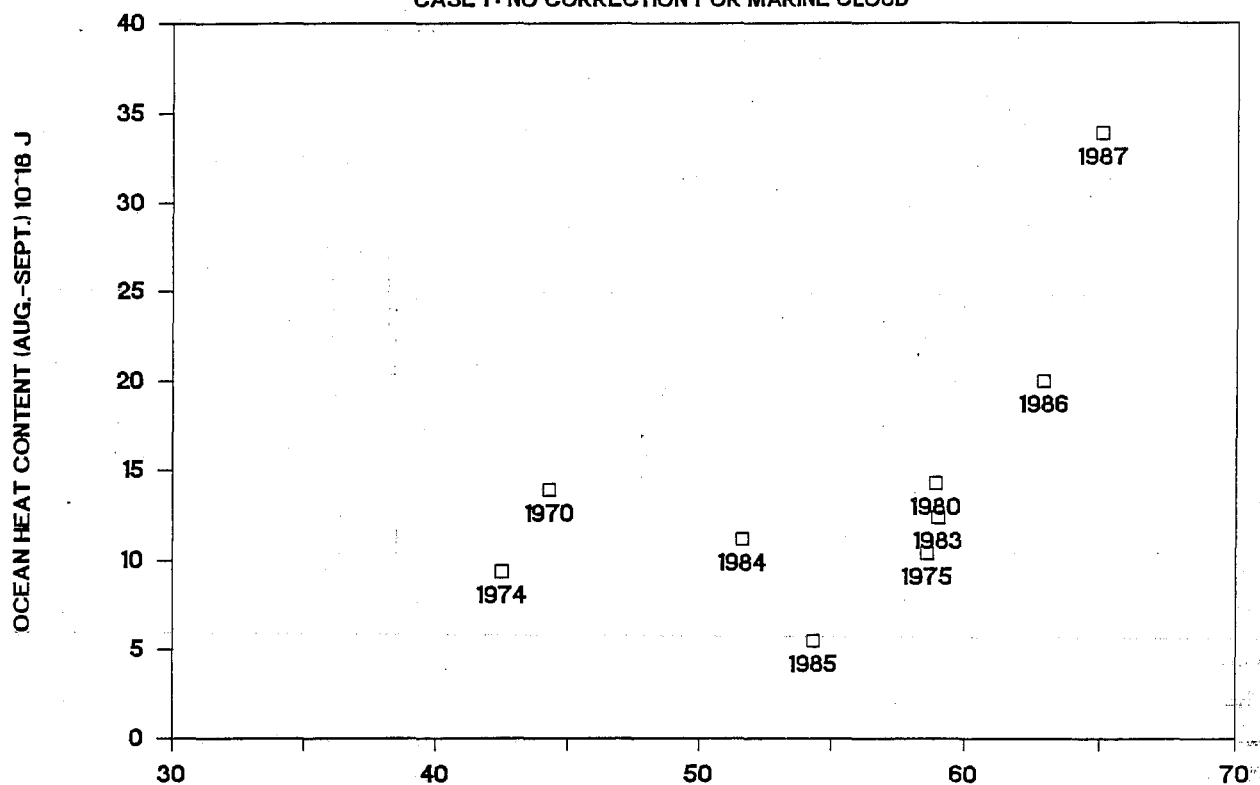


Figure 43: Estimates of heat storage in the continental shelf for those years with sufficient observations: (a) mid-July to mid-August; and (b) mid-August to mid-September.

SHELF HEAT VS. NET ATMOSPHERIC INPUT

CASE 1: NO CORRECTION FOR MARINE CLOUD



CASE 2: CORRECTIONS FOR MARINE CLOUDS

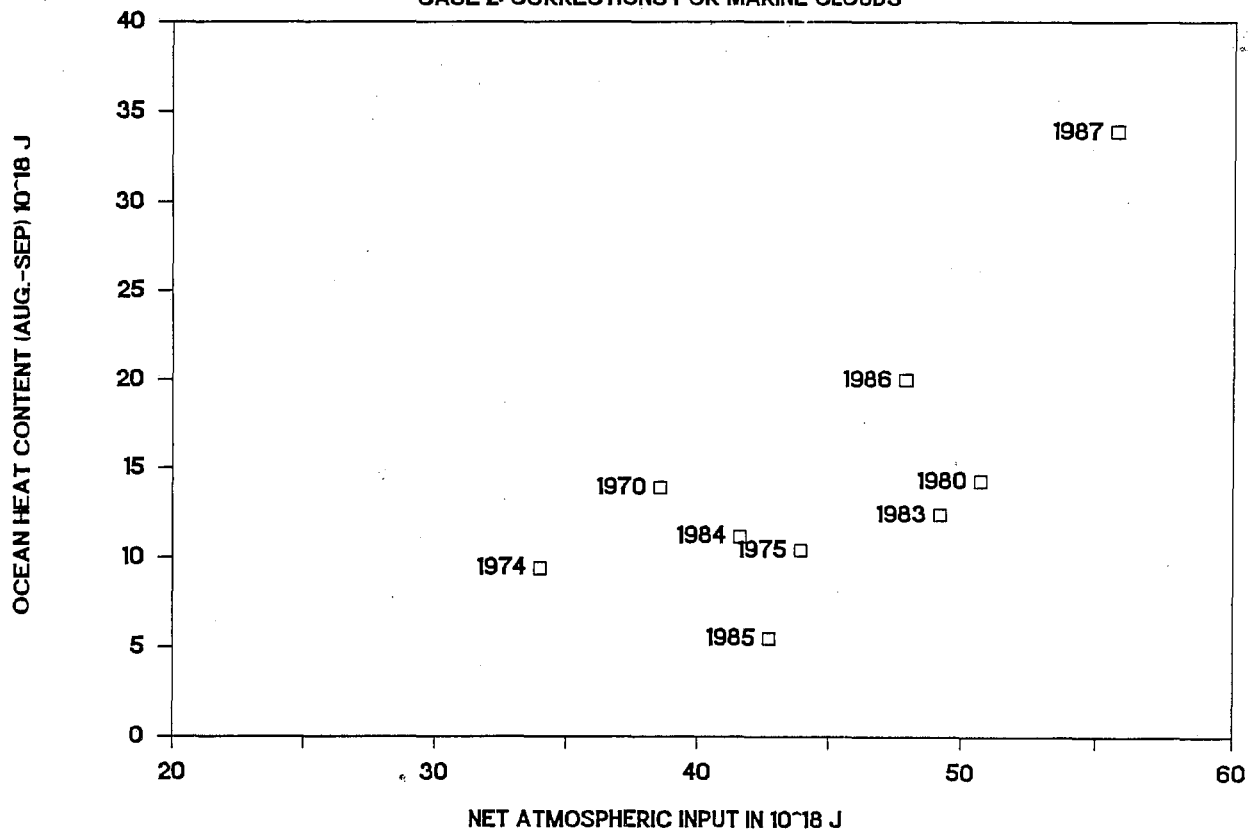


Figure 44: Yearly estimated values of heat storage (August) plotted versus net surface heat input from May to August.

notable exceptions occur in certain years (eg. 1970, when low atmospheric heat was accompanied by higher heat storage, and 1975, when the opposite situation occurred). The lack of better correspondence between surface heat transfer and ocean storage underscores the importance of other heat transfer terms (ice melt, river heat and advection) in determining the heat stored in shelf regions. The area of open water in early summer appears to be reasonably well correlated with ocean heat (Figure 24).

Comparison of freshwater and heat content in the ocean between August 15 and September 15 exhibits a considerable degree of inconsistency in most years (Figure 45a). Years with small to moderate levels of freshwater storage (1980, 1983, 1985-1987) exhibit a wide range of heat content from the smallest (1985) to the largest (1987). More consistency is apparent for years having large freshwater storage levels (1974, 1975, and 1984, which tend to have small to moderate levels of heat content. These comparisons suggest that heat accumulation in the ocean is small when freshwater accumulation is large. The converse of this statement does not appear to be applicable.

Advection of Ocean Heat--The "residual" heat term required to balance the combined sources and sinks of heat is also presented in Figures 41 and 42. This residual term is identified with advective exchanges between the heat stored over the continental shelf and adjoining oceanic areas. Note that the advection of heat could involve movement of sea-ice as well as the upper portion of the ocean. The ten-year mean residual term at the end of August was computed as -20.2×10^{18} J (-10.0×10^{18} J when the simulated reduction in solar radiation is used). However, the estimated uncertainty in these results is very large at $\pm 136\%$.

The residual heat term increases very markedly in magnitude from late July to late August by 10 to 15×10^{18} J. This sharp increase reflects a combination of opposing trends in the latter part of the summer: a decrease in ocean heat storage combined with a continuing accumulation of heat input to the ocean (atmospheric transfers and river sources less ice melt).

The advection inferred from the residual terms can also be presented as the percent of heat loss from the shelf, defined as the ratio of residual heat term to the net heat input to the shelf from non-oceanic sources (Figure 46). From mid-July to mid-August, the heat losses are comparatively small, ranging from near-zero to 47%, with the largest losses occurring in 1985-1987, when the net non-oceanic heat inputs were largest. One month later, the heat losses increased considerably to estimated values of 33 to 63%, excluding 1970 (22%) and 1987 (20%).

A comparison of estimated freshwater losses (Figure 35) reveals very different patterns for the inferred advection of heat and of freshwater. The level of freshwater loss varied enormously from year-to-year, but comparatively little within each summer; in contrast, the advective heat loss increases greatly in the late summer, but has comparatively small interannual variations. Moreover, the years exhibiting minimum or maximum levels of freshwater losses exhibit little correspondence to heat loss results.

The differences between heat and freshwater advection estimates could simply arise from the large uncertainties (estimated as $\pm 136\%$) in the estimates, arising

FRESH VS HEAT CONTENT ON SHELF (AUG)

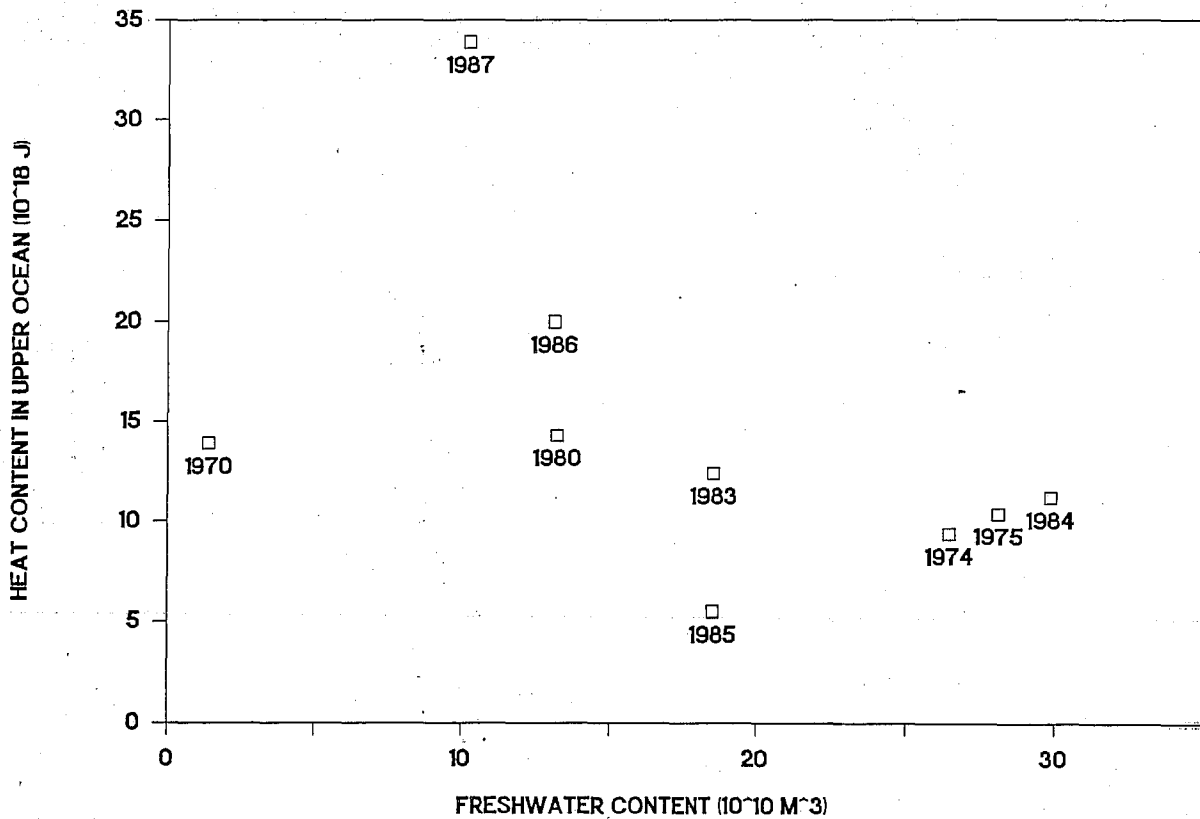
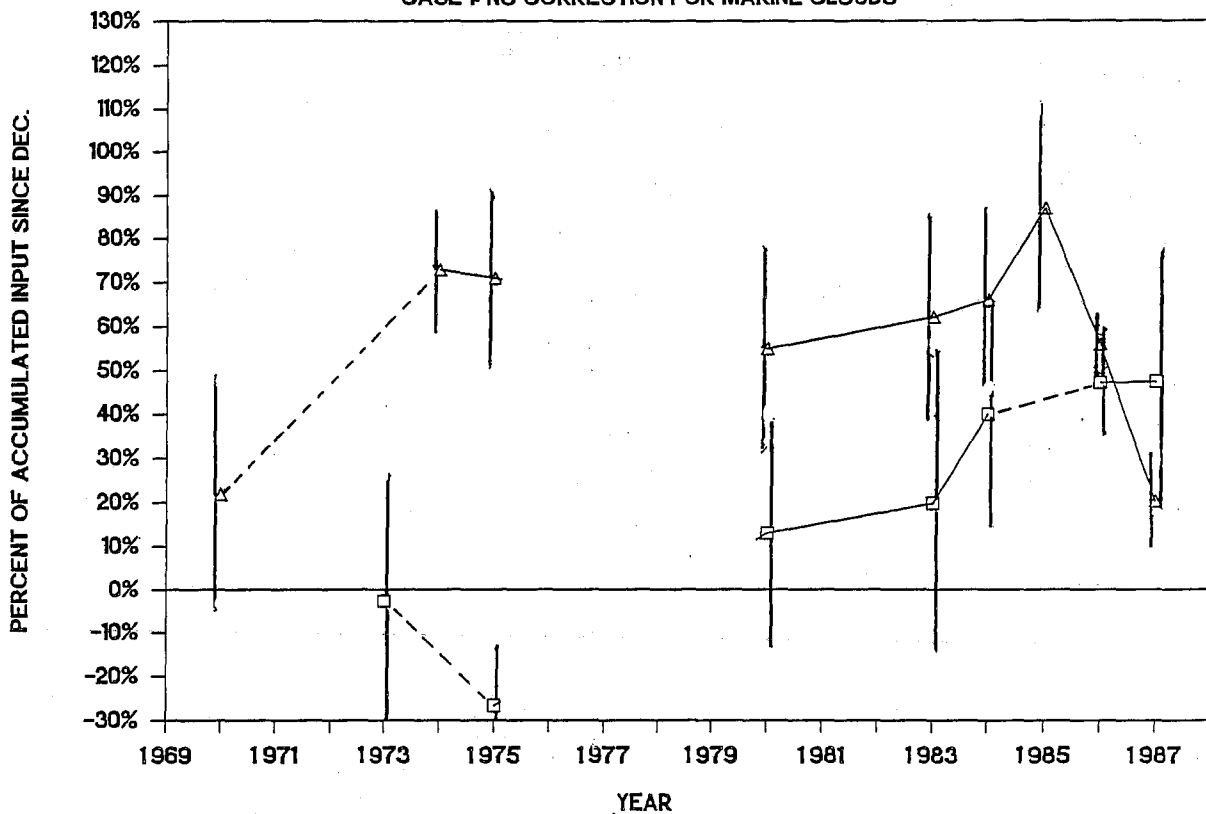


Figure 45: Estimates of freshwater content plotted versus heat content in the continental shelf for the period mid- August to mid-September.

ESTIMATED LOSS OF HEAT FROM CONT.SHELF

CASE 1: NO CORRECTION FOR MARINE CLOUDS



CASE 2: CORRECTION FOR MARINE CLOUDINESS

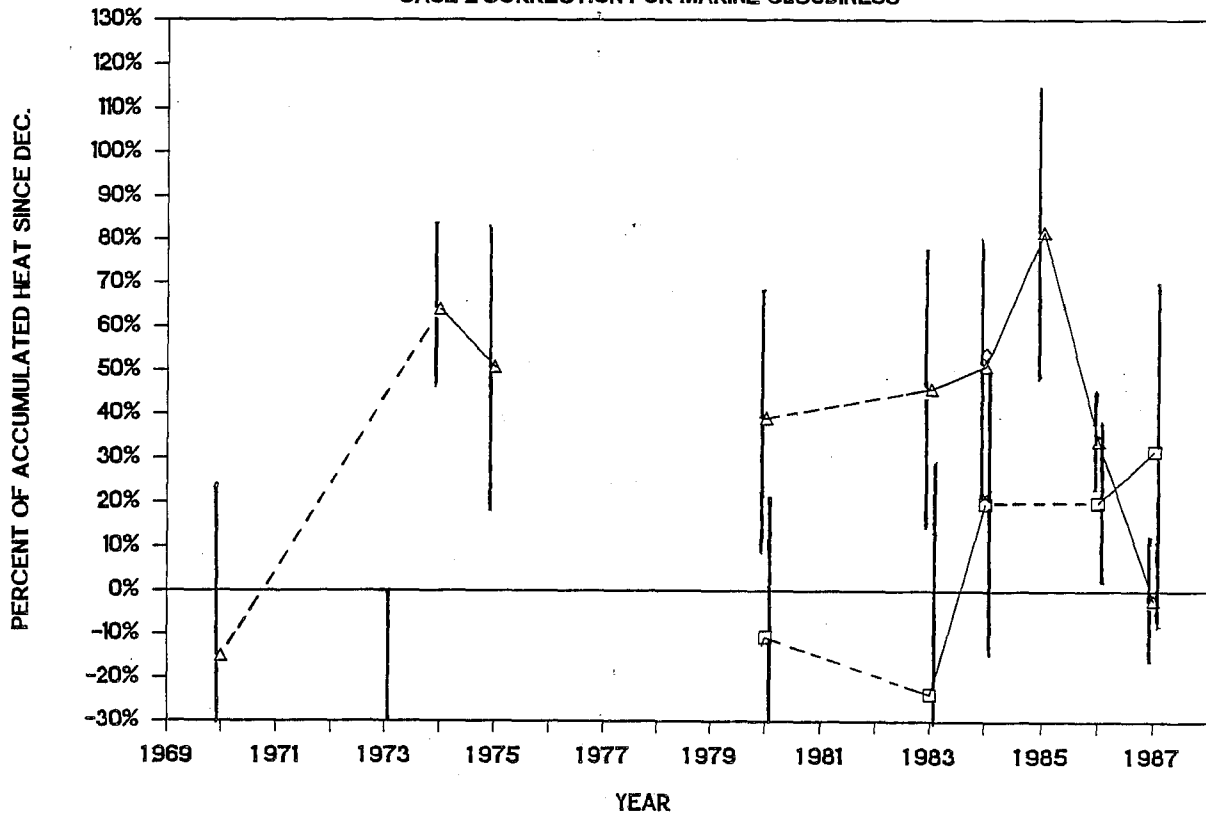


Figure 46: The computed values of heat lost from the continental shelf as a percentage of total heat input. The displayed values represent the cumulative losses from the period beginning in May to either: mid-July to mid-August, or mid-August to mid-September.

from the use of incomplete or uncertain input parameters. This may render the residual values so uncertain as to make them meaningless. The cumulative uncertainties in the residual heat estimate (Table 2) are much greater than those in the freshwater estimates (+47%). While this could explain random interannual variations, the pronounced reduction in oceanic heat content, and corresponding increase in residual losses in late summer, may still have some validity. Only a large systematic error would account for the pronounced changes in residual losses from late July to late August. While other interpretations exist (eg. turbulent heat losses in August are larger than estimated, or net solar radiation is reduced due to marine clouds), the magnitudes appear to be insufficient to negate or reverse the implied oceanic losses.

Another possible explanation is that the effects of advection on heat and on freshwater within the study area differ substantially. For freshwater, the dominant source is the Mackenzie River, which flows entirely into the study area. However, substantial quantities of oceanic heat are found just to the east of the study area in Amundsen Gulf, associated with the occurrence of the Cape Bathurst polynya in the spring of most years (Stirling and Cleator, 1981). Circumstances can be envisioned where the same pattern of upper ocean advection could result in quite different changes to heat and freshwater content: for example, under strong or prolonged easterly winds, heat and freshwater would be lost through the western boundary of the study area, but only heat would be gained through the eastern boundary, due to the presence of warm but saline water in the mouth of Amundsen Gulf (Figure 9). Under westerly winds, the waters advected into the study area from the west are generally cold and saline, so a smaller or negligible difference in changes to heat and freshwater content is anticipated.

Differences between the predominant depths of heat and freshwater storage within the water column may also have a bearing on advective exchanges. As noted in subsection 4.1, the contribution of the water column at depths exceeding 20 m can be considerable for heat, but is generally much smaller for freshwater. Thus subsurface currents may have a greater effect in the exchange of heat than freshwater.

Early Summer Quantities with Predictive Value for Net Heat Transfers--Not surprisingly, the best predictive value for surface heat transfer (Q_A) was the largest heat budget term, net solar radiation, with a correlation coefficient of 0.83 ($r^2 = 0.68$) (Figure 47). The correlation coefficient between net solar radiation to the end of June and net heat transfer to the ocean at the end of August (Q_T) was 0.83 ($r^2 = 0.68$).

The amount of open water at the end of June is also significantly correlated (Figure 48) with net atmospheric and total heat transferred to the ocean, with correlation coefficients of 0.74 and 0.33 ($r^2 = 0.55$ and 0.11, respectively).

4.4 UPWELLING CONDITIONS

Upwelling of cold, nutrient-rich water from depth onto the continental shelf has been observed on the Mackenzie Shelf and the Alaskan Beaufort Shelf in previous studies. In the eastern portion of the Alaskan Shelf (141-144°W), upwelling conditions appear to occur frequently; from an examination of 11 years of temperature and salinity data spanning 1951 to 1986, Fissel et al (1987b) found that pronounced upwelling was evident in four years, and there was evidence

NET ATMOS.(TO AUG) VS. NET SOLAR (JUNE)

CASE 1: NO CORRECTION FOR MARINE CLOUDS

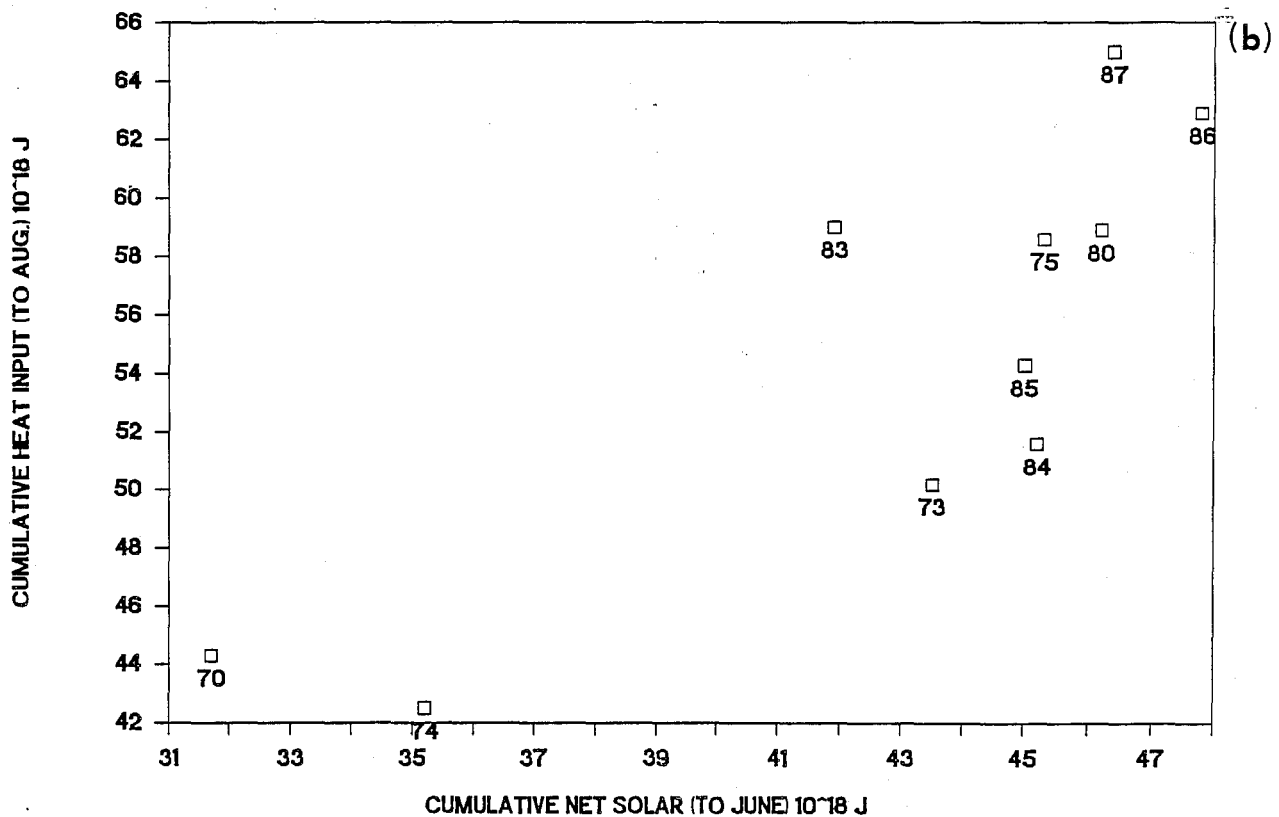
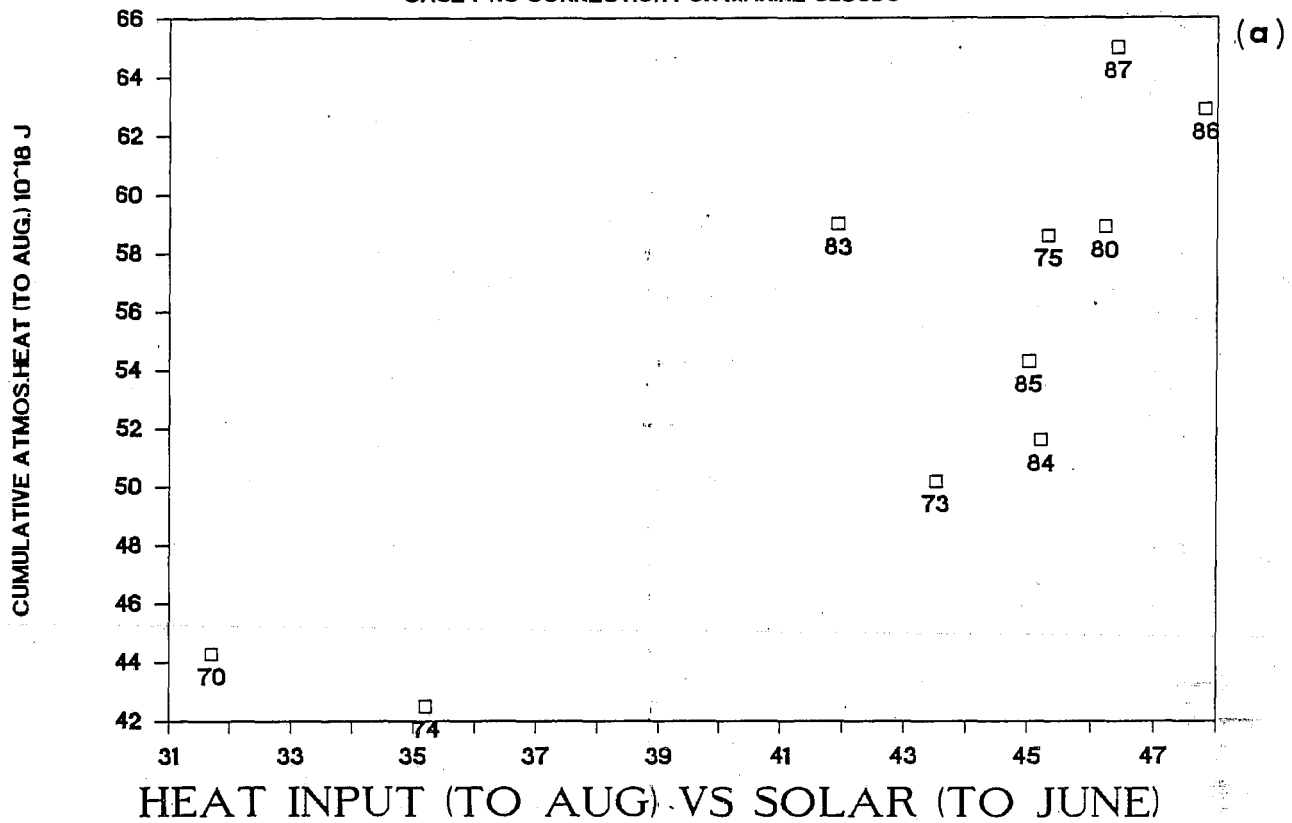
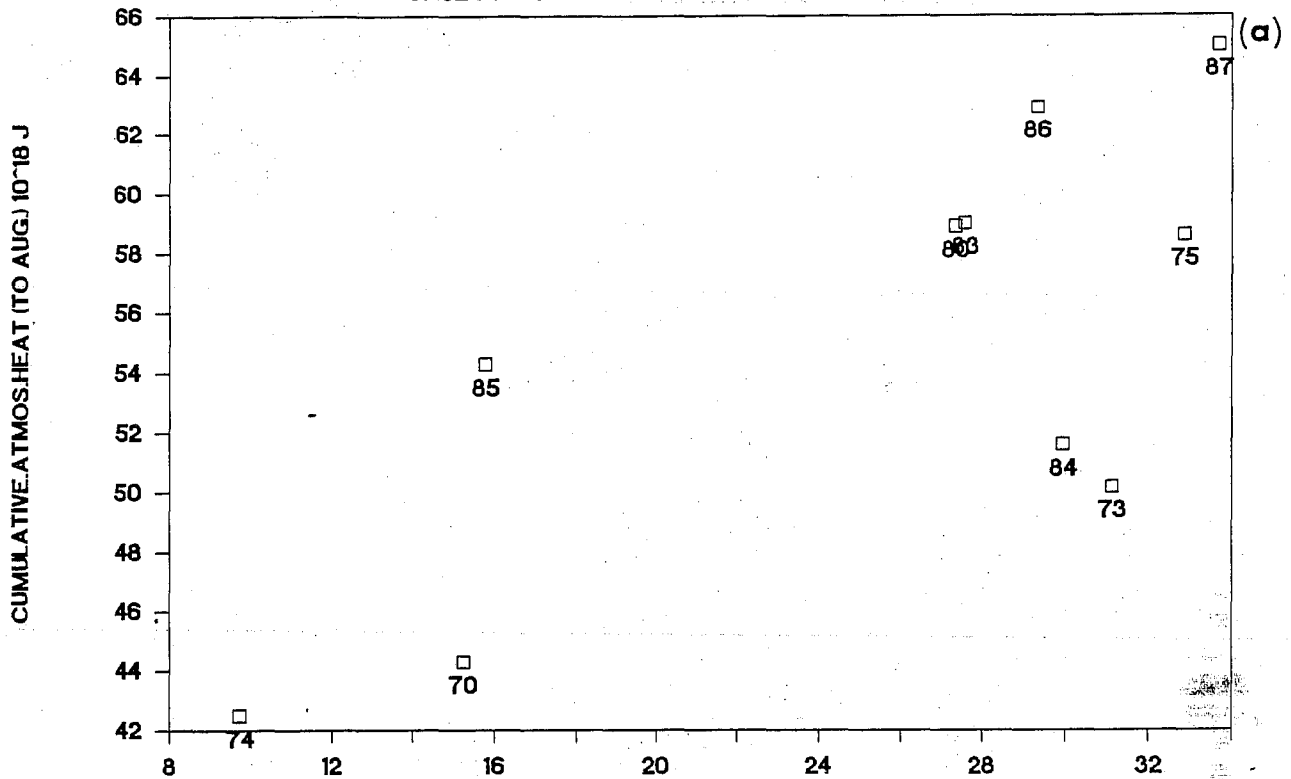


Figure 47: A scatter plot of net solar radiation to the end of June with (a) cumulative net surface heat transfer (May to August) and (b) cumulative net heat transfer to the ocean (May to August).

ATMOS.HEAT (TO AUG) VS. JUNE SEA-ICE

CASE 1: NO CORRECTION FOR MARINE CLOUDS



NET HEAT INPUT TO AUG. VS. JUNE SEA-ICE

CASE 1: NO CORRECTION FOR MARINE CLOUDS

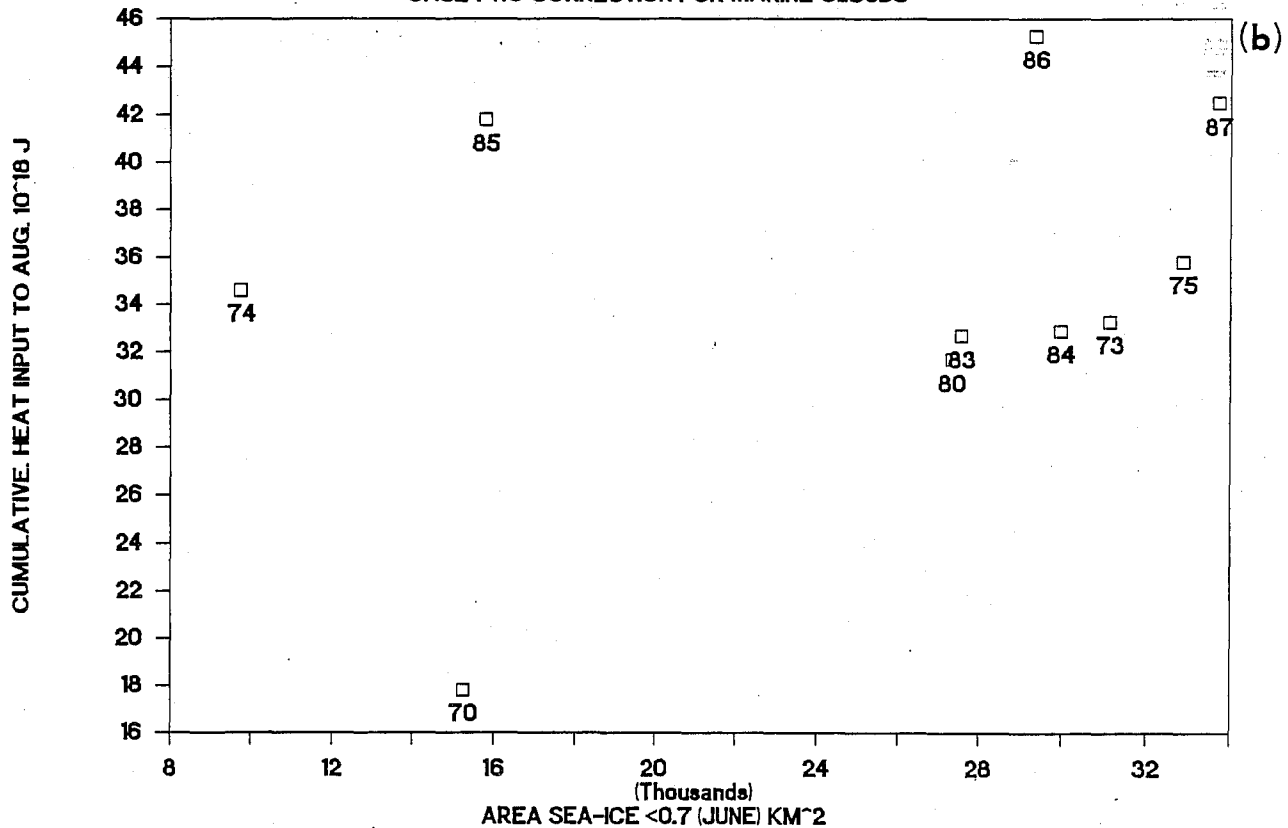


Figure 48: A scatter plot of amount of open water at the end of June with (a) cumulative net surface heat transfer (May to August) and (b) cumulative net heat transfer to the ocean (May to August).

of a reduced degree of upwelling in four other years. Strong upwelling has been attributed to classical wind-driven coastal upwelling associated with strong easterly winds, for example in 1952 on the Mackenzie Shelf (Cameron, 1953) and in 1972 on the Alaskan Shelf (Hufford, 1974). However, MacDonald et al (1987) observed upwelling in the Mackenzie Canyon area in both 1974 and 1975, at times when the local winds were not conducive to upwelling; they attributed the observed upwelling to interaction of an eastward-flowing Beaufort Undercurrent (Aagaard, 1984) with the topography of Mackenzie Canyon. Fissel et al. (1987a) noted the occurrence of upwelling of cold, clear Arctic water off the Yukon coastline between Kay and Shingle Points; upwelling in this area is related to local southwesterly winds resulting from the orographic effect of the Richardson Mountains on the regional wind patterns.

Using the vertical cross-sections of salinity and temperature assembled in this study (Appendix E), occurrences of up- or downwelling were catalogued and compared with the prevailing winds. Upwelling was somewhat arbitrarily judged to occur when the isohalines or isotherms tilted upward to the coastline, with slopes exceeding 0.001 (15 m vertical displacement over the typical shelf width of 150 km); strong upwelling conditions were taken as upward slopes exceeding 0.004. Downwelling conditions were determined as opposite directed slopes having the same magnitudes.

In some vertical cross-sections, both upwelling and downwelling conditions were simultaneously observed, most often involving upwelling over the outer shelf and slope with downward tilting isopleths located inshore (associated with the leading edge of the river plume). In such cases, the conditions representing the largest cross-sectional area were selected as the dominant condition.

For each vertical cross-section examined, the wind conditions (Appendix F) were also catalogued, according to magnitude and dominant direction over the past zero to two days and the past three to five days.

The occurrences of up- or downwelling were examined separately for the Mackenzie shelf and canyon regions (Figure 49). On the Mackenzie shelf, a further distinction was made between the inner to middle shelf and the outer shelf to continental slope area. In Mackenzie canyon and the outer shelf/slope portions of the shelf, occurrences of upwelling conditions exceeded neutral or downwelling conditions by a factor of five or more. However, over the inner shelf, the frequency of apparent up- and downwelling conditions was nearly equal.

The occurrence of upwelling appears to be unrelated to the chosen wind direction parameters for the regions examined (Figure 49). Upwelling conditions appeared to be equally likely to occur during or after westerly and easterly winds. The absence of any apparent correlation between upwelling conditions and wind direction may indicate that the frequent upwelling conditions observed result from mechanisms other than classical wind-driven coastal upwelling. Evidence exists that other mechanisms can cause upwelling (MacDonald et al., 1987; Fissel et al., 1987b) as discussed above. However, it is possible that winds are responsible for the upwelling, at least in part. However, the response is sufficiently complicated to obscure detection of a correlation through the simple empirical comparisons used in this study. One possible explanation is that oceanic response to winds is mediated by the amount of open water fetch, which varies considerably according to present and past sea-ice conditions.

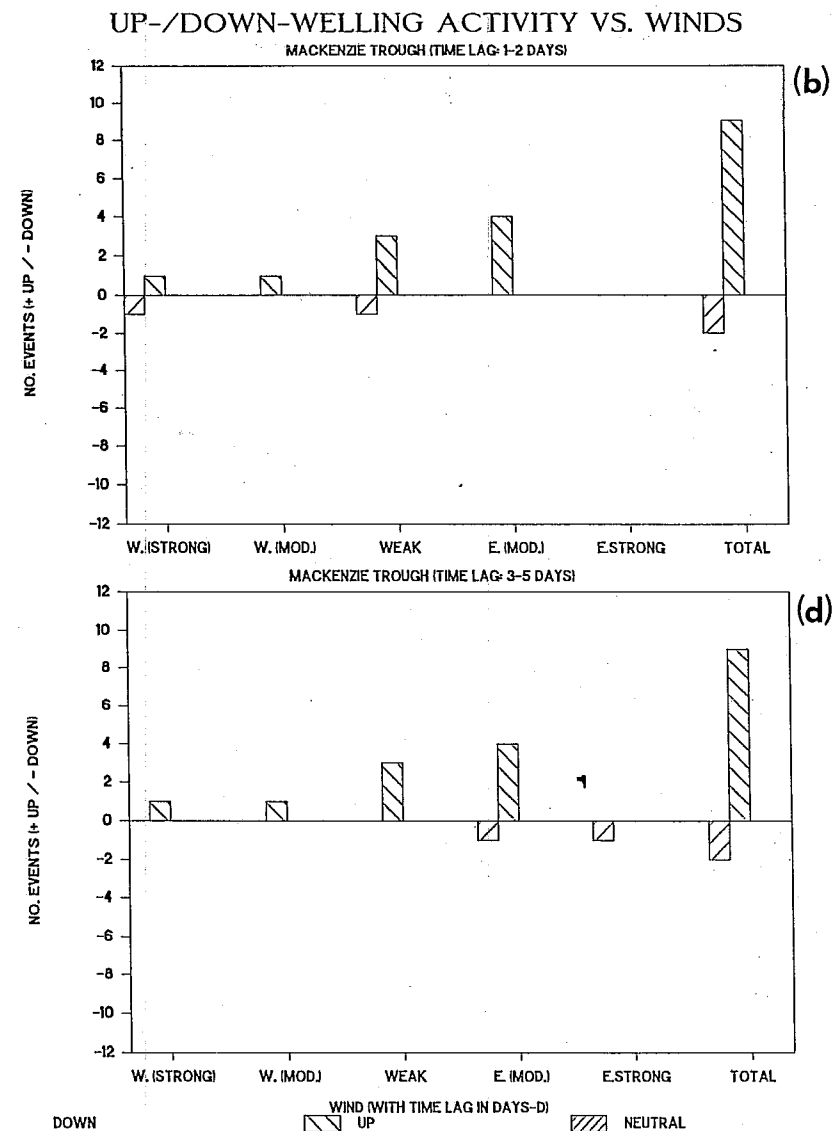
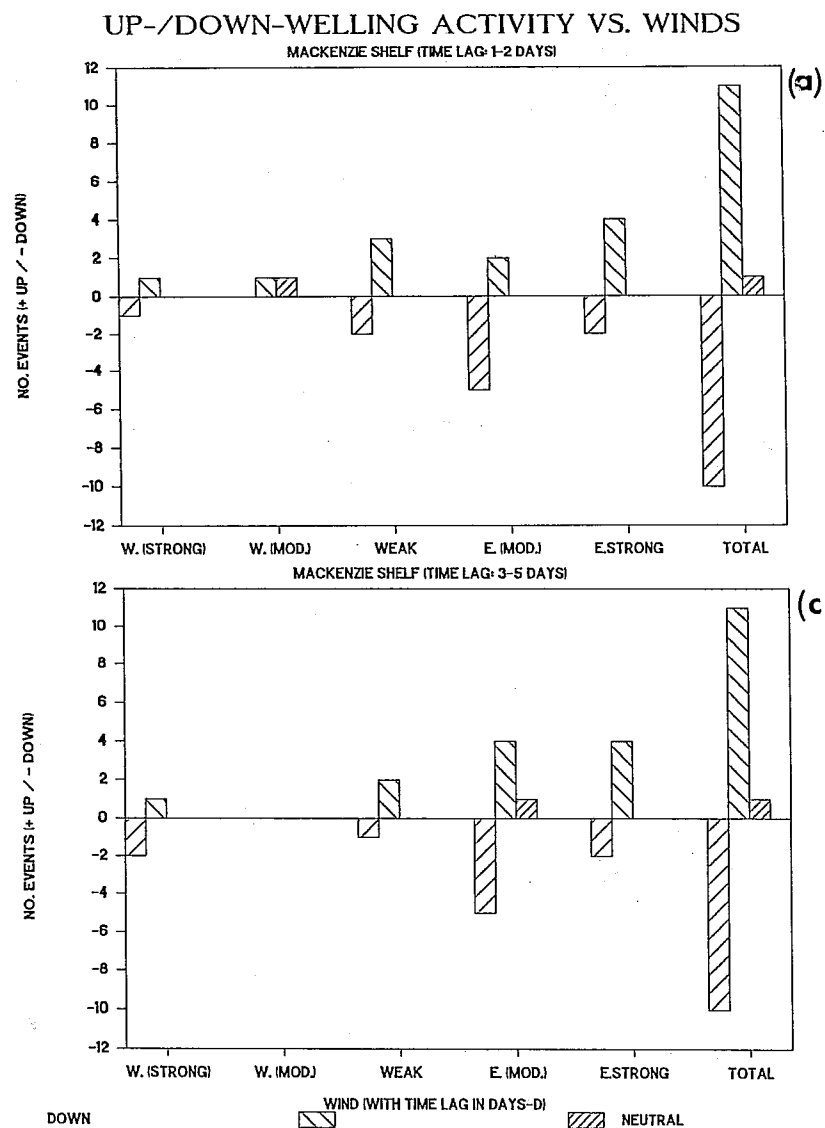


Figure 49: The number of up- or down-welling events plotted versus wind direction and magnitude categories for two different ranges of time lags between the winds and oceanographic conditions. One to two days for (a) the Mackenzie Shelf and (b) the Mackenzie Trough, and three to five days for (c) the Mackenzie Shelf and (d) the Mackenzie Trough.

5 SUMMARY AND DISCUSSION

5.1 STUDY OBJECTIVES

In this study, the variations of oceanographic conditions in the Beaufort Sea, over periods of one year or longer, were examined. All temperature and salinity data sets obtained between 1950 and 1987 (see Birch et al., 1987) were examined. From these, a total of 72 data sets, which provide suitable spatial (areal) coverage and adequate accuracy, were chosen for use in this study. The total oceanographic data consisted of approximately 1500 vertical profiles of temperature and salinity, distributed over 28 years of summer observations and eight years of spring data. Unfortunately, no suitable oceanographic data were available through most of the 1960's (1961 to 1968).

5.2 DATA SOURCES AND METHODS

A variety of non-oceanographic data sets were also assembled to examine the factors and mechanisms which determine the water properties in the southeastern Beaufort Sea. Three major data sets were processed and displayed for years with oceanographic data (1950-1961; 1969-1987).

Winds - taken from the geostrophic winds computed for marine areas (Swail, 1985) spanning the period 1950 to 1987 inclusive;

Sea-Ice - maps of sea-ice concentrations were prepared from sea-ice charts, produced since 1959 by the Canadian Ice Branch, later Ice Centre, of the Atmospheric Environment Service of Environment Canada. For years prior to 1959, only patchy maps could be prepared, especially for the years 1950 to 1953 when data were very sparse.

River Discharge - reliable measurements of the volume discharge from the Mackenzie River are available only since 1972, with the major source of information being the gauging station at the junction with Arctic Red River.

Other types of meteorological data, including solar radiation measurements, cloud cover and precipitation, were obtained from coastal weather stations in selected years of interest.

5.3 INTERANNUAL VARIABILITY OF OCEANOGRAPHIC CONDITIONS

From the temperature and salinity profile data, two integral quantities, the heat and freshwater content, were derived and displayed. The heat content was computed as the heat relative to a temperature of -1.5°C , contained in the uppermost 50 m of the water column; this approximates the limit of advective heat losses in winter and diabatic heating in summer. Freshwater content was derived as the salt deficit relative to a reference salinity of 31, again over the upper 50 m of the water column.

To examine interannual variability in oceanographic properties, monthly mean values were computed each year for five subregions: Mackenzie Bay; the nearshore portion of the Mackenzie Shelf; the middle and outer portions of the continental shelf; the adjoining continental slope; and the western entrance of Amundsen

Gulf. The computations were carried out for the months July, August and September, as well as the March-April period preceding the River freshet and sea-ice break-up. The monthly mean computations were applied to the data sets of temperature and salinity at 1 m and the heat and freshwater integral values.

The seasonal patterns in the long-term means differ considerably for the temperature and salinity quantities. Both attain yearly maximum values in July. However, the temperatures decrease throughout the summer while salinities remain nearly constant in the latter half of the summer. Also of interest is the degree of spatial differences in the mean temperature and salinity: salinities exhibit large differences among the various subregions, while the temperatures exhibited much more spatial consistency.

From the interannual variations in the monthly mean oceanographic quantities, some quasi-periodic variation was evident. The most conspicuous interannual variation occurred in surface salinity, and had an estimated period of 8-12 and an amplitude of 5 (over the continental shelf). A similar period occurred in the freshwater content, with an even larger relative amplitude amounting to 50% of the long-term mean values over the continental shelf.

The interannual variations of temperature and the heat integral have smaller amplitude than the salinity quantities. Large interannual variability of temperature and salinities occur simultaneously, but only in years having extreme conditions. Over the thirty years of oceanographic observation, extreme conditions occurred during four years: 1974 and 1985, when temperatures and salinities were unusually low, and cover was heavy; and 1958 and 1987, years of high temperatures and salinities, and extensive open water.

Yearly variations of monthly mean temperature at a salinity of 31 (a subsurface parameter) were analyzed. The results indicate that a core of warm water occurs on this salinity surface in most years. The origin of this warming at depth appears to be due to westward advection of heat from the eastern shelf Amundsen Gulf, where early clearing of sea-ice associated with the Cape Bathurst polynya results in greater heating of the upper layer of the ocean. Evidence of eastward advection of heat from the Bering Sea was limited to one year (1951).

5.4 INTERANNUAL VARIABILITY OF SEA-ICE, WIND AND RIVER DISCHARGES AND CORRELATION WITH OCEANOGRAPHIC CONDITIONS

The areal coverage of sea-ice in summer exhibited very large interannual variations, ranging from virtually complete ice cover to completely open water over the continental shelf. The period of the sea-ice variations was seven to nine years, comparable to the period evident in the upper layer oceanographic parameters.

Winds and river discharges exhibited a lesser degree of interannual variability than the sea-ice coverage. The year-to-year variations in the monthly easterly wind displacements did not exhibit any regular pattern, as they strongly reflect the synoptic scale variations associated with passing weather systems. In most years, the sea-ice coverage did appear to respond to the monthly wind displacement. A linear regression analysis revealed a statistically significant correlation, wherein increased clearing of sea-ice was associated with increased wind advection to the west (i.e. easterly winds). Based on the

regression results, a 10,000 km run of winds from the east results in an offshore retreat of the ice-edge of approximately 100 km, over the full width of the shelf zone.

The interannual variations in the Mackenzie River discharges from before freshet through the summer are relatively small in amplitude ($\pm 20\%$ of the long-term mean value). The year-to-year variations appear to be dominated by decadal periods or longer.

Regression analyses between oceanographic parameters, and sea-ice, wind, and river parameters reveal generally low levels of coupling. The highest correlations of ocean parameters occur with the clearing of sea-ice. Increased clearing of the sea-ice is associated with increased surface temperatures, heat contents, surface salinities and decreased freshwater contents, over the middle and outer continental shelf. For inshore areas, the coupling of salinity and freshwater with sea-ice clearing is also apparent, but the effect on temperature and heat content is generally reduced to below statistically significant levels.

Variations in river discharge are significantly correlated to the oceanographic parameters in the nearshore regions of the Mackenzie and Yukon shelves. However, the correlations do not extend to the middle and outer portions of the shelf, suggesting that mixing and dispersion of the river water with offshore ocean water eliminates any simple, direct effect of river discharge variations.

The oceanographic parameters exhibit little correlation with the wind run. This lack of correlation does not imply that surface winds are unimportant in determination of oceanographic distributions; rather the relationship of oceanographic conditions to the surface wind is more complex than the simple linear regression model applied. In particular, the wind runs tend to reflect intra-annual short term variations, while the oceanographic parameters exhibit a marked correlation with the interannual variations of the sea-ice and river discharge parameters.

5.5 FRESHWATER BUDGET

Computations of the freshwater budget for the continental shelf during spring and summer were made for ten years having relatively high levels of oceanographic sampling in the summer months. Discharge from the Mackenzie River represents the largest source of freshwater, which is approximately three times greater than fresh water resulting from the melting of sea-ice for the period to the end of August. If the two major sources were distributed uniformly over the continental shelf region used in the freshwater budget, they would result in a freshwater layer having a mean thickness of 3.5 m (river discharge) and 1.1 m (ice melt).

The only significant loss term, in summer, for freshwater from the continental shelf, is advection off the shelf. By estimating the storage of freshwater over the shelf, we can then estimate the losses due to advection for individual summers. The advective losses from the continental shelf (by late summer) are highly variable from year to year, ranging from losses exceeding 70% (eg. 1970, 1980 and 1987), to retention of more than 75% of freshwater input (eg. 1973, 1974, 1975 and 1984).

The magnitude of advective loss of freshwater from the shelf areas appears to be controlled primarily by the degree of ice clearing: in all years examined having small amounts of sea-ice clearing (1974, 1984 and 1985), the advective losses were small, because of the limited potential for advection and dispersal off the shelf. The converse of this statement also applies to both years (1980 and 1987) having an unusually large amount of sea-ice clearing. This relationship between losses of freshwater from the shelf and degree of clearing of sea-ice accounts for the negative correlation between freshwater content with non-ice area in several subregions of the study area (Figure 22). Looked at in another way, freshwater is concentrated in the top layer of the ocean, as also is pack ice. Those influences which clear ice from an area will also move the top layer of the ocean similarly. Therefore, small ice area will be related to effective ice advection, which is related to effective freshwater advection.

5.6 HEAT BUDGET

Heat budget computations were also carried out for the ten years over the period 1970-1987, having relatively high levels of oceanographic sampling. However, the results for the heat budget are considerably more uncertain, reflecting the larger number of processes involved in determining the heat content of the upper ocean.

Over the spring and summer months, the net of the vertical air-sea fluxes (net solar radiation less net longwave back radiation, and net losses due to the turbulent sensible and latent heat fluxes) are larger by a factor of five than the rate of heat gain by the ocean from Mackenzie River discharges, and 60% greater than the heat loss due to the melt of local sea-ice. However, the complexity of the atmospheric processes, combined with the lack of direct observations of these fluxes, results in a large uncertainty of $\pm 50\%$ in the estimate of net downward heat transfer to the ocean. When combined with the smaller uncertainties in the river and ice heat estimates, and the large uncertainty in the oceanic heat content ($\pm 27\%$), the estimated uncertainty in the net residual heat lost by the ocean is so large, at $\pm 136\%$, as to render the residual value virtually meaningless.

From May to August inclusive, the net heat input to the ocean from all external sources (surface heat exchanges and river input less losses due to sea-ice melt) was characterized by a comparatively small degree ($\pm 20\%$) of interannual variability in all but one year (1970). The level of interannual variations in heat input to the ocean is noticeably reduced in comparison with net freshwater input. The small year-to-year variation in net heat input to the ocean is a result of the strong coupling between fluctuations in the net solar radiation absorbed at the surface and heat lost to melting of sea-ice. Because much of the surface heat exchange is used to melt sea-ice, the net heat transferred into the water column remains comparatively small until sea-ice clearing is well advanced in the study area.

The heat storage in continental shelf waters, as measured from mid-July to mid-September, exhibited larger variations within the summer and smaller levels of year-to-year variability than freshwater content. In almost all years, a pronounced decrease in heat content was noted between the period mid-July to mid-August and one month later. The large loss of heat within the late summer may result from systematic errors in estimating heat exchanges; for example,

underestimation of oceanic heat losses due to turbulent heat fluxes to the atmosphere.

The differences between computed losses of heat and freshwater over interannual time scales appears to reflect the difference in the effects of advection through the eastern and western boundaries of the continental shelf study area. Unlike upper layer heat content, which tends to increase from west to east (eastern Alaska to the entrance to Amundsen Gulf), the freshwater content has a pronounced maximum over the inner to middle half of the western portion of the Mackenzie Shelf, associated with the Mackenzie River plume. Thus, the losses due to advection could differ considerably between heat and freshwater.

5.7 UPWELLING CONDITIONS

The vertical cross-section plots of temperature and salinity contours over offshore transects of the shelf waters (1950-1987) were compared with the concurrent wind data to examine the frequency of occurrence of coastal upwelling occurring under easterly wind forcing. In both the Mackenzie canyon and the outer shelf-to-slope regions of the Mackenzie Shelf, upwelling conditions occurred much more frequently than downwelling conditions. However, there was no evidence to suggest that upwelling was more likely to occur or had stronger characteristics under easterly winds. Over the Mackenzie Shelf proper, the occurrences of up- and downwelling were nearly evenly divided, but there was no apparent correlation between occurrence of upwelling with easterly winds.

Upwelling conditions in the area, although occurring frequently, do not appear to represent simple linear responses to regional wind forcing. Other mechanisms proposed in previous studies (interactions of large scale currents with sharply curving topography of the Mackenzie Canyon, or responses to local orographic-driven winds off the Yukon coastline) may be important in driving upwelling within the region.

5.8 RECOMMENDATIONS

The results of this study, derived from analyses of an extended data set spanning more than 30 years, must be considered preliminary in many respects. Further investigations that are more clearly focused can now be identified, and are included in the following recommendations:

- (1) In view of the apparent periodicities noted in the oceanographic and sea-ice quantities, the importance of extending the oceanographic time series is apparent. Efforts should be made to ensure that at least one reasonably detailed and accurate synoptic oceanographic data set is collected each summer, preferably in the latter part of August. Such a programme would avoid a repeat of the major gap in the existing data record for the 1960's. The continuation of the data set will be a valuable resource for future climatic studies involving the effects of global warming in the Canadian Arctic.
- (2) Improved techniques for heat budget studies are required to reduce the uncertainties in the computational results. The use of better marine-based parameters for atmospheric heat fluxes should be examined through a search of atmospheric data collected from (a) drillships, and (b) research

and other vessels operating in the region. Satellite data sets, such as specialized algorithms to measure cloud cover over marine areas, may also be useful.

- (3) Further analysis is required of the factors determining the area of reduced sea-ice concentrations in the summer months. The extent of clearing of sea-ice appears to be very important in controlling advective exchanges of inner shelf waters with adjoining regions, and in determining the amount of incident solar radiation absorbed by the upper ocean. A better understanding is needed of the role of: large-scale shifts in the polar pack, the degree of early season clearing of sea-ice in Amundsen Gulf and the eastern Mackenzie Shelf, and the effects of local wind forcing on sea-ice clearing patterns.

6 REFERENCES

- Aagaard, K. 1984. The Beaufort Undercurrent in "The Alaskan Beaufort Sea: Ecosystem and Environments" ed. D. Norton, Academic Press, New York. p. 47-71.
- Badgely, F.I., 1966. Heat Budget of the Surface of the Arctic Ocean. Proceedings of the Symposium on the Arctic Heat Budget and Atmospheric Circulation, 31 Jan.-4 Feb. 1966, National Science Foundation Memorandum RM-5233-NSF, pp. 269-277.
- Birch, J. R., D. D. Lemon, D. B. Fissel and H. Melling, 1987. Arctic Data Compilation and Appraisal. Vol. 12. Beaufort Sea and Amundsen Gulf: Physical Oceanography - Temperature, Salinity, Currents, Water Levels and Waves. Revised and updated to include 1914 through 1986. Can. Data Rep. Hydrogr. Ocean No. 5. 459 p.
- Burns, B.M., 1973. The Climate of the Mackenzie Valley - Beaufort Sea - Volume I. Climatological Studies No. 24, Environment Canada, Ottawa, 227 p.
- Cameron, W.M., 1953. Hydrography and oceanography of the southeast Beaufort Sea and Amundsen Gulf, including Part II (appendices): hydrographic and oceanographic observations in the Beaufort Sea, 1952. University of British Columbia, Institute of Oceanography (unpublished manuscript). 82 p.
- Danard, M. and M. Gray, 1984. Extreme wind stresses over the Beaufort Sea as determined from Tuktoyaktuk winds. Unpublished report by Atmospheric Dynamics Corp., Victoria, British Columbia for Institute of Ocean Sciences, Sidney, British Columbia.
- Davies, K.F., 1975. Mackenzie River Input to the Beaufort Sea, Beaufort Sea Technical Report 15, Department of the Environment, Victoria, B.C.
- Fissel, D.B., 1981. An analysis of current meter data obtained at Canmar drillships, 1976-1979. Arctic Sciences Ltd. report to Dome Petroleum Ltd., Calgary, Alta. (unpublished manuscript).
- Fissel, D.B. and J.R. Birch, 1984. Sediment transport in the Canadian Beaufort Sea. Arctic Sciences Ltd. for Atlantic Geoscience Centre, Bedford Institute of Oceanography, Dartmouth, Nova Scotia. 165 p.
- Fissel, D. B., M. S. W. Bradstreet and J. Moen, 1987a. Water mass distributions in the Canadian Beaufort Sea. In: Proceedings IEEE, Oceans 87. Vol. 3, pp. 910-916.
- Fissel, D. B., J. R. Marko, J. R. Birch, G. A. Borstad, D. N. Truax and R. Kerr, 1987b. Water mass distributions. In: Importance of the Eastern Alaskan Beaufort Sea to Feeding Bowhead Whales, 1985-86. W. J. Richardson Ed. Unpublished report, LGL Ecol. Res. Assoc. Inc., Bryan, TX, Arctic Sciences Ltd., Sidney, B. C., Biosonics Inc., Seattle, WA, G. A. Borstad Associates Ltd., Sidney, B. C. and University of Alaska, Fairbanks, AK for U. S. Minerals Management Service, Reston, VA.

Herlinveaux, R.H. and B.R. de Lange Boom, 1975. Physical oceanography of the southeastern Beaufort Sea. Beaufort Sea Project Tech. Rept. 18, Beaufort Sea Project, Dept. of the Environment, Victoria, B.C. (available from Micromedia Ltd., Information Access, 144 Front St. W., Toronto, Ontario, M5J 1G2).

Hufford, G.L., 1974. On apparent upwelling in the southern Beaufort Sea. J. Geophys. Res. 79(9). pp. 1305-1306.

Hufford, G.L., 1975. Some characteristics of the Beaufort Sea shelf current. J. Geophys. Res. 80(24). pp. 3465-3468.

Huyer, A., and F.G. Barber, 1970. A Heat Budget of the Water in Barrow Strait for 1962. Manuscript Report Series No. 12, Marine Sciences Branch, Department of Energy, Mines and Resources, The Queen's Printer for Canada, Ottawa.

Hydrotechnology, 1980. Wave hindcast study, Beaufort Sea. Report by Hydrotechnology Ltd., Ottawa, Ontario, for Gulf Canada Resources Inc., Calgary, Alberta. (Available from Pallister Resources Management Ltd., Calgary, Alberta, T2C 2B3, as Beaufort EIS Report RWE28). 81 p. (with appendices).

Kelly, P.M., P.D. Jones, C.B. Sears, B.S.G. Cherry and R.K. Travol, 1982. Variations in surface air temperatures: Part 2. Arctic regions, 1881-1980. Monthly Weather Review, pp. 71-83.

MacDonald, R.W., C.S. Wong and P.E. Erickson, 1987. The distribution of nutrients in the southeastern Beaufort Sea: implications for water circulation and primary production. J. Geophys. Res. (92). pp. 2939-2952.

MacNeill, M.R. and J.F. Garrett, 1975. Open water surface currents. Beaufort Sea Project Tech. Rept. 17, Beaufort Sea Project, Dept. of the Environment, Victoria, B.C. (available from Micromedia Ltd., Information Access, 144 Front St. W., Toronto, Ontario, M5J 1G2).

Marko, J. R., D. B. Fissel, M. A. Wilson, and D. Huston, 1983. Background and evaluation of impacts of Liard River hydroelectric development in the southeastern Beaufort Sea. Preliminary draft, unpublished manuscript. Arctic Sciences Ltd., Sidney, British Columbia, for B.C. Hydro and Power Authority, Vancouver, British Columbia. 81 p. plus unnumbered figures and appendices.

Maykut, G.A. and N. Untersteiner, 1971. Some Results from a Time Dependent Thermodynamic Model of Sea Ice. J. Geophys. Res. 80: 4501-4513.

Melling, H., 1983. Oceanographic features of the Beaufort Sea in early winter. Can. Tech. Rep. Hydrogr. Ocean Sci. (20). 131 p.

Melling, H. and E.L. Lewis, 1982. Shelf drainage flows in the Beaufort Sea and their effect on the Arctic Ocean pycnocline. Deep Sea Res. Vol. 29 (no. 8A). pp. 967-985.

Mountain, D.G., 1974. Preliminary analysis of Beaufort shelf circulation in summer. In: The Coast and shelf of the Beaufort Sea. J.C. Reed and J.E. Sater (Ed.). Arctic Inst. of North America, Arlington, VA. pp. 27-42.

- Murray, M. A. and M. Maes, 1986. Beaufort Sea extreme wave studies assessment. Environmental Studies Revolving Funds, Report Series No. 023. Ottawa, 97 p.
- Mysak, L.A. and D.K. Manak, 1989. Arctic sea-ice extent and anomalies, 1953-1984. Atmosphere-Ocean 27, pp. 376-405.
- Nakawo, M. and N. K. Sinha, 1981. Growth rate and salinity profile of first year sea-ice in the high Arctic. J. Glaciol., 27: pp. 315-330
- Olson, R., 1985. An Assessment of Canadian Arctic Wind Data Sets. Unpublished report by Environment Canada, Atmospheric Environment Service, Downsview, Ontario. 21 pp.
- Parker, N. and J. Alexander, 1983. Weather, ice and sea conditions relative to Arctic marine transportation. Can. Tech. Rep. Hydrogr. Ocean Sci. No. 26: xii + 211 p.
- Pond, G. S. and W. J. Emery, 1984. Descriptive Physical Oceanography. Pergamon Press, Oxford. 249 p.
- Smith, M. and B. Rigby, 1981. Distribution of polynyas in the Canadian Arctic. In: Polynyas in the Canadian Arctic, I. Stirling and H. Cleator, Eds. Canadian Wildlife Service Occasional Paper No. 45; 7-28.
- Stirling, I.S. and H. Cleator, 1981. Polynyas in the Canadian Arctic. Canadian Wildlife Service Occasional Paper No. 45, Ottawa, 73 pp.
- Swail, V.R., 1985. Geostrophic Wind Climatology of Canadian Marine Areas. Report No. 85-9, Canadian Climate Centre, Downsview, Ont. 25 p. + unnumbered appendices.
- Sweers, H.E., 1970. Oceans IV: A Processing, Archiving and Retrieval System for Oceanographic Station Data. Manuscript Report Series No. 15. Marine Environmental Data Service, Ottawa.
- Swithenback, C., 1960. Ice Atlas of Arctic Canada. Defense Research Board of Canada, Ottawa. 67 pp.
- Taylor, J. 1976. CONMAP: A Computer Program for Contouring Oceanographic Data. Technical Note No. 12. Marine Environmental Data Service, Ottawa.
- Thomas, D.J., R.W. Macdonald and A.B. Cornford, 1986. Geochemical mass balance calculations for the coastal Beaufort Sea., N.W.T., Canada. Rapp. P.V. Reun. Cons. Int. Explor. Mer., 186. pp. 156-178.
- Thomson, D. H., D. B. Fissel, J. R. Marko, R. A. Davis, and G. A. Borstad, 1986. Distribution of bowhead whales Balaena mysticetus in relation to hydrometeorological events in the southeastern Beaufort Sea, 1980-1983. Environmental Studies Revolving Fund Report No. 028, Ottawa. 119 p.
- Tummers, E.L., 1980. Heat Budgets of the Southeast Beaufort Sea for the Years 1974 and 1975. M.Sc. Thesis, U.S. Naval Postgraduate School, 205 pp.

Vowinckel, E. and S. Orvig, 1970. The climate of the North Polar Basin in *Climates of the Polar Oceans*, ed. S. Orvig. Elsevier, Amsterdam, p. 129-252.

Walmsley, J.L., 1966. Ice cover and Surface Heat Fluxes in Baffin Bay. Manuscript Report No. 2, Marine Sciences Center, McGill University, Montreal.

APPENDIX A
INFORMATION ON DATA SETS

The data set identification (i.d.) numbers, and ship/agency are derived from Birch et al. (1987). The accuracies given for temperature (T) and salinity (S) were initially based on Birch et al. (1987) but in some cases these values were modified based on the results of testing and use of the data in this study. In the comments section, the symbols T, S and ρ represent temperature, salinity and density, respectively.

DATA SET I.D.	SHIP/AGENCY	ACCURACY		TIME		# OF PROFILES		COMMENTS ON ERRORS DETECTED
		T	S	START	END	TOTAL	ERRORS	
50-0001	BURTON IS.	0.03	0.04	Aug. 19	Aug. 23	19	2	minor S spikes and ρ inversions
51-0001	BURTON IS.	0.03	0.04	Sep. 14	Sep. 21	28	8	minor ρ inversions
51-0002	CANCOLIM	0.03	0.04	Aug. 20	Sep. 15	26	0	No errors detected
52-0001	CANCOLIM	0.03	0.1	July 18	Aug. 31	172	17	Minor errors (ρ inversion, T below freeze T)
52-0002	BURTON IS.	0.03	0.04	Sep. 2	Sep. 10	10	8	minor ρ inversions
54-0001	LABRADOR	0.03	0.04	Sep. 12	Sep. 14	10	1	S spike
54-0002	BURTON IS.	0.03	0.04	Sep. 10	Sep. 13	22	3	few points outside reasonable TS curves
55-0001	NORTHWIND	0.03	0.04	Aug. 27	Sep. 4	3	0	
55-0016	BURTON IS.	0.03	0.04	Aug. 2	Aug. 2	3	2	minor errors in T and S
56-0001	REQUISITE	0.03	0.04	July 30	Aug. 27	4	1	one T < freeze T
57-0002	ATKA	0.03	0.04	Aug. 3	Aug. 15	9	2	minor ρ inversions
58-0001	BURTON IS.	0.03	0.04	Sep. 2	Sep. 4	6	0	
59-0001	T-3	0.03	0.04	June 9	Sep. 9	11	5	surface S too low
59-0002	STATEN IS.	0.03	0.02	Aug. 10	Sep. 3	13	1	one point ρ inversion
60-0001	BURTON IS.	0.03	0.02	Aug. 16	Sep. 19	22	2	minor ρ spikes
60-0003	SALVELINUS	0.03	0.04	Aug. 3	Aug. 25	6	0	
69-0001	STATEN IS.	0.03	0.02	Aug. 8	Aug. 10	4	2	minor ρ spikes
70_0002	HUDSON	0.03	0.02	Aug. 28	Sep. 23	23	5	ρ spikes
71_0001	SALVELINUS	0.03	0.02	July 19	July 19	4	0	

DATA SET I.D.	SHIP/AGENCY	ACCURACY		TIME		# OF PROFILES		COMMENTS ON ERRORS DETECTED
		T	S	START	END	TOTAL	ERRORS	
72_0001	HELICOPTER	0.03	?	Mar. 21	Apr. 9	36	21	S inversions at near surface depths
73_0002	NORTH STAR	0.50	0.70	July 20	July 27	19	0	
74_0007B	?	0.03	0.10	July 17	July 31	9	9	several missing samples
74_0007A	THETA	0.03	0.02	July 14	Aug. 16	7	0	
74_0002	THETA	0.03	0.02	Aug. 12	Sep. 3	62	31	near-surface p inversions
75_0001	AIRCRAFT	0.02	0.02	Mar. 20	May 10	20	5	suspect S - due to ice in cond. cell?
75_0002	PANDORA II	0.01	0.02	Aug. 5	Aug. 24	46	18	minor p inversions; 6 profiles exhibited large systematic differences in S in comparison to nearly simultaneous profiles of 75_0006.
75-0006	PANDORA II	0.01	0.02	Aug. 5	Aug. 23	6	0	used in place of profiles of Data Set 75_0002.
75_0009	THETA	0.03	0.02	Aug. 14	Sep. 9	23	3	minor T and S errors
76_0001	CANMAR	0.1	0.2	Aug. 9	Aug. 25	2	2	large (≈ 1) errors in S
76_0004	SLANEY	0.5	0.7	Aug. 15	Aug. 16	3	3	large errors in S
76_0020	SALVELINUS	0.03	1	Aug. 16	Aug. 24	2	2	large errors in S
77-0001	SLANEY	1	1	July 25	Aug. 11	8	8	all S profile data unreliable
77-0002	AQUA. ENV.	0.2	?	July 21	Aug. 30	4	4	near-surface values only
77-0003	PANDORA	0.02	0.02	Aug. 14	Aug. 15	5	0	

DATA SET I.D.	SHIP/AGENCY	ACCURACY		TIME		# OF PROFILES		COMMENTS ON ERRORS DETECTED
		T	S	START	END	TOTAL	ERRORS	
77-0004	CANMAR	1	1	July 27	Oct. 12	20	6	large errors in all S data.
77-0009	ENVIROCON	0.1	0.7	July 30	Aug. 29	4	1	large errors in all S data.
77-0035	SALVELINUS	0.03	1	July 28	Aug. 25	13	3	large errors in all S data
78-0001	CANMAR	1	1	July 18	Sep. 18	18	18	all T and S data has large errors of ≈ 1 .
78-0002	SEAKEM	0.06	0.04	July 19	Sep. 24	4	1	minor S error
78-0018	SEAKEM	0.08	0.04	July 20	July 20	1	0	
78-0019	CANMAR	0.08	0.04	July 29	July 29	1	0	
78-0031	FWI	0.5	0.7	Sep. 2	Sep. 4	4	0	near surface only
79-0003	CANMAR	1	1	July 17	Oct. 12	19	19	large T and S errors
79-0007	ARCTIC LAB	0.04	0.04	July 22	July 22	1	0	
79-0010	ARCTIC LAB	0.04	0.09	Sep. 25	Sep. 25	1	0	
79-0037	FWI/DFO	0.5	0.7	July 19	July 19	2	0	near surface only
80-0002	CANMAR	0.1	.1-1	Aug. 2	Sep. 27	18	6	all S in error in some profiles.
80-0003	ARCTIC LAB	0.04	0.09	Aug. 10	Sep. 26	3	0	
80-0004	ARCTIC LAB	0.03	0.04	Aug. 15	Sep. 25	3	1	minor errors
80-0025	LGL LTD.	0.1	1.0	Aug. 14	Aug. 27	7	7	large (≈ 1) S errors
81-0001	IOS	0.003	0.01	Mar. 18	Apr. 18	48	1	minor S error
81-0002	CANMAR	0.1	0.1-1	Aug. 12	Aug. 26	4	2	large S errors in 2 profiles
81-0003	ARCTIC LAB	0.03	0.04	July 26	July 26	1	0	
81-0027	LGL LTD.	0.1	0.1	Aug. 1	Aug. 25	13	3	minor p inversions

DATA SET I.D.	SHIP/AGENCY	ACCURACY		TIME		# OF PROFILES		COMMENTS ON ERRORS DETECTED
		T	S	START	END	TOTAL	ERRORS	
82-0118	CANMAR	0.1	0.1-1	July 30	Oct. 5	12	2	2 profiles with all S data in error
83-0058	ARCTIC LAB	0.10	0.02	Aug. 21	Aug. 23	24	0	only surface values
83-0065	AGC	0.03	0.10	July 20	July 28	25	2	minor T and S spikes
83-0069	CANMAR	0.1	0.1-1	July 23	Sep. 19	15	4	all S in error on one profile
84-0044	AGC	0.01	0.025	July 18	July 20	13	0	
84-0048	CANMAR	0.1	0.1	July 19	Sep. 9	6	1	minor errors
84-DFO	FWI/DFO	0.02	0.03	July 14	Sep. 9	15	0	
85-0017	FWI/DFO	0.02	0.03	Mar. 27	?????	69	3	minor ρ inversions
85-0032	IOS/DFO	0.01	0.02	Apr. 13	Apr. 19	18	0	
85-0033	CANMAR	0.1	0.1-1	Aug. 10	Oct. 1	15	7	all S values in error on 4 profiles
86-0010	IOS/DFO	0.01	0.02	Mar. 23	Mar. 30	21	0	
86-DFO	FWI/DFO	0.02	0.03	Mar. 23	Sep. 20	80	3	all S in error on one profile
86-0003	IOS	0.01	0.02	Sep. 10	Sep. 14	39	0	
86-0004	LGL LTD.	0.05	0.1	Aug. 28	Sep. 8	161	9	minor ρ inversions
87-IOS	IOS/DFO	0.01	0.02	Mar. 24	Mar. 27	26	0	
87-DFO	FWI/DFO	0.02	0.03	Mar. 19	Aug. 27	45	0	
87-NGP	IOS/DFO	0.02	0.15	Mar. 30	June 4	51	0	